

# Application of Remote Sensing in Earth Sciences – A Review

Adel Shirazy  
PhD  
Shahrood University of  
Technology  
Shahrood, Iran

Aref Shirazy  
PhD Candidate  
AmirKabir University of  
Technology  
Tehran, Iran

Hamed Nazerian  
MSc  
University of Catania  
Catania, Italy

**Abstract:** The application of remote sensing sciences in the field of geology is very diverse and wide. One of its most important applications in earth sciences is geological mapping. Mineral exploration using remote sensing techniques is done in different ways, one of them is the mapping alteration zones related to mineral resources. Given the importance of remote sensing and geosciences in today's industry and given that deposit-related alteration areas are one of the most important exploratory keys. In this review study the mapping methods and alteration zones detection using remote sensing techniques and other applications of remote sensing in earth sciences and its generalities are explained.

---

**Keywords:** Remote Sensing, ETM, ASTER, Alteration, Exploration, Earth Sciences.

---

## 1. INTRODUCTION

Mineral resources as the first link in the production chain play an undeniable role in the development, growth and prosperity of a country and form the basis of the economy and industry [1-4]. From the beginning of its creation and throughout history, human beings have used minerals according to their needs and knowledge [5, 6]. In other words, these minerals form the basis of civilization. Therefore, mineral exploration has special importance as the first step in this cycle [7, 8]. Along with the production and advancement of science, technology, and innovations such as remote sensing, GIS, and global positioning systems, traditional methods of mineral exploration have been replaced by new methods [9, 10].

Remote sensing is technique of collecting information about land surface features without physical contact with them. Remote sensing has great potential for identifying altered areas associated with deposit masses thus is known as a standard method in the field of mineral exploration and it can help to study geochemical explorations [11-15]. [Remote sensing data] has special capabilities compared to data collection methods due to its integrity and breadth, spectral diversity, duplication of coatings, and cheapness, which today is the first factor in the study of land surface and its constituent factors [16]. The digital nature of data has made it possible for computer systems to use this data directly [17, 18]. Quick access to remote areas and their high accuracy are the special advantages of this technology. Remote sensing techniques play an important role in locating mineral deposits and significantly reduce the costs of initial exploration and semi-detailed studies. It is very useful to use satellite imagery when making geological maps, improving the quality of maps and preparing thematic maps. Remote sensing is used in various sciences such as geology, archeology and environmental sciences. A new generation of advanced remote sensing has been used in recent decades in the mineral exploration, the exploration of oil reserves, the environmental study and agriculture [19].

The application of remote sensing in the field of geology is very wide, one of which is related to geological mapping

using remote sensing. Some geological surveys using remote sensing :

- Identify the type of stone [20].
- Structure identification [21].
- Structural and hybrid mapping [22].
- Remote geochemistry [23].
- Exploration of oil reserves [24].
- Exploration of mineral resources [25].
- Water resources [26].

Exploration of mineral resources by remote sensing is done by the following three methods [27].

- Alterations mapping
- Structures mapping
- Hyperspectral mapping

In this study, has tried to collect and present methods related to the application of remote sensing in mineral resource exploration [28-30].

## 2. REMOTE SENSING & LITHOLOGY

In this section, the properties of the igneous, sedimentary and metamorphic rocks that help us to identify them using satellite images processing and remote sensing techniques, are mentioned [31].

### 2.1 IGNEOUS ROCKS

Intrusive igneous rocks usually cover tens of square kilometers areas and have a relatively homogeneous texture. These rocks may have joints, faults, or arc-shaped dykes in their margins and be affected by joint systems throughout the area. Intrusive coarse-grained rocks are easily eroded into well-drained and thick soils, while fine-grained rocks are more resistant to erosion. Felsic intrusive stones like granites, are lighter in color, while mafic intrusions, such as gabbro, are darker in color. Mafic minerals are usually eroded by clay due to erosion and alteration, and show a milder topography than granite soils. Ultramafic units, carbonates and kimberlites have an unusual morphology and narrow rangelands [32].

One of the characteristics of intrusive igneous rocks is the presence of veins filled with mineral deposits, which are

usually observed at the site of ring, radial faults or at their intersection. These streaks are usually characterized by their associated faults, their resistance to erosion, or their light color. Extrusive igneous rocks often have specific areas. Volcanoes, volcanic cones, and lava flows are all easily recognizable. Craters are often identified by radial or ring dykes and craters filled by lakes. Most of the volcanic rocks are granular and have very strong layers that form steep precipices. It is difficult to distinguish tuffs from erodible sedimentary rocks. They have very bright colors. Basalts are often dark and sometimes seen as flowing lavas. In some areas, basalts form dark, resistant layers that cover tens of square kilometers. Most of the volcanic soils contain red soils, which are formed as a result of rapid weathering of ferrous minerals. These features can be used to detect igneous rocks using remote sensing methods [33].

## 2.2 METAMORPHIC ROCKS

Metamorphic rocks can be identified by adhesions and scratches. Low-pressure rocks, such as schists, are usually dark in color and highly erodible along their foliation, but in some areas they may be difficult to distinguish from sedimentary rocks. Metamorphic rocks, unlike intrusive igneous rocks, are heterogeneous and therefore do not have uniform color and surface texture [34].

## 2.3 SEDIMENTARY ROCKS

Sedimentary rocks are characterized by strong and weak alternating layers with various thicknesses and colors. The appearance of different types of rocks depends on their grain size, composition and weathering environment [10].

## 2.4 SANDSTONES

The sandstones are mainly composed of quartz and feldspar and form resistant ridges. Of course, this resistance depends on the type and degree of cementation of the sandstones. Silica cements are more resistant than calcite cements and both are more resistant than clay and gypsum cements. High porosity sandstones usually have little surface runoff and canals flow at a distance from each other. High permeability promotes the growth of plants with deep roots in sandstones. Due to the high fragility and strength of sandstones, joint systems are widely used [35].

## 2.5 SHALES

Shales are either clay particles or clay-sized quartz. Due to their fineness, they are highly erodible and form shallow valleys in wet areas. Due to the high surface flow, the waterways flow at a very short distance from each other. Because Chilean units are more likely to be malleable, the joints in them do not develop well. Shales are prone to landslides and generally have a mild topography [36].

## 2.6 CARBONATITES

Carbonatites are crystalline and therefore resistant to physical weathering. In arid areas, they form bumps and break easily. In humid areas they are resistant but have a circular morphology. Carbonates are usually light in color, although they may darken due to weathering. One of the important features of carbonates is the presence of karsts or wells in them. They create areas of spots [37].

In such areas, the pattern of canals is erratic because the canals suddenly collapse into the wells or all the precipitation penetrates between the joints. In arid areas, carbonates produce little soil, have steep valleys, and most plants grow in wells where moisture accumulates. In wet areas, plants are more concentrated. Residual clays with carbonates form red soils in wetlands. There is no clear way to distinguish between

limestone and dolomites except by high-resolution imaging spectroscopy in areas where vegetation is scarce or non-existent. Dolomites are often highly fractured and erode more easily than limestone. Therefore, dolomites may be black in a certain area if lime is gray [38].

## 2.7 EVAPORATION

Evaporates, such as halite and gypsum or anhydrite, are present only in arid areas on the surface. Because they are soluble in water. They are recognizable because they are very bright and white. They are found in the form of domes, salt lakes and rarely in sand dunes. Subsurface evaporations are the evaporative layers below the earth's surface. They are usually characterized by the morphology which is created on the surface. Salts usually form dome-shaped diapirs. The moving nuclei of thrust folds, like salt domes in the folded Zagros belt, sometimes reach the surface in the form of domes [39].

## 2.8 SPECTRAL LITHOLOGY

Satellite images can be effective in identifying different stratigraphic units by determining the spectral characteristics of rocks and minerals. For example, Hunt and Salisbury provided near-infrared and infrared wavelength reflection curves for sandstone, shale, and limestone. According to these curves, units with similar stratigraphy show similar reflection curves, based on which many geologists have mapped rock units in different areas using their respective reflection curves. In Fig1 Spectral diagrams of minerals in sedimentary rocks are presented, which comparison between these curves with the main curves help us in the exploration and detection of sedimentary rocks [40].

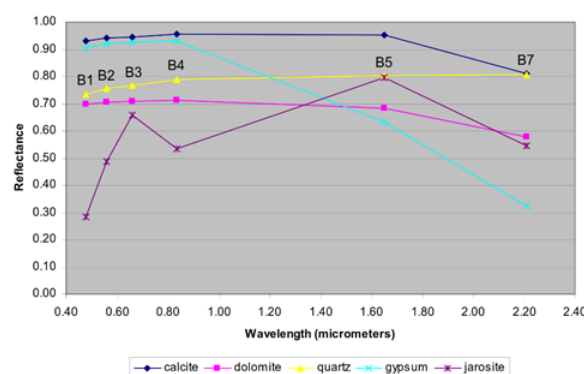


Figure 1: Reflection curves for some minerals found in sedimentary rocks

## 3. REMOTE SENSING AND EXPLORATION OF MINERALS

To date, two different methods have been used in studies related to mineral exploration using remote sensing techniques [8].

- 1- Pattern mapping of fractures and faults at the regional and local scale to detect their control over critical reserves. For example, a comparison of the pattern of ridges in Nevada with areas with mineral reserves showed that mineral deposits occur along these ridges and their focus is at the intersection of these ridges. According to the studies of Nicholas (1974) and based on the pattern of local fractures in Landsat images in Colorado, it was found that more mineral deposits are formed in areas with high fracture density.

2- Detection of rocks that have undergone hydrothermal alteration and may be associated with mineral deposits. In the meantime, Landsat image TM has been most used in this field, especially for the detection of alteration minerals such as iron oxides, clays and alunites.

The reflectance spectra of minerals are well known. Many studies have been done to determine the reflection spectrum of rocks. The reflectance spectra of minerals are measured by spectroscopic instruments of varying resolution and stored in spectral libraries that are stressed in digital formats. When a beam of light hits the surface, some of it is absorbed and some is scattered or reflected. The reflected rays of different objects are measured in the laboratory or in the desert. Field spectrometers reflect the reflection of objects by dividing the radiant energy reflected from the intended target by the radiant energy reflected from a reference (radiant material)100%). Barium sulfate is usually used for reference in field spectrometers. Sunlight is usually sufficient for the light source [41].

### 3.1 SPECTRAL CHARACTERISTICS OF CLAY MINERALS

Clay minerals generally include smectite, kaolinite and illite. Smectite is a group of clay minerals that is characterized by three layers including two layers of silicon and oxygen tetrahedron and one layer of aluminum and hydroxyl octahedron, the most important member of which is montmorillonite. In these layers, water molecules are absorbed between the layers. Montmorillonite approaches a strong absorption spectrum 1.4, 1.9, 2.2 micrometers. The spectra of illite, montmorillonite and muscovite have almost the same absorption bands. Like montmorillonite, illite shows an absorption band of 1.4 and 1.9, as well as 2.2, 2.3 and 2.4 micrometers [42].

Kaolinite is one of the clays that consists of two layers of silica in the form of tetrahedron and aluminum in the form of octahedron. Absorption properties of the whole kaolinite range are 2.2 micrometers and 1.4 micrometers. Figure 2 shows the reflection spectra of the three groups of illite, kaolinite and montmorillonite in the short infrared spectral range [43].

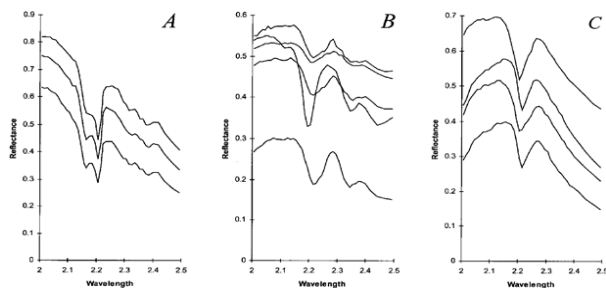
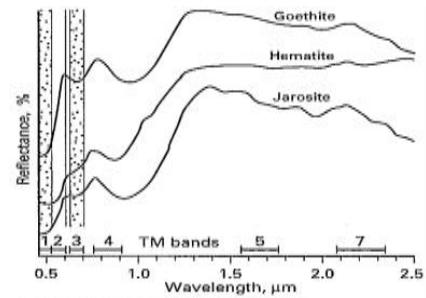


Figure 2: Spectral range reflection spectrum SWIR Three groups (A illite, B kaolinite and C montmorillonite)

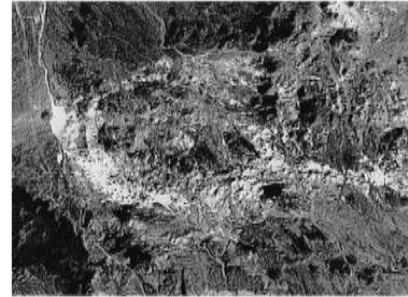
### 3.2 SPECTRAL CHARACTERISTICS OF IRON OXIDES

The spectrum of iron oxides has the highest reflection in the visible red band, 0.7  $\mu\text{m}$  and the lowest reflectance at 0.9 and 0.4  $\mu\text{m}$ . Reflective spectra of iron oxides, mostly hematite, goethite, and limonite, were studied by Rowan to identify the alteration zone associated with the Goldfield mineralization in Nevada (Figure 3). The reflection spectra of some iron oxides

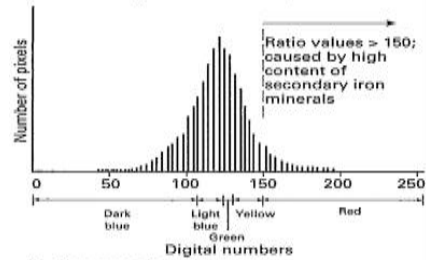
from the data TM in the Goldfield mine is shown in the figure 3 [44].



A. Laboratory reflectance spectra.



B. Ratio image of TM bands 3/1.



C. Histogram for 3/1 image.

Figure 3: Curve of reflection spectra of iron oxides and bandwidth of 1/3 of TM data in Goldfield mine

## 4. APPLICATION OF LANDSAT IMAGES

The Landsat remote sensing satellite was designed and built by the American Ground Observation Satellite Company. Landsat is the name of a series of satellites designed to collect information from terrestrial sources in a regular and systematic framework. [Satellite] information can be used to determine land use, geological and mineralogy exploration, forestry and agriculture management, and cartography [45].

### 4.1 DETECTION OF CLAY MINERALS BY DATA TM

Reflectance spectra of alunite and three important clay minerals are shown in figure 4. These minerals show the least reflection and the most absorption in band 7TM but they have the most reflection in the band 5 TM. Images from comparison can emphasize these spectral differences. Band ratios 5/7 in pictures ETM+ Or TM is effective in detecting clay minerals. Table 1 shows how to distinguish 5/7 ratio of altered stones from unaltered stones. The reflection of unaltered rocks in band 7 is similar to band 5 but both rocks have the same reflection in band 5. Therefore, the ratio of 5/7 non-altered rocks is equal to one, while in altered rocks it is 1.45 because the altered rocks have less reflection in band 7. The numbers in the table are typical and can be different for other examples. Figure 4 shows a 5/7 aspect ratio image of the

Goldfield mine that shows a higher aspect ratio value with a lighter tone, as well as a 5/7 aspect ratio image histogram that shows the aspect ratio of the altered rocks [46].

**Table 1: Ratio values of 5/7 for altered and unmodified rocks in Goldfield mine**

Type of stone	Band reflection 5	Band reflection 7	Ratio 5/7	Digital number ratio 5/7
Unaltered stones	160	160	1.00	100
Altered stones	160	110	1.45	145

## 4.2 DETECTION OF FERROUS MINERALS BY DATA TM

Iron ores are the second class of markers of altered rocks in Figs 3. The reflection spectra of these minerals are shown. They are in the blue band TM The least reflection and in the red band TM. They have the most refinement. So ratio of 3/1 in pictures TM is effective. In the second picture of figure 4 high digital values are displayed in clear case only [47, 48].

## 5. USING HYPERSPECTRAL IMAGES TO EXPLORE MINERALS

Hyperspectral scanners are special type of multispectral scanners that have tens of bands with a width of approx 0.1  $\mu\text{m}$ . These images can provide more accurate and detailed data on minerals. There are two ways to produce images that specify the frequency and distribution of individual minerals by these images [49]:

1. As mentioned, many alteration minerals, especially clays, reflect a similar spectrum. Absorption spectra of clays with slight differences is 2.2 micrometers. These slight differences help to identify the range of different clay minerals. Image processing programs can range from one pixel AVIRIS compare the reference for known minerals in comparison with the laboratory range. This process is a kind of supervised classification and can only be effective for soil segregation in which there is only one single mineral.
2. Resolution AVIRIS is 20 by 20 meters. In areas with complex geology, a pixel with an area of 400 square meters contains different types of minerals. This pixel is a mixed pixel which is called a spectrum because it is a mixture of the spectra of different minerals in a cell that occupy 20 by 20 meters. These single minerals are called spectral samples. Distinctive digital programs are used to extract the spectrum of each individual mineral for each mixed pixel. For each sample, a sample frequency image is generated that shows its relative frequency.

TM images shows a broad pattern of hydrothermal alteration, while AVIRIS images show the distribution of individual alteration minerals.

## 6. USE OF ASTER IMAGES IN MINERAL EXPLORATION

Over the past decade, new remote sensing satellites, hyperspectral, and multispectral satellites have been launched into space, providing data with higher spectral resolution that can be useful for mineral exploration. In addition, laboratory spectral data for rocks and minerals such as spectral libraries USGS and JPL are considered as a complement to spectral measurements and allow geologists to identify individual rock units. Recent advances in remote sensing have made the use of this technology an important tool in mineral exploration, especially for areas with difficult access or areas without topographic and geological maps [50].

As mentioned, over the years a wide range of TM images with four bands VNIR and two bands SWIR has been used to detect iron oxides in bands VNIR and clay minerals in SWIR. However, ASTER images are similar to TM images in terms of spatial resolution, but existence of 6 bands SWIR increased ASTER ability relative to TM images. Another advantage of ASTER images is the existence of 5 thermal bands that allow the detection of quartz, potassium-containing feldspar, minerals containing  $\text{CO}_3$  and gives igneous rocks to geologists using spectral radiation curves and band ratios.

Each of the image bands of ASTER like TM Indicates some minerals. Absorption properties of bands 1 and 3 of ASTER mainly identifies iron oxides. While the absorption spectra of the bands 5 and 6 identifies aluminum hydroxides in clay minerals, alunite and muscovite. Band 7 also identifies iron hydroxides such as jurassites and ferrous muscovites, and band 8 is used to identify minerals containing magnesium hydroxide such as epidote, chlorite, and carbonate. Laboratory reflection data curves of kaolinite, alunite, muscovite and montmorillonite minerals corresponding to channels SWIR and VNIR that are extracted from the spectral library of ASTER Are shown in Figure 4 [51].

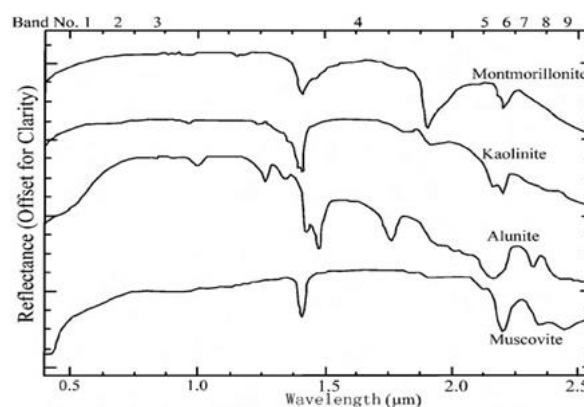


**Figure 4: Laboratory reflection data curve of kaolinite, alunite, muscovite and montmorillonite minerals from spectral library ASTER**

Dittomaso and Robinstein (2007) studied spectral reflection of alteration minerals in porphyry mine Infiernillo in Argentina by pictures of ASTER. In Figure 5 The first curves correspond to the combination of muscovite and illite. The second curve is consistent with the combination of iron

oxides and jurassite, the third curve shows a combination of illite and kaolinite, which shows small absorption properties at 2.16  $\mu\text{m}$ . Curve four shows a combination of illite and jurassite with absorption properties at 0.8 and 2.26  $\mu\text{m}$ . Curve 5 is consistent with chlorite. They use these spectral sections as a reference for mapping alteration minerals using images [52].

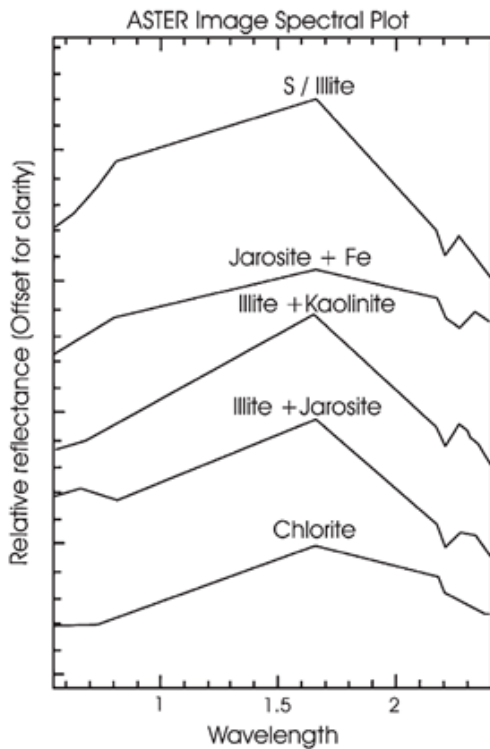


**Figure 5: Spectral reflection of alteration minerals in porphyry mine Infiernillo in Argentina**

Ravan and March (2003) presented spectral characteristics of important rock-forming minerals in the pass mountain in California, the results of calibration and re-sampling of locally measured reflective of 9 bands SWIR and VNIR. Comparison of laboratory reflection spectra with high resolution of selected minerals with reflectance spectra of ASTER images from resampling shows that ASTER image, despite [50] their low resolution, are recognizable and interpretable. The effect of factors such as the presence of mineral-mineral mixtures, plant-mineral mixtures, variable grain size and atmospheric effects reduces the quality of the reflected spectra in the images. The differences in the reflectance spectrum between carbonate minerals (calcite and dolomite) and muscovite minerals (aluminum-bearing and iron-bearing muscovite) are significant in both ASTER and laboratory spectra. Figure 6 shows the steps of calibrating [ASTER images for mapping. Ninomia (2003) presented a mineralogical index using 6 SWIR channels that are used to detect alteration minerals [53].

$$\begin{aligned} \text{OHI} &= (\text{band7} / \text{band6}) \times (\text{band4} / \text{band6}) \\ \text{KLI} &= (\text{band4} / \text{band5}) \times (\text{band8} / \text{band6}) \\ \text{ALI} &= (\text{band7} / \text{band5}) \times (\text{band7} / \text{band8}) \\ \text{CLI} &= (\text{band6} / \text{band8}) \times (\text{band9} / \text{band8}) \end{aligned}$$

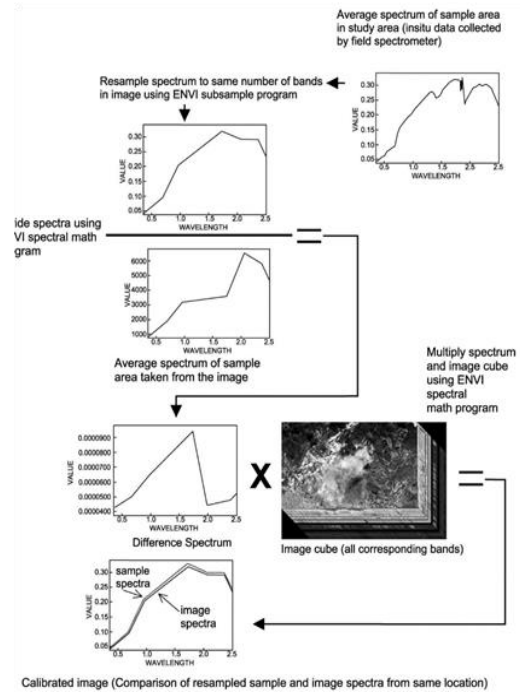


**Figure 6: Steps to calibrate data ASTER by reflectance spectral measurements to map alteration zones in Pass mountain, California**

OHI Index of minerals containing OH and KLI Kaolinite profile and ALI Alunite profile and CLI Is the calcite index as well as ninomia (2003) Index for Quartz in thermal bands ASTER-TIR Introduced, thus the quartz spectrum in bands 10 and 12 are absorbed and show a small radiative peak at 11 band:

$$Q_i = (b_{11} \times b_{11}) / (b_{10} \times b_{12})$$

It is expected that the amount of  $Q_i$  will be high for quartz and low for potassium feldspar [8].

## 7. CONCLUSION

The application of remote sensing in geology is very diverse and wide. One of the most important of these applications is geological mapping using remote sensing. In this study, generalities of satellite images and how to analyze and use them were expressed. Information was also provided on a range of minerals as well as various rocks. Due to the increasing development of science, it is suggested that you always expand the relationship between the two by studying new research in the field of remote sensing and earth sciences.

## REFERENCES

- [1] Khakmardan, S., A. Shirazi, A. Shirazy, and H. Hosseingholi, *Copper Oxide Ore Leaching Ability and Cementation Behavior, Mesgaran Deposit in IRAN*. Open Journal of Geology, 2018. **8**(09): p. 841.
- [2] Khakmardan, S., R.J. Doodran, A. Shirazy, A. Shirazi, and E. Mozaffari, *Evaluation of Chromite Recovery from Shaking Table Tailings by Magnetic Separation Method*. Open Journal of Geology, 2020. **10**: p. 1153-1163.
- [3] Doodran, R.J., S. Khakmardan, A. Shirazi, and A. Shirazy, *Minimalization of Ash from Iranian Gilsonite by Froth Flotation*. Journal of Minerals and Materials

- Characterization and Engineering, 2020. **9**(1): p. 1-13.
- [4] Campbell, J.B. and R.H. Wynne, *Introduction to remote sensing*. 2011: Guilford Press.
- [5] Shirazi, A., A. Shirazy, S. Saki, and A. Hezarkhani, *Geostatistics Studies and Geochemical Modeling Based on Core Data, Sheytoor Iron Deposit, Iran*. Journal of Geological Resource and Engineering, 2018. **6**: p. 124-133.
- [6] Sabins Jr, F.F., *Remote sensing--principles and interpretation*. 1987: WH Freeman and company.
- [7] Alahgholi, S., A. Shirazy, and A. Shirazi, *Geostatistical Studies and Anomalous Elements Detection, Bardaskan Area, Iran*. Open Journal of Geology, 2018. **8**(7): p. 697-710.
- [8] Sabins, F.F., *Remote sensing for mineral exploration*. Ore geology reviews, 1999. **14**(3-4): p. 157-183.
- [9] Shirazi, A., A. Shirazy, S. Saki, and A. Hezarkhani, *Introducing a software for innovative neuro-fuzzy clustering method named NFCMR*. Global Journal of Computer Sciences: Theory and Research, 2018. **8**(2): p. 62-69.
- [10] Gupta, R.P., *Remote sensing geology*. 2017: Springer.
- [11] Shirazi, A., A. Hezarkhani, A. Shirazy, and I. Shahrood, *Exploration Geochemistry Data-Application for Cu Anomaly Separation Based On Classical and Modern Statistical Methods in South Khorasan, Iran*. International Journal of Science and Engineering Applications, 2018. **7**: p. 39-44.
- [12] SHIRAZI, A. and A. HEZARKHANI, *Predicting gold grade in Tarq 1: 100000 geochemical map using the behavior of gold, Arsenic and Antimony by K-means method*. 2018.
- [13] Shirazy, A., A. Shirazi, M.H. Ferdossi, and M. Ziaii, *Geochemical and Geostatistical Studies for Estimating Gold Grade in Tarq Prospect Area by K-Means Clustering Method*. Open Journal of Geology, 2019. **9**(6): p. 306-326.
- [14] Shirazy, A., M. Ziaii, A. Hezarkhani, T.V. Timkin, and V.G. Voroshilov, *Geochemical behavior investigation based on k-means and artificial neural network prediction for titanium and zinc, Kivi region, Iran*. Известия Томского политехнического университета, 2021. **332**(3): p. 113-125.
- [15] Woźniak, S.B. and D. Stramski, *Modeling the optical properties of mineral particles suspended in seawater and their influence on ocean reflectance and chlorophyll estimation from remote sensing algorithms*. Applied Optics, 2004. **43**(17): p. 3489-3503.
- [16] Scafutto, R.D.P.M., C.R. de Souza Filho, and W.J. de Oliveira, *Hyperspectral remote sensing detection of petroleum hydrocarbons in mixtures with mineral substrates: Implications for onshore exploration and monitoring*. ISPRS Journal of Photogrammetry and Remote Sensing, 2017. **128**: p. 146-157.
- [17] Shirazy, A., A. Shirazi, and A. Hezarkhani, *Behavioral Analysis of Geochemical Elements in Mineral Exploration*. 2020, Germany: LAP LAMBERT Academic Publishing.
- [18] Shirazy, A., *Behavior of Gold, Arsenic, and Antimony Elements: K-Means Method, Matlab, and SPSS-Software*. 2020: GRIN Verlag.
- [19] Shirazi, A. and A. Shirazy, *Introducing Geotourism Attractions in Toroud Village, Semnan Province, IRAN*. International Journal of Science and Engineering Applications, 2020. **9**(6): p. 79-86.
- [20] Jaiswal, R., S. Mukherjee, J. Krishnamurthy, and R. Saxena, *Role of remote sensing and GIS techniques for generation of groundwater prospect zones towards rural development--an approach*. International Journal of Remote Sensing, 2003. **24**(5): p. 993-1008.
- [21] Ye, Y., J. Shan, L. Bruzzone, and L. Shen, *Robust registration of multimodal remote sensing images based on structural similarity*. IEEE Transactions on Geoscience and Remote Sensing, 2017. **55**(5): p. 2941-2958.
- [22] Van Leeuwen, M. and M. Nieuwenhuis, *Retrieval of forest structural parameters using LiDAR remote sensing*. European Journal of Forest Research, 2010. **129**(4): p. 749-770.
- [23] Khan, S.D. and S. Jacobson, *Remote sensing and geochemistry for detecting hydrocarbon microseepages*. Geological Society of America Bulletin, 2008. **120**(1-2): p. 96-105.
- [24] Brekke, C. and A.H. Solberg, *Oil spill detection by satellite remote sensing*. Remote sensing of environment, 2005. **95**(1): p. 1-13.
- [25] Pour, A.B., M. Hashim, and M. Marghany, *Using spectral mapping techniques on short wave infrared bands of ASTER remote sensing data for alteration mineral mapping in SE Iran*. International journal of physical sciences, 2011. **6**(4): p. 917-929.
- [26] Kalashnikova, O.V. and R. Kahn, *Ability of multiangle remote sensing observations to identify and distinguish mineral dust types: 2. Sensitivity over dark water*. Journal of Geophysical Research: Atmospheres, 2006. **111**(D11).
- [27] Schowengerdt, R.A., *Remote sensing: models and methods for image processing*. 2006: Elsevier.
- [28] Shirazy, A., M. ZIAII, and A. HEZARKHANI, *Geochemical Behavior Investigation Based on K-means and Artificial Neural Network Prediction for Copper, in Kivi region, Ardabil province, IRAN*. 2020.
- [29] Shirazy, A., M. Ziaii, A. Hezarkhani, and T. Timkin, *Geostatistical and Remote Sensing Studies to Identify High Metallogenic Potential Regions in the Kivi Area of Iran*. Minerals, 2020. **10**(10): p. 869.
- [30] Ширازی, А., З. Мансур, А. Хезархани, Т.В. Тимкин, and В.Г. Ворошилов, *ИССЛЕДОВАНИЕ ГЕОХИМИЧЕСКОГО ПОВЕДЕНИЯ ТИТАНА И ЦИНКА НА ОСНОВЕ МЕТОДА К-СРЕДНИХ И ИСКУССТВЕННЫХ НЕЙРОННЫХ СЕТЕЙ ДЛЯ ПРОГНОЗИРОВАНИЯ НОВЫХ ПЛОЩАДЕЙ, РЕГИОН КИВИ, ИРАН*. Izvestiya Tomskogo Politekhnikeskogo Universiteta Inzining Georesursov, 2021. **332**(3): p. 113-125.
- [31] Ninomiya, Y. and B. Fu, *Thermal infrared multispectral remote sensing of lithology and mineralogy based on spectral properties of materials*. Ore Geology Reviews, 2019. **108**: p. 54-72.
- [32] Salisbury, J.W. and L.S. Walter, *Thermal infrared (2.5–13.5 μm) spectroscopic remote sensing of igneous rock types on particulate planetary surfaces*. Journal of Geophysical Research: Solid Earth, 1989. **94**(B7): p. 9192-9202.
- [33] Planke, S., H. Svensen, R. Myklebust, S. Bannister, B. Manton, and L. Lorenz, *Geophysics and remote sensing, in Physical geology of shallow magmatic systems*. 2015, Springer. p. 131-146.

- [34] Khan, S.D., K. Mahmood, and J.F. Casey, *Mapping of Muslim Bagh ophiolite complex (Pakistan) using new remote sensing, and field data*. Journal of Asian Earth Sciences, 2007. **30**(2): p. 333-343.
- [35] Legg, C., *Remote sensing and geographical information systems: geological mapping, mineral exploration and mining*. 1994.
- [36] Rencz, A.N. and R.A. Ryerson, *Manual of remote sensing, remote sensing for the earth sciences*. Vol. 3. 1999: John Wiley & Sons.
- [37] Van der Meer, F.D., H.M. Van der Werff, F.J. Van Ruitenbeek, C.A. Hecker, W.H. Bakker, M.F. Noomen, M. Van Der Meijde, E.J.M. Carranza, J.B. De Smeth, and T. Woldai, *Multi-and hyperspectral geologic remote sensing: A review*. International Journal of Applied Earth Observation and Geoinformation, 2012. **14**(1): p. 112-128.
- [38] Dubucq, D., L. Turon, B. Blanco, and H. Bideaud, *Earth observation remote sensing for oil and gas: A new era*. The Leading Edge, 2021. **40**(1): p. 26-34.
- [39] Serkan Öztan, N. and M. Lütü Süzen, *Mapping evaporate minerals by ASTER*. International Journal of Remote Sensing, 2011. **32**(6): p. 1651-1673.
- [40] Shirazy, A., A. Shirazi, S. Heidarlaki, and M. Ziiai, *Exploratory Remote Sensing Studies to Determine the Mineralization Zones around the Zarshuran Gold Mine*. International Journal of Science and Engineering Applications, 2018. **7**(9): p. 274-279.
- [41] Manuel, R., M.D.G. Brito, M. Chichorro, and C. Rosa, *Remote sensing for mineral exploration in central Portugal*. Minerals, 2017. **7**(10): p. 184.
- [42] Goetz, A.F., B.N. Rock, and L.C. Rowan, *Remote sensing for exploration; an overview*. Economic Geology, 1983. **78**(4): p. 573-590.
- [43] Calvin, W.M., E.F. Littlefield, and C. Kratt, *Remote sensing of geothermal-related minerals for resource exploration in Nevada*. Geothermics, 2015. **53**: p. 517-526.
- [44] Shirazi, A., A. Hezarkhani, A. Shirazy, and I. Shahrood, *Remote sensing studies for mapping of iron oxide regions, South of Kerman, Iran*. International Journal of Science and Engineering Applications, 2018. **7**(4): p. 45-51.
- [45] Safari, M., A. Maghsoudi, and A.B. Pour, *Application of Landsat-8 and ASTER satellite remote sensing data for porphyry copper exploration: a case study from Shahr-e-Babak, Kerman, south of Iran*. Geocarto international, 2018. **33**(11): p. 1186-1201.
- [46] Safari, M., A.B. Pour, A. Maghsoudi, and M. Hashim, *TARGETING HYDROTHERMAL ALTERATIONS UTILIZING LANDSAT-8 AND ASTER DATA IN SHAHR-E-BABAK, IRAN*. International Archives of the Photogrammetry, Remote Sensing & Spatial Information Sciences, 2017. **42**.
- [47] Bersi, M., H. Saibi, and M.C. Chabou, *Aerogravity and remote sensing observations of an iron deposit in Gara Djebilet, southwestern Algeria*. Journal of African Earth Sciences, 2016. **116**: p. 134-150.
- [48] Ahmadi, H. and H. Uygucgil, *Targeting iron prospective within the Kabul Block (SE Afghanistan) via hydrothermal alteration mapping using remote sensing techniques*. Arabian Journal of Geosciences, 2021. **14**(3): p. 1-22.
- [49] Agharezaei, M. and A. Hezarkhani, *Delineation of geochemical anomalies based on Cu by the boxplot as an exploratory data analysis (EDA) method and concentration-volume (CV) fractal modeling in Mesgaran mining area, Eastern Iran*. Open Journal of Geology, 2016. **6**(10): p. 1269-1278.
- [50] Ahmadi, H. and K. Kalkan, *Mapping of Ophiolitic Complex in Logar and Surrounding Areas (SE Afghanistan) With ASTER Data*. Journal of the Indian Society of Remote Sensing, 2021: p. 1-14.
- [51] Ahmadi, H. and A.B. Rahmani, *STUDY ON THE MINERAL ANOMALIES OF MUQUR-CHAMAN FAULT AND ITS COMPARISON WITH HARIRUD (HERAT) FAULT (AFGHANISTAN) USING GEOPHYSICAL AND REMOTE SENSING (ASTER-HyMap) DATA*. Геология и охрана недр, 2018(1): p. 28-38.
- [52] Shirazi, A., A. Shirazy, and J. Karami, *Remote Sensing to Identify Copper Alterations and Promising Regions, Sarbishe, South Khorasan, Iran*. International Journal of Geology and Earth Sciences, 2018. **4**(2): p. 36-52.
- [53] Mora, J., C. Armas-Herrera, J. Guerra, A. Rodríguez-Rodríguez, and C. Arbelo, *Factors affecting vegetation and soil recovery in the Mediterranean woodland of the Canary Islands (Spain)*. Journal of arid environments, 2012. **87**: p. 58-66.

# Teaching and Learning Arabic as a Second Language: A Case Study of Dubai

Mohamed Moghazy  
University of Illinois  
Urbana and Champaign  
USA

---

**Abstract:** Enrolment into Arabic as a second language (ASL) in Dubai has increased steadily due to the high influx of immigrant populations. Although Arabic is the primary language in Dubai mandatory taught in primary schools in Dubai, training and learning face challenges that affect learning a teaching objective. The extant investigation aimed to examine the teaching and learning of ASL in Dubai through exploring the importance of ASL, ALS programs in Dubai, ASL changes and solutions, and the role of technology infusion and motivation in ASL training and learning. The examination utilized a qualitative case study where seven teachers and eight learners were interviewed. The researcher analyzed the data using thematic analysis. The data obtained revealed that ASL is important among non-Arabic natives and immigrants since its improved communication and interaction. The main challenge noted included curriculum shortcomings, inadequate training and learning, poor technology utilization, and insufficient learning times. The findings suggested curriculum review, increase in the technology used in training and learning, and allocation of more time for ASL lessons to curb the challenges. The examinations discuss the policy, practice, and research implications of the findings. Although the findings are insightful in ASL training and learning in Dubai, the researcher recommended extensive research using different methodologies, sample sizes, and other cities in the UAE.

**Keywords:** Teaching and Learning Arabic; Challenges; ASL; Arabic in Dubai

---

## 1. INTRODUCTION

The Arabic language is increasingly receiving recognition in the international community as more countries realize its importance in international communication. The acceptance of Arabic as a working language by the UN set the path for implementing Arabic in educational discourses (UN, 2019). The UNESCO conference of 1948 that convened in Beirut, Lebanon, endorsed the Arabic language to facilitate UN summits convened in Asian or Arabic-speaking countries (UNESCO, 2019). The recognition of Arabic as a crucial communication language worthy of status that Chinese, Russian, and Spanish received in the UN in 1974 increased the adoption of Arabic in global meetings. The language was subsequently incorporated into the education acumen (UN, 2019). Since Arabic is spoken in Dubai, most schools have responded to the growing need for learning Arabic as a second language (ASL). Mercer and MacIntyre (2014) examined the second language acquisition process and constrained and noted that it faces numerous hurdles.

## 2. RESEARCH QUESTIONS

- i. What is the importance of teaching and learning ASL in Dubai?
- ii. What are the challenges facing the learning and instruction of ASL in Dubai?
- iii. What are the solutions to the challenges experienced in teaching and learning of ASL in Dubai?
- iv. What is the role of motivation and technology in training and learning ASL in Dubai?

## 3. LITERATURE REVIEW

### 3.1 Importance of learning and teaching Arabic as a second language

Although learning ASL is demanding and challenging, it crucial to learn when considering living or working in UAE (Salameh, 2018). According to Kataw (2016), learning ASL is crucial for communication with residents and literacy. Habbal (2017) conducted a qualitative investigation of Arabic discourses in a classroom setting and the benefits that accrue to learners and teachers. Other researchers found that the increased demand for the ASL had increased worldwide, particularly in countries that have close political and economic ties with the Arab countries (Habbal, 2017). Other researchers who concluded that learning and teaching Arabic were challenging include Moeller, and Catalano (2015), Alkutich (2017), and Kharkhurin (2015), who hypothesized that there were benefits that made learners and teachers partake in ASL.

Habbal (2017) examined classroom discourses between teachers and learners to comprehend the perceived benefits and importance of learning and teaching ASL. The researcher used the second language attainment framework and the Vygotsky model to assess the significance of learning ASL to learners and the motivations of teaching ASL among teachers (Habbal, 2017). The findings of the study depicted that learning and teaching of ASL were crucial because they fostered secure interaction among learners and teachers (Habbal, 2017). The analysis revealed that there were learner-specific reasons for learning ASL, such as working in an Arabic country and social interactions. The researcher examined the increasing demand for ASL or AFL and found that Arabic is central to Arab culture and religion. Besides, the increased expatriation drives the teaching and learning of ASL (Hussein & Gitsaki, 2018).

### 3.2 Role of technology in teaching and learning ASL

The changes in technology and its permeation in modern pedagogy led to the invention of technology that simplifies TAFL and learning ASL (Shehab & M Zeki, 2015). Alhumaid (2015) examined the perspectives regarding the infusion of technology in teaching and learning ASL in the UAE. The researcher investigated perspectives regarding the infusion, competence, and ease of learning and found that contemporary learners are accustomed to technology in learning foreign languages due to its ease of navigation, customization, and independence. Learners can search for vocabularies and get their meaning in Arabic instantly (Alhumaid, 2015). The qualitative investigation concluded that technology was inevitable in TAFL and TASL. Al Musawi et al. (2016) also conducted a similar study to be part of the 3-year project to support the development of software for teaching and learning ASL.

The investigators examined the application of technology in teaching Arabic and found that teachers used technology to introduce their lessons (Al Musawi et al., 2016). However, the teachers did not use technology to explain concepts or illustrations. A related investigation on an infusion of YouTube in teaching and learning the Arabic language found that technologies such as YouTube effectively teach Arabic (Albantani & Madkur, 2017). The researcher argued that contention on the use of technology in instructing foreign dialects should not be on the legitimacy or validity of using the technology or the bi-argument of using technology but on the infusion of technology in foreign language curriculums (Albantani & Madkur, 2017). According to the researcher's arguments of Albantani and Madkur (2017), the benefits of using technology outweigh the demerits.

However, the researchers had reservations about the little research on the demerits of infusion of technology in learning Arabic. Laabidi and Laabidi (2016) examined challenges faced in infusing ICT in TAFL and found a shortage of research studies that examined hurdles faced in the use of ICT in instructing and learning foreign languages. Omari (2015) also examined computer-aided techniques in instruction and learning of Arabic using a mixed design and found that the permeation of pedagogy compels teachers to assimilate technology in their instruction. The findings of the studies review are useful to this investigation. However, a salient drawback is the lack of examination of technology's challenges and implementation strategies in TASL.

### 3.3 Role of Motivation in Teaching and Acquisition of ASL

Please Mahdikhani (2016) examined motivation and its implication on the acquisition of foreign languages. According to Mahdikhani (2016), motivation is the driving force that propels learners to master new words. The examination of Anjomshoa and Sadighi (2015), Ordem (2017), and Zaman (2015) also found that motivating learners and teachers boost their morale to instructors learn the second language. Farhat and Benati (2018) examined the impacts of motivations on the acquisition of modern ASL. The researcher found that motivation creates an enabling environment for instructors and learners of ASL. However, the major drawback of the motivation arguments is that the approach advocates for comprehension of human behaviors and revives forces for actions using a single approach. Farhat and Benati (2018) explained that motivation is a complex concept and can be exhaustively examined under a single method or this

study. The findings of this study are useful to the current investigation since they illuminate the role of motivation in the acquisition of ASL. The present research will examine the concept in detail.

### 3.4 Challenges of Teaching Arabic as a Second Language

The review in the sections above showed that most studies had a shallow examination of the challenges faced in TAFL and TASL. First, cultural barriers affect the TAFL process due to cultural diversity among learners in Arabic as a second language. Elachachi (2015) examined the cultural barriers of Arabs affecting the learning of foreign languages among native Arabic speakers. Elachachi (2015) found that cultural differences affect learner interpretation, pronunciation, grammar, and comprehension. Additionally, Haron and Ahmed (2016) examined the challenges faced in learning Arabic and found that internal obstacles originated from the learner and external agents. The internal challenges were related to the knowledge of Arabic, where vocabulary was identified as the chief challenge. Poor grammar was also cited as the second challenge in teaching and instructing Arabic.

Interestingly, the discoveries also showed that learners who learn Arabic have a phobia for using the new words they learn when speaking. According to Haron and Ahmed (2016), learner tend to use Arabic acquired sparingly in fear of being judged or making mistakes when speaking. Haron and Ahmed (2016) explained that low vocabulary was limited to insufficient content. A similar study revealed two principal challenges in teaching and learning ASL or AFL (Yang & Chen, 2016). Cultural factors affect TAFL and TASL through affective learner perspectives of learners regarding the Arabic language and the link between language and Arab culture. Azaryad-Shechter (2018) also added that grammar was a prevalent challenge in foreign language teaching and erudition in Arabic and other foreign languages.

Unal and Ilhan (2017) assessed challenges facing in teaching and learning the Arabic language among nonnative and found that learning foreign or second languages have loopholes that allow the ad-hoc implementation of strategies that teacher service as effective. For instance, the infusion of ICT in overseas languages and second language teaching largely remains a contentious trend to be implemented by teachers and school administration. Therefore, curriculum shortcomings also challenge learning and teaching ASL. Al-Busaidi (2015) also found that diglossia and triglossia aspects of Arabic were barriers in learning standard Arabic as a secondary language. Al-Busaidi (2015) also examined program-related challenges and found that TAFL lacks clarity of objectives, coordination, qualified and experienced teachers, insufficient presentation of Arab culture, and insufficient teaching and learning resources.

### 3.5 Solutions to the Challenges facing the teaching of Arabic

As seen in the review, TAFL encounters numerous challenges that impact the curriculum delivery of ASL. Worryingly, numerous researchers examined the challenges faced in TAFL but ignored the solutions to the challenges of instructing and learning Arabic. A search on the internet revealed a worrying deficit in scientific inquiries into the solutions to challenges in teaching and learning ASL. Masood (2015) examines the challenges and solutions in teaching Arabic, focusing on interpretations and translation of Arabic. Although Masood

(2015) sought to examine the challenges and solutions, the researcher focused more on challenges than solutions.

Notably, there were no clear solutions enumerated for the challenges faced in teaching and learning ASL. Alipicheva, Khalevinab, Trubcheninovac, and Fedulova (2017) also examined practical solutions to challenges that face TAFT and other foreign languages. The researchers suggested that online and distance learning tools solve the major challenges to the teaching of ASL through instant translation, availability, and customization of the technology (Alipicheva, Khalevinab, Trubcheninovac & Fedulova, 2017). The high interactivity of the tools also increases learning outcomes and makes the learning of a foreign language interesting. The current research studies will explore the solutions to the challenges.

#### **4. THEORETICAL REVIEW: THEORIES OF SECOND LANGUAGE ACQUISITIONS**

First, the mother tongue transfer theory illuminates the concept of second language acquisition and holds that second language is transferred through interactions with vernacular. According to the mother tongue theory, learners use their vernacular knowledge to acquire an additional language. The theory supports the use of mother tongue translation in the classroom to translate the second language vocabulary to vernacular for easier comprehension. Although the theory is effective in learning the second language, it has been criticized for its detrimental effect on the learning progress of learners in acquiring a new language. For instance, Zhao (2019), Wang (2015), and Wang and Xiang (2016) discredited the use of vernacular in teaching and learning foreign languages due to the numerous disadvantages it has, such as delayed achievement of learning outcomes.

Secondly, the cultural introject theory argues that a second language is gained from social-cultural practices. Schumann (1978) proposed the theory, which argued that cultural introjects influence the acquisition of an additional language (Beliles, 2015). The ease of acquiring an additional language depends on the ability of the learner to adapt to new cultures. According to Schumann (1978), second language acquisition was determinant of the distinction between the target language and the cultural language of the learner (Beliles, 2015). Other factors, such as culture, awareness, and tolerance, were evinced to influence the additional language attainment process. The cultural introjection theory proposed that second language acquisition depends on their ability of the learner to acquire the culture of the target language. The theory proposed that learning the target culture promoted learning of the language since language is part of the culture. Understanding cultural aspects enables faster comprehension of second language.

Lastly, Krashen's second-language acquisition theory explained that second learning is based on five hypotheses: learning, affective filter, input, natural order, and monitor (Sun, 2017). The learning proposition explains that learning of the second language happens subconsciously without teachers, like acquiring the first language in children (Ma & Chen, 2017). According to the Krashen theory, acquisition affects learning. It continues to monitor the hypothesis where the acquired knowledge starts speaking of acquired words while the learning system monitors the use of the acquired language. The input aspect is concerned with the acquisition process (Liu, 2017). The natural order hypothesis holds that attaining additional dialect follows a foreseeable normal order in which learners can learn consciously or subconsciously.

According to the affective filter of Krashen theory, numerous affection variable impacts second language acquisition (Sun, 2017).

#### **Key Research Gaps**

The review in this section revealed several research gaps that require extensive research to illuminate learning and teaching ASL. For instance, some studies explored challenges face in teaching and learning ASL, more research work is required on the challenges. There is a gap in solutions to the challenges facing teaching and learning ASL since the literature review and scrutiny of databased yield two suitable studies only. Besides, the studies fell short of the expectation in addressing the solutions to the challenges facing learning and instruction of ASL. The extant investigation seeks to bridge the informational gap by examining the challenges and solutions of TAFL and TASL.

### **5. METHODOLOGY**

#### **5.1 Research method and its justification**

Quinlan, Babin, Carr, and Griffin (2019) noted that differing arguments and definitions characterize research methods discourses. In some cases, researchers such as Bell, Bryman, and Harley (2018) refer to designs such as qualitative, quantitative, or mixed methods. Some researchers, such as Drake, Rancilio, and Stafford (2017), discuss methods as the instruments used to gather data. In this context, the research methods refer to the tools used to glean data from the participants. Notably, the researcher used interviews to glean data from respondents. Rosenthal (2016) and Alshenqeti (2014) explained that interviews are suitable for qualitative methods since they explore experiences and allow extensive examination of the subject under scrutiny. Therefore, interviews were justified because the investigator aimed to glean data on teachers' and learners' experiences and perceptions of teaching and learning ASL.

#### **5.2 Study Location and Population**

The researcher examined the teaching and learning of ASL in Dubai. The study of teaching and learning of ASL was suitable in Dubai because Dubai is a growing multicultural and multilinguistic cosmopolitan city with an increasing demand for ASL among immigrants and locals who speak colloquial Arabic. Thomure (2019) examined the Arabic language systems in Dubai and the larger UAE and found that the demand for Arabic was increased among immigrants and locals who speak other languages. Therefore, the blend of the learners in Dubai city provided a suitable location and population for examining teaching and learning ASL practices. The study population comprised the teachers and learners taking ASL or AFL.

According to Achkhanian (2016), the increasing influx of immigrants in the UAE has increased enrollment in Arabic learning centers. For instance, in 2016, the average enrolment for ASL in the Arabic learning center located in Dubai World Trade Centre was slightly over 1000 students, with the majority being between 20-45 years. The demand for modern standard Arabic (MSA) is rising because Arabic is the primary language in schools. For instance, in 2015, 38% of the total enrolment were Emiratis (Pennington, 2015). Clarke

(2016) also revealed that in 2016, the immigrant population in the UAE was over 90%. The population in Dubai has increased rapidly in the last three years, considering the increasing immigration to Dubai. Therefore, the population for this study is vast and impractical to glean data from all the population members, thus necessitating sampling. The sampling procedures and sample size obtained is described in the subsection below.

### 5.3 Study Location and Population

The number of learners taking ASL is many; thus, it is impractical to investigate all due to resources constraint. Taherdoost (2016) explained six steps for choosing a sampling method for qualitative methods. According to Taherdoost (2016), the procedure for sampling begins with a definition of the population and selecting the sampling frame to ensure that the sample obtained will be a reliable representative of the entire population. The researcher then chooses the sampling technique, a sample size, collects data, and then assesses the response rate. However, Palinkas et al. (2015) asserted that researchers should first assess the response rate before deciding the sample size. Notably, the researcher chose a qualitative sampling method since the study was qualitative. The investigator combined purposeful and convenience sampling. The convenience sampling was appropriate since it enabled the investigator to choose reachable participants due to resource constraints. Additionally, the purposeful sampling was appropriate as it allowed the investigator to choose participants that would provide useful information regarding the study. Benoot, Hannes, and Bilsen (2016) explained that although the purpose and convenience sampling are different, they are complementary in choosing a reliable and enough sample size. The investigator chose a sample of 15 interviewees, where 8 were learners taking ASL, and 7 were teachers of ASL.

### 5.4 Data Collection and Recording Procedures

The investigator used interviews to glean data. The interviewing procedure was as follows. The researcher approached the potential respondents and established a rapport. The investigator explained the intentions to interview the respondents regarding the teaching and learning of ASL in Dubai. The investigator requested the respondents for time to explain more about the study. The researcher gave the potential interviewer a consent form explaining all aspects of the study, such as confidentiality, privacy, potential harm, intention to withdraw, and other aspects of the study. The process of getting informed consent from the responses explains all risks, benefits, or implications that may befall the interviewees upon participation be divulged to the interviewees (Manti & Licari, 2018). Once the respondents participate orally or through writing, the interview took place conveniently for the participants. The interview discussions were recorded using an aural phone recorder and later transliterated for further scrutiny.

### 5.5 Data Analysis Methods

The investigator used a thematic approach to analyze data. First, the researcher coded the data gleaned to ensure that patterns and themes were formulated. The researcher used an open coding technique to identify close relationships and patterns in the data. The preliminary codes also identified crucial information. The preliminary codes later formulated final codes that constituted the study themes. The researcher used the final codes to come up with a theme under which the data was discussed. Elliott (2018) explained that the thematic approach relies on coding for data analysis and discussion. The investigator discussed the teaching and learning of ASL in Dubai under the themes formulated through open coding.

### 5.6 Data Reliability and Validity

Validity aspects examine the extent of the study in examining the subject intended to be examined (Noble & Smith, 2015). Dikko (2016) also added that reliability is critical since it is the basis upon which the findings are assessed for application in other contexts. The validity discussed, in this case, is the validity of the interviews in examining the teaching and learning ASL in Dubai. Leung (2015) examined the reliability, generalizability, and validity in qualitative research and asserted that they are the fundamental basis of research. Findings must be reliable, valid, and generalizable. First, the investigator tested the interview questions to ensure that they were reliable in examining the subject. The researcher avoided ambiguity in questions. The researcher also ensured that the university research committee authorized the interview process, and the respondents consented to the interview to ensure that the research findings were authentic and rational.

## 6. DATA PRESENTATION, ANALYSIS, AND DISCUSSION

### 6.1 Introduction to Data Presentation and Analysis

Notably, the investigator first prepared data through validation, checking for completeness, then coded the data. Coding was essential in theme formulation under which the data would be presented, analyzed, and discussed. The analysis and discussion in this chapter utilized a thematic approach, as earlier noted and explained in the preceding chapter. The themes formulated through open coding as detailed in chapter three are: a program of teaching Arabic in Dubai, challenges facing teaching and learning of ASL in Dubai, solutions to the challenges, the role of technology, role of motivation, and perceptions regarding the current programs for training and learning of ASL in Dubai. Although the researcher targeted 15 interviews comprising a blend of Arabic trainers and scholars, the investigator invited 17 potential interviewees. The response rate was 15 because two declined the invitation citing lack of time due to their busy work schedules. Nonetheless, the response rate met the researchers' target sample. The researcher used alphabets to code the identity of interviewees from A to O. The interview

had seven questions, one on biographic information and six scrutinizing the subject matter of this investigation.

## 6.2 Data Presentation and Data Analysis

The research asked interviewees to identify whether they were teachers or learners since their responses would be impacted by being teachers or learners. For instance, the challenges faced by the two categories of respondents are different. There were eight scholars and seven teachers.

### 6.2.1 Learning programs of ASL in Dubai and their importance

First, the researcher enquired about the learning programs of Arabic in Dubai. The data gleaned showed that there were numerous learning programs for ASL, but there was autonomy to the institutions to customize the programs to meet the diverse demand of their customers. The Arabic language is implemented based on the specific institution requirements and standards guided by the government policies on foreign language teaching. Respondent J explained that the current education system had emphasized English as a foreign language and less of AFL. Respondent D also added that “most of the programs support Arabic as a primary language, not as a secondary language.” Respondents H, C, and E explained that currently, there are bilingual programs where English, and Arabic are used as the main languages of communication.

Further, respondent N added that every institute has its outline guided by the curriculum for delivering modern standard Arabic, but the interpretation is left to the instructor’s interpretation. Notably, respondent A, B, C, D, E, F, G, H, I, J, K, L, M, N, O had similar explanations that there are numerous challenges as noted in their use of words like “many”, “various”, “numerous” and “a lot” to describe the programs of ASL in Dubai. For instance, respondent F said: “Well, there are various programs based on learner’s specific needs. For instance, there are programs for the beginner and or professionals who want to master the language. Also, we have online courses for those who want to do self-study.”

The respondents also explicated that Arabic teachers are subjected to rigorous training to attain a diploma in teaching Arabic. The testing and teaching are guided by government education policies and standards, as outlined by KHDA. Respondent N said that “there are a variety of programs all which KHDA must approve.” Most Arabic teaching job requirements stipulated that prospecting ASL teachers must have a bachelor’s degree in ASL specialization or at least a diploma in teaching the Arabic language. Arabic is mandatory in the UAE learning system. Most of the existing programs on learning and teaching Arabic focus on Arabic as the primary language and less on ASL. The investigator also asked about the importance of teaching and learning ASL in Dubai.

Respondents G, I, E, A, J, D, F, C, L, and K explained that gaining literacy of ASL facilitated communication with the locals since Arabic is a primary language in Dubai. 60% of

the respondents (B, D, E, G, I, J, L, N, O) said that the literacy of Arabic supported their business communication and interactions with customers. Notably, one participant said that learning Arabic diversified the language portfolio since they liked learning new languages. Teachers explained that it is important to teach Arabic since it shares the rich culture and heritage of the UAE. Besides providing them with job opportunities, some teachers explained that it promotes Islamic religion among learning since Arabic is the language of the Holy Quran. For instance, participant C said:

“It is important since most Dubai locals use Arabic as their only primary language. Thus, knowledge of the language ensures that the language barrier is broken, especially for foreigners. We also believe Arabic is the holy language of the Quran; hence, learning it helps one have a deeper understanding of our religion.”

The data presented and discussed above illuminated the importance of teaching and learning ASL in Dubai and the programs available to learners prospecting to enroll in ASL. The findings above achieved the first objective research question on the importance and programs of ASL in Dubai. The data presented in the current and subsequent questions represented the responses of 15 interviewees subjected to seven scrutiny questions. All the interviewees answered all research questions, thereby promoting an in-depth comprehension of the aspects under investigation.

### 6.2.2 Role of technology in learning and training of ASL in Dubai

All the interviewees explained that technology infusion in the instruction of ASL was a prime milestone in the teaching of foreign languages in Dubai. The interviewees explained that technology promoted translation and learning after classes. One can search for the meaning of Arabic words, translate Arabic to other languages, and vice versa. Besides, interviewee A, B, C, D, E, F, G, H, I, J, K, L, M, N, O explained that technology-supported online learning programs such as live training via skype, online learning Moodle’s, online management classes, and submission of assignments. Respondent M asserted that technology “has made life easier for teachers and us through the translation tools.” Respondent A, B, C, D, E, F, G, H, I, J, K, L, M, N, O had positive perceptions regarding the infusion of technology in learning ASL. A teacher (respondent B) said that technology eased their work since they could manage classes online, exchange learning materials with scholars over the internet. The perception of technology is evident in the assertion:

“Technology has made learning Arabic very easy, especially for foreigners, especially translation tools. Particularly, an online program can translate any major language into Arabic. In my case, as a teacher, I utilize the internet by sending learning materials and doing online Arabic language webinars.”

Another teacher, respondent E, illustrated that technology had improved performance because learners can research material

over the internet. The findings presented in this section answer achieves objective five by providing enriched responses to question five on the role of technology in teaching ASL in Dubai. The findings meet the objective above because they fostered the comprehension of technology and motivation in teaching and learning in Dubai. The findings explained the impacts of technology on teaching and learning ASL in Dubai.

### 6.2.3 Role of motivation in learning and instruction of ASL in Dubai

The respondents elucidated that learning ASL is a challenging task and requires scholars to strive hard. Regarding this, respondent J asserted that “learning Arabic is difficult, particularly grammar and vocabulary, which requires one to be in the right mind to embrace the challenge.” The respondent further explained that attitude and motivation towards Arabic learning was the fundamental aspect of learning ASL. Respondent M added that “motivation is crucial in learning as it enables scholars to strive to be proficient in Arabic.” Further respondent C asserted that:

“I think learners are motivated to Arabic because of its association with the religion while foreigners are motivated by the feeling of belonging that comes with the ability to communicate with the locals in their native language. Still, some learners are interested in business communications to ensure that they can communicate with their customers and suppliers.”

Further, respondent O asserted that the “motivation concept is the most fundamental aspect utilized in illuminating the success of learning and teaching as an overseas or second language.” The respondent went further to illustrate the intrinsic and extrinsic motivation aspect of learning Arabic in the assertion that “learning of Arabic can be motivated by the desire for self-fulfillment and actualization.” In this sense, respondent O asserted that “learning Arabic is motivated by the joy that accrues after gaining proficiency in ASL.” Additionally, respondent F explained that extrinsic motivation was essential in learning Arabic and emanated from external factors such as the need for reward, recognition, and fear of punishment, among others.

### 6.2.4 Challenges facing training and learning of ASL in Dubai

The researcher inquired about the challenges that instructors and learners face when learning or training ASL in Dubai. The trainers and learners pointed out numerous challenges. Teachers expressed that behavior management was a significant challenge since most learners, especially in lower and upper primary schools, required constant monitoring and managing behavior during and after classes. For instance, respondent D said that “learners in primary school are very playful, thus making it hard to control a class with a big number” Other challenges identified were assessment, teaching, and performance evaluation. Limited input time and impractical expectations from learners lead to teachers’

frustrations when objectives are unmet regarding this. Respondent G, a teacher, explained that.

“learning Arabic for nonnative requires patience and extensive input in teaching since young learners do not understand Arabic faster. Therefore, expecting learners to understand and be proficient in Arabic in a few lessons is impractical. Teachers end up frustrated when the learning objectives are unmet.”

The respondents also listed insufficient teaching aids, resources, and technology infusion in Arabic as limiting factors. This is evident in the respondent’s D assertion that”

“Unlike other major languages like English, French and Spanish, which has many print materials to help teachers and instructors, Arabic falls short of resources to make the learning of the language effective and interesting. Also, time dedicated to young learners in the classroom is hard enough.”

Similarly, respondent A explained that the current curriculum is a challenge because of its lack of focus on ASL since it focused on Arabic as a primary language. Inadequate professional development of Arabic teachers was outlined as a prime challenge. Learners also reported that transition from primary to secondary and finally to tertiary institutions was challenging because each level came with increased demands on ASL. Colloquialism and mother tongue affected the learning of MSA. Participant K said that learning grammar and vocabulary was also challenging. Insufficient e-learning facilities in Arabic were a challenge; thus, students had to rely on personal technologies to learn MSA. The data provided and analyzed in this subsection illuminated the challenges facing instruction and learning of ASL in Dubai. The interviewees obtained rich data on the difficulties from fifteen respondents. The data presented in this section answered the second research question. The findings in this section achieved objective two.

### 6.2.5 Solutions to the challenges

The investigator asked the respondents about the solutions they could suggest for improving the instruction and teaching of ASL in Dubai. Respondent A, B, C, D, E, F, G, H, I, J, K, L, M, N, O suggested the infusion of technology in Arabic teaching. All the teachers also explained that the current curriculum requires evaluation and revision to offer a comprehensive guide to ASL and AFL teaching, assessment, methodology, and learning. A teacher, respondent B, also suggested improving infrastructure in public schools to match the standard in private schools. Respondent B illustrated the above assertion in the statement that:

“There is a huge disparity in resource and infrastructure of training and learning ASL and AFL between public schools and private schools. Most private schools have the needed infrastructure and resources such as books, technology, enough teachers, and supportive administration compared to public schools”.

Additionally, respondent I suggested that classrooms should have “inspiration boards where a learner can practice their Arabic writing skills on the board.” Respondent J, a teacher, suggested improving progress tracking systems for the achievement of learning outcomes. Another teacher (respondent A) recommended using ‘Boomerang’ or an independent model where scholars are empowered to create practical solutions to their problems and homework instead of relying on friends and parents to help with the assignments. The findings presented above answer question three, thus achieving objective three to challenge facing learning and instruction—besides, the data respondent to all research questions and objectives.

## 7. DISCUSSION OF FINDINGS

The data gleaned revealed the myriad programs available in ASL and AFL pedagogy in Dubai. Dubai has a diverse population comprising tourists, expatriates, scholars, and natives, among others. Different population segments of learners have different language needs. For instance, a tourist or a foreign investor's language needs are different from a learner intending to become an Arabic teacher. Therefore, the wide variety of programs is essential for addressing the needs of all ASL or AFT. Besides, customization is necessary to ensure that programs meet the specific needs of different categories of learners. For instance, a tourist visiting Dubai for three months will not enroll in a one-year program. Instead, they will enroll in shorter vacation programs. The data showed that the high number of programs had a chief implication on policies.

The data depicted a need for a policy review to capture the emerging trends and the growing number of ASL and AFT programs in Dubai. The study was championed to ensure learners got high-quality ASL education. The finding of Thomure (2019), Lewicka and Waszau (2017), Ahmad (2018), and the Mother Tongue Center (2019) reviewed in the literature section two supports the findings of this study on the variety of ALS programs in Dubai. Besides, the results on perceptions of training and learning ASL showed that the variety of ASL and AFL programs was preferred to a universal program since it met the needs of a diversified learning population in Dubai. The positive perspectives towards technology and motivation showed that instructors and learners comprehend the essence of technology in curriculum delivery and achievement of learning outcomes in contemporary language pedagogy. The results above concur with findings researchers reviewed in literature such as Alish (2016), Al Musawi et al. (2016), Abdalla (2015a), Ismail and Ibrahim (2018), Abedalla (2015b), Al Suwaiyan (2018), and Carroll et al. (2017). Therefore, the literature sources reviewed above supported the findings of this study.

Contrary to the perceptions and conclusion of Bani-Khaled (2014) that Arabic would fade away, the results counterargued that Arabic was growing due to the increasing demand for ASL and ASL. The results obtained in this study also supported the infusion of technology. Technology has become a necessity in modern pedagogy. Technology positively

impacts ASL and AFL since it makes learning more accessible, convenient, and automated. Respondents that used technology in learning Arabic supported the adoption of technology due to the myriad benefits that accrued to learners and teachers following its adoption. Some findings of the literature sources reviewed concurred with the results of this study. For instance, learners elucidated that they check the meaning of words and phrases or translate sentences instantly, as Alhumaid (2015), Albantani and Madkur (2017), and Omari (2015) found in their studies reviewed in the literature review.

However, some respondents noted a need for policy development on the infusion of technology in learning and training ASL and AFL. In line with Laabidi and Laabidi (2016) discoveries, the findings portrayed that more policies on the technology implementation, online learning Arabic and CATL of Arabic are required but recommended extensive research first. Results also revealed that teachers experience more challenges than learners. Most of the challenges facing teaching ASL were emanated from external factors such as curriculum, policies, infrastructure, technology infusion, and learners' attitudes. For instance, the lessons set for Arabic lessons were not enough for learners to gain proficiency. The results disclosed that the learners' challenges were internal.

The impacts of vernacular were identified as a prime challenge to learning and training MSA: cultural variations and the use of vernacular affected the learning of MSA, such as accents and pronunciation. The above findings were supported by the results of Al-Busaidi (2015), Unal and Ilhan (2017), Elachachi (2015), and Haron and Ahmed (2016) reviewed in the literature section. A review of curriculum, policies, and implementation of ASL and AFT syllabus was suggested as participants argued that they impact the delivery, testing, and performance management of ASL. Additionally, incorporating technology in the ASL curriculum was essential in modern globalized learning of foreign languages. The results presented, analyzed, and discussed above led to the discoveries summarized below.

## 8. LIST OF ABBREVIATED TERMS

AFL-Arabic as a foreign language

ASL-Arabic as a second language

CATL- Computer-Aided Techniques of Learning

CMALT- Committee for Modernization of Arabic Language Teaching

EFL- English as a Foreign Language

KHDA- Knowledge and Human Development Authority

T AFL-Teaching Arabic as a Foreign Language

TASL-Teaching Arabic as a Second Language

Definitions of key terminologies

Diglossia- denotes the usage of two dialects of a language, also referred to as bilingualism. (Bracker, 2018). For instance, the Arabic language has several dialects that

affect the learning and teaching of ASL to locals and foreigners.

Multilingualism- Multilingualism in this investigation is applied in the context of using multiple languages in the education system (Yoon, 2016)..

## 9. REFERENCES

- [1] Abedalla, R. (2015a). The Use of Mobile Assisted Language Learning Applications in Learning Arabic. *Issues in Information Systems*, 16(2), 63-73. Retrieved from [http://www.iaicis.org/iis/2015/2\\_iis\\_2015\\_63-73.pdf](http://www.iaicis.org/iis/2015/2_iis_2015_63-73.pdf).
- [2] Abedalla, R. (2015b). *Students' perceptions of the use of mobile applications technology in learning Arabic as a second language* (Ph.D.). Robert Morris University.
- [3] Achkhanian, M. (2016). Rise in the number of expats learning the Arabic language Despite the false notion that learning Arabic is difficult, more people seem to be taking the plunge. *Gulf News*. Retrieved from <https://gulfnews.com/going-out/society/rise-in-number-of-expats-learning-the-arabic-language-1.1672641>.
- [4] Ahmad, A. (2018). *The impact of the KHDA policy on teaching Arabic as a first language: An exploratory study among selected schools in Dubai* (masters). British University, Dubai.
- [5] Al Musawi, A., Al Hashmi, A., Kazem, A., Al Busaidi, F., & Al Khaifi, S. (2016). Perceptions of Arabic language teachers toward their use of technology at the Omani basic education schools. *Education and Information Technologies*, 21(1), 5-18. doi: 10.1007/s10639-013-9305-5
- [6] Al Suwaiyan, L. (2018). Diglossia in the Arabic language. *International Journal of Language & Linguistics*, 5(3). doi: 10.30845/ijll.v5n3p22
- [7] Albantani, A., & Madkur, A. (2017). Musyahadat Al Fidyu: You Tube-based teaching and learning of Arabic as foreign language (AFL). *Dinamika Ilmu*, 17(2). doi: 10.21093/di.v17i2.854
- [8] Al-Busaidi, F. (2015). Arabic in Foreign Language Programmes: Difficulties and Challenges. *Journal of Educational and Psychological Studies [JEPS]*, 9(4), 701. doi: 10.24200/jeps.vol9iss4pp701-717
- [9] Alhumaid, K. (2015). *Perspectives and usage of technology of Arabic language teachers in The United Arab Emirates* (Ph.D.). The University of Kansas.
- [10] Alipicheva, A., Khalevinab, S., Trubcheninovac, A., & Fedulova, A. (2017). Practical solutions to foreign language training courses implemented using distance learning tools. *International Electronic Journal of Mathematics Education*, 12(1), 59-68. Retrieved from <https://www.iejme.com/download/practical-solutions-to-foreign-language-training-courses-implemented-using-distance-learning-tools.pdf>.
- [11] Alkutich, M. (2017). Curriculum delivery constraints of Arabic language as a foreign language in the UAE. *International Journal of Science and Engineering Applications*, 6(9), 241-247. doi: 10.7753/ijsea0609.1001
- [12] Alosch, M. (2016). Review of the book teaching and learning of Arabic as a foreign language: A guide for teachers, by Karin C Ryding. *Al-'arabiyya: Journal of The American Association of Teachers of Arabic*, 49(1), 139-142. Retrieved from <https://www.muse.jhu.edu/article/637817>.
- [13] Alshenqeeti, H. (2014). Interviewing as a data collection method: A critical review. *English Linguistics Research*, 3(1). doi: 10.5430/elr.v3n1p39
- [14] Anjomshoa, L., & Sadighi, F. (2015). The importance of motivation in second language acquisition department of foreign. *International Journal on Studies in English Language and Literature*, 3(2), 126-137. Retrieved from <https://pdfs.semanticscholar.org/b8c3/de1c37f994d830dc3b3ffaeda59742f6daf.pdf>.
- [15] Azaryad-Shechter, D. (2018). Overcoming the grammar barrier in foreign language learning: The role of television series. *Journal of Language and Education*, 4(2), 92-104. doi: 10.17323/2411-7390-2018-4-2-92-104
- [16] Bani-Khaled, T. (2014). Attitudes towards standard Arabic: A case study of Jordanian undergraduate students of English. *International Journal of Linguistics*, 6(4), 154. doi: 10.5296/ijl.v6i4.5959
- [17] Beliles, E. (2015). *The effect of attitude toward the target language and culture, and of input on English second language proficiency in a study-abroad immersion setting* (Masters). The University of Stellenbosch.
- [18] Bell, E., Bryman, A., & Harley, B. (2018). *Business research methods*. Oxford university press.
- [19] Benoot, C., Hannes, K., & Bilsen, J. (2016). The use of purposeful sampling in a qualitative evidence synthesis: A worked example on sexual adjustment to a cancer trajectory. *BMC Medical Research Methodology*, 16(1). doi: 10.1186/s12874-016-0114-6
- [20] Berryman, D. R. (2019). Ontology, Epistemology, Methodology, and Methods: Information for Librarian Researchers. *Medical Reference Services Quarterly*, 38(3), 271-279.
- [21] Bracker, P. (2018). Linguistic Fields: Multilingualism, Sociolinguistics. *Multilingual*, 37(6), 727-729. doi: 10.1515/multi-2017-0076
- [22] Carroll, K., Al Kahwaji, B., & Litz, D. (2017). Triglossia and promoting Arabic literacy in the United Arab Emirates. *Language, Culture, and Curriculum*, 30(3), 317-332. doi: 10.1080/07908318.2017.1326496
- [23] Clarke, K. (2016). Arabic in UAE schools — the needs and the challenges. *Khaleej Times*. Retrieved from <https://www.khaleejtimes.com/nation/education/should-arabic-become-a-compulsory-language-in-uae-schools>.
- [24] Dikko, M. (2016). Establishing construct validity and reliability: Pilot testing of a qualitative interview for research in Takaful (Islamic insurance). *The Qualitative Report*, 21(3), 521-528.
- [25] Drake, B. F., Rancilio, D. M., & Stafford, J. D. (2017). Research methods. In *Public Health Research Methods for Partnerships and Practice* (pp. 174-187). London: Routledge.
- [26] Elachachi, H. (2015). Exploring cultural barriers in EFL Arab learners' writing. *Procedia - Social and Behavioral Sciences*, 199, 129-136. doi: 10.1016/j.sbspro.2015.07.496

- [27] Elliott, V. (2018). Thinking about the coding process in qualitative data analysis. *The Qualitative Report*, 23(11), 2-14. Retrieved from <https://nsuworks.nova.edu/cgi/viewcontent.cgi?article=3560&context=tqr>.
- [28] Farhat, A., & Benati, A. (2018). The effects of motivation on processing instruction in the acquisition of Modern Standard Arabic gender agreement. *Instructed Second Language Acquisition*, 2(1), 61-82. doi: 10.1558/isla.34879
- [29] Faryadi, Q. (2007). *Techniques of teaching Arabic as a foreign language through constructivist paradigm: Malaysian perspective* (Ph.D.). UiTM Malaysia.
- [30] Habbal, M. (2017). *Classroom discourse in an Arabic foreign language classroom and the perceived benefits of interactions among learners: A case study of college-level Heritage Language Learners (HLLs) and Foreign Language Learners (FLLs)* (Ph.D.). Ohio State University.
- [31] Hanson, S. (2017). Putting the epistemology back: Writing against ontology in HE philosophy. *Journal for Critical Education Policy Studies*, 15(1), 1740-2743.
- [32] Haron, S., & Ahmed, I. (2016). Challenges in learning to speak Arabic. *Journal of Education and Practice*, 7(24), 80-85. Retrieved from <https://files.eric.ed.gov/fulltext/EJ1112863.pdf>.
- [33] Hussein, M., & Gitsaki, C. (2018). 6 Foreign language learning policy in the United Arab Emirates: Local and global agents of change. *UN (Intended) Language Planning in A Globalizing World: Multiple Levels of Players at Work*, 97-112. doi: 10.1515/9783110518269-006
- [34] Hyland, K. (2016). Methods and methodologies in second language writing research. *System*, 59, 116-125.
- [35] Ismail, R., & Ibrahim, R. (2018). Teachers' perception of digital game: A preliminary investigation towards educational game application for islamic religious primary schools. *2018 International Conference on Information and Communication Technology for The Muslim World (ICT4M)*. doi: 10.1109/ict4m.2018.00016
- [36] Kataw, Y. (2016). *Teaching Arabic as a foreign language: The role of communicative competence, pragmatics, and literacy* (Masters). Utah State University.
- [37] Kharkhurin, A. (2015). Introducing bilingual creative education to the UAE school curriculum. *Mental Health and Psychological Practice in the United Arab Emirates*, 199-209. doi: 10.1057/9781137558237\_18
- [38] Laabidi, Y., & Laabidi, H. (2016). Barriers affecting successful integration of ICT in Moroccan universities. *Journal of English Language Teaching and Linguistics*, 1(3). doi: 10.21462/jeltl.v1i3.29
- [39] Leung, L. (2015). Validity, reliability, and generalizability in qualitative research. *Journal of Family Medicine and Primary Care*, 4(3), 324. doi: 10.4103/2249-4863.161306
- [40] Lewicka, M., & Waszau, A. (2017). Analysis of textbooks for teaching Arabic as a foreign language in terms of the cultural curriculum. *Universal Journal of Educational Research*, 5(1), 36-44. doi: 10.13189/ujer.2017.050105
- [41] Liu, L. (2017). The application and enlightenment of second language acquisition theory in English teaching. *Proceedings of the 7Th International Conference on Education, Management, Information, and Mechanical Engineering (EMIM 2017)*. doi: 10.2991/emim-17.2017.251
- [42] Ma, F., & Chen, J. (2017). Second language acquisition theory-based bilingual teaching methods of computer science. *Proceedings Of 4Th International Conference on Education, Language, Art, and Intercultural Communication (ICELAIC 2017)*. doi: 10.2991/icelaic-17.2017.24
- [43] Mahdikhani, Z. (2016). An overview of motivation: The challenges and the importance of motivation for second language acquisition. *Journal for the Study of English Linguistics*, 4(1), 53. doi: 10.5296/jsel.v4i1.9407
- [44] Manti, S., & Licari, A. (2018). How to obtain informed consent for research. *Breathe*, 14(2), 145-152. doi: 10.1183/20734735.001918
- [45] Masood, M. (2015). *Arabic in Pakistan problems and solutions in the field of teaching and testing* (Masters). Universität Leipzig.
- [46] Mercer, S., & MacIntyre, P. (2014). Introducing positive psychology to SLA. *Studies in Second Language Learning and Teaching*, 2(1), 153-172. doi: 10.14746/ssllt.2014.4.2.2
- [47] Moeller, A., & Catalano, T. (2015). Foreign language instruction and learning. *International Encyclopedia of The Social & Behavioral Sciences*, 327-332. doi: 10.1016/b978-0-08-097086-8.92082-8
- [48] Omari, S. (2015). The effect of computer-assisted language learning on improving Arabic as a foreign language (AFL) in higher education in the United States. *Procedia - Social and Behavioral Sciences*, 192, 621-628. doi: 10.1016/j.sbspro.2015.06.109
- [49] Omary, F., & Qudah, M. (2015). The curriculum and its effect on teaching a second language: Arabic for non-speakers as an example. *Arabic Language and Literature*, 19(2), 41-64. doi: 10.18630/kaall.2015.19.2.003
- [50] Ordem, E. (2017). A longitudinal study of motivation in foreign and second language learning context. *Journal of Education and Learning*, 6(2), 334. doi: 10.5539/jel.v6n2p334
- [51] Palinkas, L., Horwitz, S., Green, C., Wisdom, J., Duan, N., & Hoagwood, K. (2015). Purposeful sampling for qualitative data collection and analysis in mixed method implementation research. *Administration and Policy in Mental Health and Mental Health Services Research*, 42(5), 533-544. doi: 10.1007/s10488-013-0528-y
- [52] Pennington, R. (2015). Special report: Arabic 'at risk of becoming a foreign language in UAE'. *Abu Dhabi*. Retrieved from <https://www.thenational.ae/uae/education/special-report-arabic-at-risk-of-becoming-foreign-language-in-uae-1.21382>.

- [53] Quinlan, C., Babin, B., Carr, J., & Griffin, M. (2019). *Business research methods*. South-Western Cengage.
- [54] Rosenthal, M. (2016). Qualitative research methods: Why, when, and how to conduct interviews and focus groups in pharmacy research. *Currents in Pharmacy Teaching and Learning*, 8(4), 509-516.
- [55] Salameh, W. (2018). *Arabic as a foreign language (AFL): Northern UAE AFL Teachers' Perceptions of the Integrated Approach* (Ph.D.). The British University in Dubai.
- [56] Schumann, J. H. (1978). *The pidginization process: A model for second language acquisition*. Rowley, MA: Newbury House.
- [57] Shehab, R., & M Zeki, A. (2015). Web Assisted Language Learning System for Enhancing Arabic Language Learning Using Cognates. *Journal of Technology*, 77(19). doi: 10.11113/jt.v77.6538
- [58] Sun, Y. (2017). Krashen's second language acquisition theory in business English teaching. *Proceedings of the 2017 4Th International Conference on Education, Management, and Computing Technology (ICEMCT 2017)*. doi: 10.2991/icemct-17.2017.299
- [59] Taherdoost, H. (2016). Sampling methods in research methodology: How to choose a sampling technique for research. *SSRN Electronic Journal*, 5(2), 18-27. doi: 10.2139/ssrn.3205035
- [60] Tavakoli, P., and Jones, R. (2018). An overview of approaches to second language acquisition and instructional practices. Cardiff: Welsh Government report number 12/2018 Retrieved from <http://gov.wales/statistics-and-research/overview-approaches-second-languageacquisition-instructional-practices/?lang=en>.
- [61] The Mother Tongue Center (2019). The mother tongue – Arabic language center. Retrieved 15 November 2019, from <https://mothertongue.ae/>
- [62] Thomure, H. (2019). Arabic language education in the UAE: Choosing the right drivers. *Education in The United Arab Emirates*, 75-93. doi: 10.1007/978-981-13-7736-5\_5
- [63] UN. (2019). What are the official languages of the United Nations? *Ask DAG!* Retrieved from <http://ask.un.org/faq/14463>.
- [64] Unal, M., & Ilhan, E. (2017). A case study on the problems and suggestions in foreign language teaching and learning at higher education. *Journal of Education and Training Studies*, 5(6), 64. doi: 10.11114/jets.v5i6.2302
- [65] UNESCO. (2019). History of the Arabic language at UNESCO | *United Nations Educational, Scientific, and Cultural Organization*. Retrieved from <http://www.unesco.org/new/en/unesco/resources/history-of-the-arabic-language-at-unesco/>.
- [66] Wang, R., & Xiang, X. (2016). On the function of mother tongue transfer in English vocabulary acquisition. *Theory and Practice in Language Studies*, 6(11), 2208. doi: 10.17507/tpls.0611.19
- [67] Wang, S., & Zhu, P. (2015). Exploring a research method - interview. *Advances in Social Sciences Research Journal*, 2(7), 161-165. Retrieved from [https://journals.scholarpublishing.org/index.php/ASSRJ/article/view/1270/pdf\\_187](https://journals.scholarpublishing.org/index.php/ASSRJ/article/view/1270/pdf_187).
- [68] Wang, Y. (2015). Negative transfer of mother language in English compositions by Jiujiang university students. *SHS Web of Conferences*, 14, 01008. doi: 10.1051/shsconf/20151401008
- [69] Yang, X., & Chen, D. (2016). Two barriers to teaching culture in the foreign language classroom. *Theory and Practice in Language Studies*, 6(5), 1128. doi: 10.17507/tpls.0605.29
- [70] Yoon, H. (2016). 'Writing' children's literate identities: The meaning of language in multilingual, multicultural contexts. *Multicultural Education Review*, 8(2), 65-82. doi: 10.1080/2005615x.2016.1166722
- [71] Zaman, J. (2015). *Role of motivation in second language learning: A study of private university students in Bangladesh* (Masters). BRAC University.
- [72] Zhao, Y. (2019). Negative transfer of mother tongue in English. *Creative Education*, 10(05), 940-946. doi: 10.4236/ce.2019.105070
- [73] Ding, W. and Marchionini, G. 1997 A Study on Video Browsing Strategies. Technical Report. University of Maryland at College Park.
- [74] Fröhlich, B. and Plate, J. 2000. The cubic mouse: a new device for three-dimensional input. In Proceedings of the SIGCHI Conference on Human Factors in Computing Systems
- [75] Tavel, P. 2007 Modeling and Simulation Design. AK Peters Ltd.
- [76] Sannella, M. J. 1994 Constraint Satisfaction and Debugging for Interactive User Interfaces. Doctoral Thesis. UMI Order Number: UMI Order No. GAX95-09398., University of Washington.
- [77] Forman, G. 2003. An extensive empirical study of feature selection metrics for text classification. *J. Mach. Learn. Res.* 3 (Mar. 2003), 1289-1305.
- [78] Brown, L. D., Hua, H., and Gao, C. 2003. A widget framework for augmented interaction in SCAPE.
- [79] Y.T. Yu, M.F. Lau, "A comparison of MC/DC, MUMCUT and several other coverage criteria for logical decisions", *Journal of Systems and Software*, 2005, in press.
- [80] Spector, A. Z. 1989. Achieving application requirements. In *Distributed Systems*, S. Mullender

# Optimization of Hybrid Energy Systems for Rural Electrification

Ekpo, Andifiok Aloysius  
Department of Electrical/Electronic  
University of Port Harcourt  
Port Harcourt, Nigeria.

Dr Nelson Ogbogu  
Department of Electrical/Electronic  
University of Port Harcourt  
Port Harcourt, Nigeria.

---

**Abstract:** This study is an optimization of hybrid energy system in Nigeria, the energy requirement of Ikot Inyang rural community is satisfied after carrying out the design and simulation of different variables, the optimal systems were a system that consisted of 5 wind turbines, solar models and a diesel generator as energy sources. Ikot Inyang is a rural community located in Akwa Ibom state, South-South Nigeria, the community is connected to the national electricity network (grid) but the power supply is rarely consistent. The load estimate analysis showed that Ikot Inyang had peak load 58.62kW and peak energy demand per day as 670.65kWh. Eight (8) different design plans were considered and simulations were carried out using HOMER software. Several factors were used to determine the most optimal system, which includes the Net Present Cost, Levelized Cost of Energy, Renewable Fraction and system emissions. This was carried out for the 25 years project life time. The design plans were made of stand-alone systems as well as combination of many generating sources with battery included in some systems, various simulations were carried out. HOMER Presented the most technical and economical solution to meet the load demand at the least Net Present Cost, least Levelized Cost of Energy and allowable Renewable fraction. The most optimal solution for Ikot Inyang involved a combination of a 50Kw diesel generator, 5 Bergey Excel 10 wind turbine, 134kW solar model, 204 strings of Hoppecke 12 OPzS 1500 battery and 2 Leonics MTP-413F 25kW converter. The dispatch method used for this system was the Load Following dispatch method. This method produced at least Net Present Cost of \$1.7M (N349.36M), Levelized Cost of Energy of \$0.228 (N74.74), considerably high Renewable Fraction of 84.7%, When this result was compared with a diesel generator only system, it showed 77.2% reduction in the diesel saving fuel cost. Comparison with a design plan consisting of diesel generator only showed that 202,155kg of carbon dioxide is saved per year and 1,262kg of carbon monoxide is saved per year when making use of the most optimal system design.

**Keywords:** HOMER, Renewable Fraction, Levelized Cost of Energy, Net Present Cost, Optimal System Design

---

## 1.0 INTRODUCTION

Up to two billion people around the world have no accessibility to grid connected electricity most of which are underdeveloped communities (rural area) according to the research carried out by the United Nations Environment Program (UNEP) [1]. The Inaccessibility to electricity in the rural has directly influenced rural population migration and reduction in the workforce in the rural communities which mostly deal with agricultural produce which also contributes significantly to an economy.

In Nigeria, the power generated and supplied to national grid is still very small compared to the country's load demand, and the geography of some rural communities makes it difficult for them to have access to the nation's grid supply, hence the need for off-grid power generation becomes inevitable [2]. As started by [3], over 100 local government areas in Nigeria are still not connected to the nation's grid system, hence the need for off-grid electrification cannot be over emphasized.

In the last decade, rural electrification in Nigeria with renewable energy with off-grid connection has become a suitable alternative for communities where connection to the grid is neither is not present or economically viable [4].

Harsh terrains and isolation of rural communities are among the various factors are responsible for the poor distribution of electrical resources [5]. Nevertheless, the main reason for

poor distribution is that it is not economically feasible, it is too expensive to expand the grid over long distances just to supply a small number of people with electricity in a rural community [5]. Because of this, the only viable option to consider that is economically feasible, reliable and dependable is to make use of Hybrid Energy System (HES). Hybrid Energy System (HES) is very cost friendly and can be utilized where difficult terrains are found and where energy supplied to the grid is limited and insufficient. Hybrid Energy System (HES) is a good alternative for supplying electricity to the rural areas rather than connecting to the national grid where the community is either isolated or situated at a location with a harsh terrain.

Hybrid Energy Systems (HES) is mostly made of a backup generator which supplements the output power for a Solar PV and wind systems during periods of peak loads and poor resource availability. One of the greatest advantages of Hybrid Energy Systems is the ability for energy sources to complement each other. Here the strengths (merits) of each sources type are used to complement the weaknesses (demerits) of each other [6].

Stand-alone Hybrid Energy Systems incurs less cost and has a higher reliability than single systems either photovoltaic (PV) or wind systems [7]. Also, the installation of PV module to meet load demand at all times, will lead to excessive generation for certain month of increase and

maximum solar radiation leading to wastage of energy generated for some months.

HOMER (Hybrid Optimization Model for Electrical Renewables) was developed in USA by National Renewable Energy Laboratory, according to (Jose´ et al., 2009), this is the software mostly utilized for optimization of Hybrid Energy Systems.

## 2.0 REVIEW OF RELATED LITERATURES

The standard of living of any economy depends massively on the accessibility to sustainable, reliable and affordable energy supply. For the growth, development and stability of the economy of any nation, sufficient and consistent energy supply is a necessity. A nation cannot beyond a certain level without access to an energy source [8].

United Nations Environmental Program (UNEP) conducted a survey, the survey revealed that close to two billion people around the globe have no access to electricity from the nation's grid system and the people in this group are people are mostly residents of rural communities [8],[9].

Population rise which leads to proliferate socio-economic activities which in turn increased energy demand, this continuously increases energy demand must be met by continuously increasing energy supply. The appropriate measuring yardstick for sustainable socio-economic growth is electricity supply. According to [8], Close to forty percent of the population of Nigeria are not connected to the national grid system, this are mostly people living in the rural communities of Nigeria and they rely on biomass (wood, dung etc), batteries and at other times self-generation of electricity.

According to [10], the supply of grid-based electricity to some rural and remote communities fronts some serious economic challenges, especially when the community has a difficult geographical terrain and is scantily populated. In Nigeria, due to insufficient and inconsistent supply, preference of supply is given to commercially productive areas and areas economically beneficial to the power company, this is mostly cities and urban areas because they are densely populated. For some rural areas in Nigeria, although connected to the nation's grid system, due to insufficient energy supply which cannot match load demand, rural and remote communities are mostly load-shedded making to complement grid supply with self-powered generation.

[11], stated that globally more than 1.7 billion people live independent of the grid-based electricity supply. This doesn't include those connected to the grid but with epileptic supply of electric energy. World bank energy facts as quoted by [2], approximately 1.2 billion people globally which amounts to 20% of the population globally are without access to electricity supply and approximately all the people in this class are residents of developing countries. In the past India was among this group, but excluded themselves because they restructured their interconnected system to not

only be grid dependent but they developed distributed energy generation which included standalone, mini and micro power plants.

### 2.1 Rural Electrification and Hybrid Renewable Energy System

Population growth, technological advancements and improvement in the growth in the standard of living has led to global rise in energy consumption and demand. Due to this fact, many rural and remote communities are deprived of electricity as they are not seen as priority and because electricity supply cannot match the teeming energy demand. The answer to this issue is to increase the amount of electricity generated and supplied and to reduce transmission losses. But most of world electricity plants are power by fossil fuels. Fossil fuels are exhaustible and it cannot meet future electricity needs due to their negative influence on the environment. Making use of renewable resources not as an immediate replacement but as alternatives and supplements to fossil fuels is rapidly becoming the most efficient method of electricity generation. When renewable is generated individually and in small unit, it becomes a very costly option and it comes with so many technical difficulties due to intermittent availability of renewable resources and their unpredictable nature. The solution to this problem is the utilization of Hybrid Renewable Energy Systems [12].

Hybrid Renewable Energy Systems is the merging of renewable, conventional energy sources and different kinds of energy storage to meet both or either grid connect and standalone loads. Hybrid Renewable Energy Systems are mostly utilized in rural areas and secluded communities.

When this is method is used, the uncertain and unpredictable nature of renewable resources, the demerits of traditional resources all supplement for each other. When the electricity production of the renewable energy sources is not large enough to meet the required load, the remaining load is met by a back-up energy sources, either from the storage or from the conventional energy sources. Also, when the renewable sources produce more than required electric energy, the required energy feeds the load and the left over is sent to be stored by the different kinds of storage utilized either battery or pump storage but the most popular and economically available option is the use of battery cells.

The use of Hybrid Renewable Energy Systems is more reliable and efficient that the renewable sources especially in a standalone/off-grid mode. Hybrid Renewable Energy Systems has been implemented in places such as estates, university, factories etc. In this scenario when, during off peak periods when the electricity from the grid is cheapest, the load demand is met by energy from the grid, but at peak periods, electric energy demand is met by Hybrid Renewable Energy sources and the extra energy is either stored by the energy storage systems or sold to the grid [13]. Also, the energy stored in energy sources are utilized to meet extra electricity demand or they are sold for profits into the grid. There are great advantages of Hybrid Renewable Energy Systems which includes; reduced levelized cost of energy, reduction in CO<sub>2</sub> emission, protection of the environment by

cutting down the emission of greenhouse gases, poisonous substance and industrial waste, generation of cheap electricity for rural communities, increased reliability, dependency and efficiency. According to all the above listed advantages meets all the criteria of Sustainable Development which are made of the environmental, social and economic aspects [14].

For design and optimization purposes, many theoretical approaches have been adopted and many simulation and optimization models has been developed and has been discussed in details by [15]. [16], worked on the design and control techniques in order to simulate and optimize a stand-alone Hybrid Renewable Energy Systems, another optimization tool and techniques were developed for optimal design by [17] and they developed models for the Optimization in microgrids with hybrid energy systems. A critical review on the developments in Hybrid wind/Photovoltaic energy systems with a battery storage system and a converter by [18] and they shared their findings.

There have been other studies carried out on Hybrid Renewable Energy Systems on either grid-connected systems or standalone systems which includes energy management, cost analysis, optimization techniques, software and simulation designs, planning criteria and other design parameters have been reviewed in [19], [20].

Many authors have made use of HOMER in their study and their design of optimal hybrid energy systems. [21] worked on the rural village electrification in South Africa: role of energy efficient in off-grid PV/dg system, in their works the made the relationship between the process of optimization and sizing the various component of a Hybrid Renewable energy systems and the energy efficiency. This investigation was carried out in a rural community in south Africa, covering 30 households. He summarized that the reduction in the operation time of a diesel generator can be cut down by up to 20%, if households made of efficient lamps and energy save appliances which would also lead to the reduction of CO<sub>2</sub> emission.

An evaluation of hybrid wind/diesel energy potential in pemanggil island Malaysia, was carried out by [22], they examined the potential energy output of a wind/diesel hybrid with battery storage. They examined extensively the influence of wind speed, penetration, and energy stored in the battery on the cost of energy, annual operational hours of the diesel generator and energy production. An analysis of hybrid wind/fuel cell /battery/ diesel energy system under alaska condition was designed and simulated by [23], they designed was simulated with the aim of reducing the gas emission by 37% in comparison with the previously existing system.

[24], in their paper on Modelling of solar/diesel/battery hybrid power systems for far-north Cameroon, this was meant for the electrification of domestic households and schools in the rural community in northern Cameroon. [25], worked on assessment of off-shore wind farms in Malaysia, and in their work, they concluded that there was great wind

potential if a wind turbine is placed along the South China sea coast line and optimized accordingly. here their design was made with Vestas V-47 and V-48 wind turbine and hence economic optimization and feasibility studies were performed accordingly. [26], worked on Balancing cost, operation and performance in integrated hydrogen hybrid energy system designed to feed and supply small rural community with electricity. They focused on designing and optimizing a hybrid energy system whose primary sources was hydrogen, this was to enable them to obtain a hydrogen independent system. They also collectively developed an algorithm for determining the correct size of individual system and for the optimizing the system collectively.

Biomass gasifier-based hybrid energy system for rural areas was designed by [27], this incorporated a biomass gasifier plant as one of the energy sources joined with other renewable sources of energy. To determine optimal designs of hybrid energy systems, some factors are considered which includes; load demand, non-linear seasonal variations, sizing and constraints of equipment as well as cost. Making use of HOMER software, [28], worked on the potential of grid connected photovoltaic array in Zimbabwe. Their analysis showed that to make generation of electricity from solar photovoltaic competitive, the electricity market was to increase the tariff of electricity to a minimum of \$0.15/kWh in specific areas whose minimum daily solar irradiation is at least 5.6Wh/m<sup>2</sup>.

[29], carried out an analysis on the technical and economic assessment of power generation from landfill gas in south Africa, in the investigation he also analyzed the environmental impact of making the hybrid system a standalone system or grid-based system respectively. He came a conclusion that either standalone system or grid-tied systems are both feasible, however that it was cheaper to install a standalone system than a grid-tied system.

In a research work carried out by [30] on the technical and economic analysis of different micropowers in providing network load and optimal selection with real load analysis of a 20kv/400v station in bushar province of Iran, simulations were made based on different hybrid configurations, the objectives were to determine technical and economic feasibility as well as determine their impact on the environment. When considering the most optimal system in terms of cost, technicality as well as environmental impact, solar photovoltaic stood out as the most optimal system.

[31], worked on the Sizing methods for stand-alone hybrid systems based on renewable energies and hydrogen, here he made a comparison of methods of sizing stand-alone hybrid systems, these methods are as follows: Simulink optimization model in MATLAB, use of equations, HOGA and HOMER software. The results shown by all the different methods all lied within acceptable ranges, but the more expensive systems were given by HOGA and HOMER models. Also, [32], made a comparison between Lindo simulation software and HOMER in modelling Electrical renewable energy systems with the aim to meet the load requirement of Jaunpur block of Uttaranchal state of India.

From the results obtained, it indicated that HOMER presented systems with the higher cost of energy, hence they concluded that HOMER was a more extensive software as it took into consideration the individual costs of components such as batteries, converters, grid energy cost were as Lindo software only took into consideration the cost of components directly related with the renewable energy systems only.

[33], stated that there are many environmental influences resulting from the use of hybrid systems. He also stated that utilizing renewables systems especially hybrid systems has the capacity to reduce the emission of greenhouse gases and it will serve and preserve from extinction the convention and expendable sources of energy. He was also to estimate to a certain amount of accuracy the cost of energy saved and the percentage of CO<sub>2</sub> saved annually.

In this study, different HES configurations are modeled using both the meteorological and surveyed load data collected from a typical remotely located village in Akwa Ibom State of Nigeria with the aim of determining most suitable option that will optimally meet their energy demand economically while taken into consideration the environmental impact.

## 2.2 WIND ENERGY POTENTIAL IN NIGERIA

There are many researches highlighting the potential of wind energy resource in Nigeria. [34], carried out an analysis gathering wind speed data from up to 30 stations in Nigeria, and he concluded the average wind speed lies between 1.5 to 4.1m/s per year and 5.7-22.5W/m<sup>2</sup> of power flux density. [35] gathered also a 10-year wind data from the year 1979-1988, he studied higher winds and surface winds and he also considered maximum gusts. According to [36] in their study on the cost benefits and statistical analyses of the potential of wind energy of a site in Maiduguri, he made his simulations using Weibull statistics and he carried out his analysis using a Ten years data of wind speed gathered between 1995-2004. In was discovered by [37] that the greatest wind speed is obtained in the region of high altitude and elevation above sea level also topographies in the middle the ware upland and the boundaries to the north of Nigeria has high potential for the harvest of wind energy. He made a discovery that the wind speed in the north was the highest and was about 4.0-7.5m/s while that of the south was about 3.0 to 3.5m/s at the elevation of 10m.

## 2.3 SOLAR ENERGY POTENTIAL IN NIGERIA

In terms of unlimited capacity of generation, the most favourable source of renewable energy. The energy radiated from the sun per second is equated to  $3.8 \times 10^{23}$  kW. The majority of this transmitted energy reaches the earth atmosphere through the process of electromagnetic radiation and this energy at the point of entering the earth's atmosphere is approximately 1.5kw/m<sup>2</sup>.

The total solar energy reception of Nigeria is about  $5.08 \times 10^{12}$  kWh daily and if a solar generator (PV or other solar technologies) which has an efficiency of as low as 5% efficiency is used to cover just one percent of nation's

surface, a total of  $2.54 \times 10^6$  MWh of electrical energy is obtainable [38]. The equivalent of this energy can also be derived from 4.66 million barrels of oil daily. Typical application of solar energy could either be used directly or converted into electrical energy for carrying the following such as heating, cooking, distillation, refrigeration and air condition and other industrial applications.

## 3.0 RESEARCH METHODS

### 3.1. Description of the Site

Ikot Inyang is a rural community or village (a remote area) in Ikot Ekpene Local Government Area in Akwa Ibom State, South-South Nigeria. It is located at 5°9'36.8604" N and 7°41'13.9416" East (Latitude: 5.160239, Longitude: 7.687206). It has a population of about 450 residents which majority are indigenes and the rest are mostly student. The data utilized for the simulation which includes the wind speed and the solar irradiation were obtained or downloaded using HOMER software and this data were gathered for over a period of twenty-two (22) years by the National Aeronautical and Space Administration (NASA) whose headquarters is at the United States.

### 3.2 FACTORS FOR THE SELECTION OF THE MOST OPTIMUM HYBRID SYSTEM

The determination of the most optimum solution of the hybrid energy will be based on set criteria and the utilization of different yardstick with which the optimum system should score high when judged based on the all the criteria. This includes: The Net Present Cost, Levelized cost of Energy, Carbon Emission Intensity as well as the Renewable Fraction (RF).

#### 3.2.1 NET PRESENT COST

Net Present Cost is the summation of the cost of the system throughout life cycle of the system. The life cycle cost of the system includes the cost of equipment purchase and setting up (capital cost), replacement cost, cost of operation, fuel cost stands, maintenance cost, tax as well as cost of fulfilling community developmental services. When the most important consideration is cost reduction, the energy system result with the lowest Net Present Cost is selected.

$$NPC = C_0 + C_r + \sum_{t=1}^N \frac{C(t)}{(1+in)^t} - R \quad (3.1)$$

Where  $C_0$ = initial capital,  $C_r$  for the replacement cost when  $t = 0$ ,  $R$  = the Residual value at the time,  $t=0$ ,  $C(t)$  is the cost per annum which is a function of time and is given as:

$$C(t) = C_{mo}(t) + C_f(t) \quad (3.2)$$

Where  $C_{mo}$  is the cost of maintenance and operation and  $C_f(t)$  is the fuel cost in  $t$  numbers of years.

$$C_{mo} = C_{mo}, 1 \sum_{t=1}^N \frac{1}{(1+in)^t} = C_{mo}, t \times PR_L \quad (3.3)$$

$$C_f = C_f, 1 \sum_{t=1}^N \frac{1}{(1+in)^t} = C_f, 1 * PR_L \quad (3.4)$$

$$PR_L = \sum_{t=1}^N \frac{1}{(1+i)^t} = \frac{(1+in)^{N-1}}{i(1+in)^N} = \frac{1}{C_{RF}} \quad (3.5)$$

Where N is the total number of years of the project otherwise known as the project lifetime and “in” represents the interest rates annually respectively.

Overall annualized cost ( $A_y$ ) which is given as sum total of the cost associated with the project as well as other cost as stated in equation (ii).

$$A_y = NPC \times C_{RF} \quad (3.6)$$

Where  $C_{RF}$  is the capital recovery cost and  $A_y$  represents the overall annualized cost.

As inflation values are not indicated in the analysis, the expenses per year remains the same year after year, as there is no situation like that, hence, this analysis is theoretical and not factual. As a result of that we can rewrite the equation as follows

$$NPC = C_0 + C_r + C_{mo} + C_f - R \quad (3.7)$$

### 3.2.2 LEVELIZED COST OF ENERGY

This can be defined as the mean cost of per kilowatt-hour (kWh) of usable electrical energy generated by a system during the period of useful life. This is also the minimum price the energy consumer is expected to pay for the supply and utilization of a kilowatt-hour of electrical energy.

To calculate the Levelized Cost of Energy, there has to be a division of the cost of electrical energy produced by the system per year (annualized cost) by the actual useful energy which is generated by the system during the same time frame.

$$LCOE = \frac{A_{nc}}{T_L} \quad (3.8)$$

Where LCOE is the levelized cost of energy,  $A_{nc}$  is the total cost of electric energy produced per year (also known as the Annualized cost) and  $T_L$  total electrical load supplied by the energy system annually.

### 3.2.3 CARBON EMISSION INTENSITY

This is the amount of carbon emitted by the energy system in the process of generating electrical energy. This is also the percentage of carbon produced by an energy system.

Mathematical, Carbon Emission Intensity  $C_i$  of any energy system is given as

$$C_i = \sum_1^n E_n \times P_n \quad (3.9)$$

Where  $E_n$  is the potential carbon emission of each energy generating source per kilowatt-hour of energy produced by a single source and  $P_n$  is the amount of energy generated by each different type of generating source.

### 3.2.4 RENEWABLE FRACTION

Renewable fraction is the comparison of the total amount energy produced by a renewable energy sources with the total amount of energy produced by entire hybrid energy system. Renewable fraction is needed as high as possible but also considering the consequences it has on the Net Present Cost of the energy system, this is due to the fact that at most times, the load demand is expected to be met in totality by a renewable source(s) of energy. The Renewable Fraction of a hybrid energy system is given as:

$$RF(\%) = \left[ 1 - \frac{\sum_1^i P_{d,t}}{\sum_1^i P_{r,t}} \right] \times 100 \quad (3.10)$$

Where  $P_d$  is the power generated by the fossil generator (e.g. diesel generator) and  $P_r$  is the power produced by the renewable energy sources (e.g. Wind and solar PV).

### 3.3 ENERGY DEMAND ESTIMATION AND HOURLY PROFILING OF IKOT INYANG RURAL COMMUNITY

This profiling was carried out and results were based on the oral interview performed on the indigenes and residents of the community. In this study, loads will be classified into social infrastructural loads (SL) and domestic loads (DL). A total of 75 residential buildings has been profiled. To estimate the loads, we make an assumption that the loads of all residential buildings are similar and hence energy requirement are equal as well. One building is used to carry out all the domestic load estimates and it is purely based on the necessities of the people in the area, obtained during the oral interviews performed. Some loads have been removed due to the fact that very few residential buildings have it like air-conditioner, heat extractors, washing machine etc. Electrical appliances were scheduled and profiled according to their use and according to the time of use with a 24hours time frame. For residential buildings the loads were divided to 2 loads with predictable patterns of utilization and loads whose patterns of utilization are not predictable but based on individual’s priorities and preferences.

There is also a secondary school, a primary health care centre and four (4) shops the loads from these locations forms the social infrastructural load in the area. Load estimation will be made according the devices and appliances utilized. The unpredictable loads are loads which is assumed to run continuously throughout the 24hour period

and consume a consistent amount of energy all through the day, however it can be turned off based on individual's preference and not on any predictable pattern. Predictable loads are those that are turned off when their work is done and it doesn't run throughout the day (24hours). When carrying out and estimation of load (energy) demand of the shops only a shop will be considered and the value of the estimation will be multiplied across the four shops, as assumption is made that all shops utilize similar equipment and hence consumes the same quantity of energy and 6 shops were counted and another additional 2 were forecasted. All infrastructural loads are considered predictable loads as the operation time can be estimated without much error. Estimation and scheduling are done throughout the 24hours period. The unpredictable load is assumed to run continually and the predictable load are scheduled and profiled during off peak periods. 6 water pumps were seen in the community and an additional four for future loads is added making it 10. Due to individual preference, a diversity factor of 0.7 is applied throughout all loads connected to the system. From figure 3.1, it can be seen that peak period occurs at 14.00 to 15.00 (2pm to 3pm) with total system load as high as 32.55kW when the diversity factor is applied. The peak kW demand is given as 58.62kW, the mean load demand on the system per hour is given as 27.94 kW, while the annualized scaled average load requirement is given as 670.65kWh per day

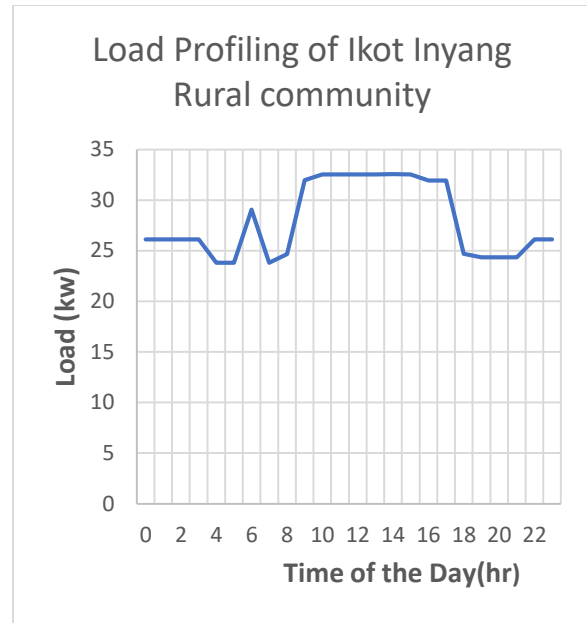


Figure 3.1 Hourly load scheduling for Ikot Inyang rural community

### 3.4 SYSTEM DESIGN

Table 3.2.: Optimal Hybrid Energy system design plan for Ikot Inyang Rural community

Plan	Battery	Diesel	Solar PV	Wind turbine
A	×	✓	×	×
B	✓	✓	×	×
C	✓	×	✓	×
D	✓	×	×	✓
E	✓	✓	✓	×
F	✓	✓	×	✓
G	✓	×	✓	✓
H	✓	✓	✓	✓

The different plans that will be used for discussions and conclusions will be drawn from here. Figure 3.3. will be used to make comparison to discover which of the plans provides a more optimal, energy efficient and cost beneficial system. The criteria that will be used to determine the most efficient and optimal system is as discussed above which includes the Net Present Cost, Renewable fraction, Carbon Emission Intensity and Levelized cost of energy.

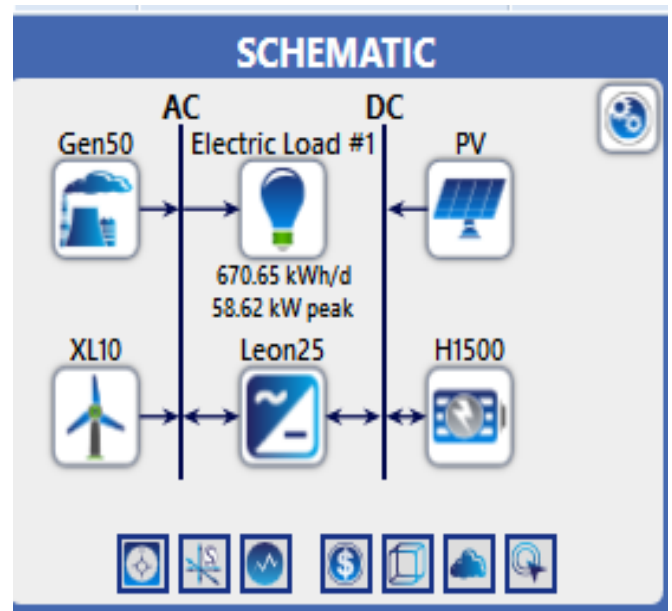


Figure 3.2.: Design schematic of optimal hybrid energy system in Ikot Inyang rural community

### 3.5 WIND ENERGY DATA

The wind energy resource data is downloaded directly from HOMER software, and the data is downloaded from NASA

(The National Aeronautics and Space Administration) data base.

Often times, wind speed data obtained at certain heights are not similar to the wind speed obtained at a certain hub height when making use of wind turbines used for commercial purposes worldwide. Because of this factor, definition of windspeed from the height of installation (Hub height) is very important in order to obtain a more accurate data. Power law equation gives the solution for obtaining wind speed at a specific wind hub. This wind speed will alter the wind speed obtained from the National Aeronautical and Space Administration (NASA) database and the modified wind speed data will be entered into HOMER to carry out the simulations in order to obtain more accurate data with consideration to the hub height. The hub height has to high especially when the installation is onshore and in an open area in order to avoid obstructions of wind paths resulting in utilization of maximum wind speed, hence maximum power is obtained that is potential available in that area.

$$W_{s_2} = W_{s_1} \left(\frac{d_2}{d_1}\right)^m \quad (3.11)$$

Here  $W_{s_2}$  is the wind speed at the height (distance of the ground)  $d_2$  and  $W_{s_1}$  is the wind velocity at the height  $d_1$  also  $m$  is called the shear exponent and it depends on the stability of the atmosphere on the surface where the components are mounted. The shear component factor is site-specific and has a rating between 0.00001 – 3m. Ikot Inyang rural community is located in tropical rainforest vegetation and hence the shear component was assumed to be 0.1 which was taken into consideration during the calculation to obtain the wind speed used for the simulation. The mean wind speed data is obtained monthly from the National Aeronautical and Space Administration (NASA) database for the period of 10years, and the anemometer height was 10m. This information was used to calculate the windspeed of the turbine at the specific height. The Hub height for Ikot Inyang was chosen by design to be 80m.

Applying power equation to the wind speed we have:

$$W_{s_2} = W_{s_1} \left(\frac{80}{10}\right)^{0.1} = W_{s_1}(8)^{0.1} = W_{s_1} \times 1.23 \quad (3.12)$$

$$W_{s_2} = W_{s_1} \times 1.23 \quad (3.13)$$

Table 3.3.: Wind speed data for Ikot Inyang Rural Community

Months of the Year	WS <sub>1</sub>	WS <sub>2</sub>
<b>January</b>	2.750	3.395
<b>February</b>	2.970	3.656
<b>March</b>	2.710	3.336
<b>April</b>	2.390	2.942
<b>May</b>	2.230	2.745
<b>June</b>	2.810	3.459

<b>July</b>	3.210	3.952
<b>August</b>	3.370	4.148
<b>September</b>	2.960	3.644
<b>October</b>	2.350	2.893
<b>November</b>	2.250	2.770
<b>December</b>	2.400	2.954

$W_{s_2}$  = Calculated wind speed at the hub height of 80m,  $W_{s_1}$  = Wind speed data from NASA. The Average annual wind speed is 3.32. The lowest wind speed was in may which was 2.745 m/s. The calculated wind speed data is used for the simulation of the work.

### 3.6 SOLAR ENERGY RESOURCES

The data solar irradiation resources gathered here is downloaded using HOMER which was collected from the National Aeronautical and Space Administration (NASA) database. The scaled annual mean solar irradiation of Ikot Inyang rural community was 4.71 kWh/m<sup>2</sup>/day. The month with the highest solar irradiation is February which is 5.59 kWh/m<sup>2</sup>/day and the lowest solar irradiation occurs in Augusts which is 3.77 kWh/m<sup>2</sup>/day.

Table 3.4.: Solar radiation data for Ikot Inyang Rural community

Months	Clearness Index	Solar Radiation (kWh/m <sup>2</sup> /day)
January	0.583	5.530
February	0.559	5.590
March	0.511	5.320
April	0.490	5.090
May	0.469	4.720
June	0.438	4.310
July	0.388	3.850
August	0.369	3.770
September	0.381	3.940
October	0.425	4.270
November	0.507	4.840
December	0.570	5.290

### 3.7 SIZING/MODELLING OF SYSTEM COMPONENTS

In order to accurately size components, there has to correctly estimate the load/energy requirement of the community. The energy requirement of Ikot Inyang community has been accurately stated to be 670.65Kwh/day with the peak load of the system at 58.62Kw.

#### 3.7.1 SIZING OF THE PHOTOVOLTAIC SYSTEM

The system peak load of the system at 58.62 Kw which is being considered for the design of the photovoltaic energy

system. HOMER optimizer is used to obtain the most economic and optimal system. HOMER will specify the solar model sizes as well as quantity needed to produce the meet the required energy demand. In the solar PV model, there is a direct proportionality between the direct incident solar radiation and the output power from the solar model. The cost of solar panel ranges from \$2.5 to \$4.5 per watt depending on quality, hence the capital cost per Kilowatt is approximately \$2500.

Table 3.5: Solar PV design variables (Inputs) considerations

INPUT TYPE	VARIABLES	VALUE	UNIT
TECHNICAL	Panel Tilt angle	0	Degree
	Azimuth angle	0	Degree (W of S)
	Derating factor	95	Percentage (%)
	Ground reflectance	20	Percentage (%)
	Solar tracking system	Nil	Nil
	Lifetime	25	Years
	Temperature coefficient	0.5	%/°C
	COST	Capital cost	2,500
Replacement cost		2,500	\$/Kw
Operation and maintenance cost		25	\$/year

The specific solar model has not been specified because the installation engineer can choose to purchase from a different manufacturer. The capital and replacement cost given in table 3.7 includes the cost of purchase, cost of transportation, cost of labour and other associated cost during installation of the solar model.

### 3.7.2. SIZING OF BATTERY SYSTEM

In order accurately estimate battery size, HOMER implements the following sets of equations by determining the excess energy the Hybrid Energy System generates.

$$S_{BS} = \frac{\sum_{i=0}^{8760} E_x(t) \times C_{ef}}{V_l} \quad (3.14)$$

Where  $E_x$  is the excess electrical energy generated that is evacuated to be stored by the storage system (battery),  $C_{ef}$  is the charging efficiency and  $V_l$  is the voltage level of the battery.

The excess electrical energy generated and evacuated to be stored ( $E_x$ ) can also be written as:

$$E_x(t) = \sum_{i=0}^{8760} E_s(t) - E_u(t) \quad (3.15)$$

Where  $E_s$  is the sum total of the electrical energy generated by all the renewable sources combines (i.e. the solar PV and Wind turbine) per hour and  $E_u$  is the total functional electrical energy utilized per hour. In circumstances where the total generated electrical energy from the renewable sources in the energy system is exceed the energy consumed by the system connected loads, the remainder of the energy will be stored in the battery. Likewise, when the energy generated by the renewable energy systems is less than the system connected load at any instance of time, the battery will be discharged to meet load requirement or the diesel backup generator will be dispatched to meet the required load.

In order to determine the optimal battery size, HOMER optimizer is utilized during the simulation, the battery sizing and quantity can be reduced or increase in order to obtain the most technically optimal and economically feasible system. Excess electrical energy generated is determined at the end of the simulation and is carefully detailed in the results of the optimization. Hoppecke 12 OPzS 1500 is the energy storage system used for the simulation. Hoppecke is a vented, lead acid, tubular-plate and deep-cycle battery.

Table 3.6: Storage system design variable (Inputs) considerations

INPUT TYPE	VARIABLES	VALUE	UNIT
TECHNICAL	Battery model	Hoppecke 12 OPzS 1500	Nil
	Nominal Capacity	3.59	Kwh
	Nominal Voltage	2	Volts (v)
	Maximum charge rate	1	A/Ah
	Capacity ratio	0.317	Nil
	Float life	10	Years
	Minimum state of charge	40	%
	COST	Capital cost	400
Replacement cost		350	\$/Kw
Operation and maintenance cost		15	\$/year

### 3.7.3 SIZING OF THE POWER CONVERTER

In order to accurately determine the size of power converted needed, the error margin has to be applied and put into consideration. Therefore, to calculate the minimum size of the converter, taking into consideration equation (xvi), and assuming an error margin of 5% and a capacity factor of 0.9.

$$P_m = \frac{P_{lf} + E_r}{C_f} \quad (3.16)$$

Where  $P_m$  is the overall power derived,  $P_{lf}$  is the peak load factor and  $C_f$  is the capacity factor.

Ikot Inyang community has a peak load of 58.62Kw. Applying the error margin of 5% and the capacity factor of 0.9, we have:

$$P_c = \frac{58.62 \times 1.05}{0.9} = 68.39 \approx 68.4\text{kW} \quad (3.17)$$

With our design, we make use of a 25kW converter system based on availability, HOMER will optimize it and find the quantity required to meet the system load demand. The converter size is set at \$400 per kilowatt and it's meant to last for a minimum of 15 years. The converter model used Leonics MTP – 413F 25kW. To carry out simulation is done by search space optimizer, with the sizes specified as 0kW, 25kW and 50kW respectively.

Table 3.7: Converter system design variable (Inputs) considerations

INPUT TYPE	VARIABLES	VALUE	UNIT	
TECHNICAL	Converter model	Leonics MTP – 413F 25kW	Nil	
	Rated Power	25	kW	
	Relative capacity	80	%	
	Inverter efficiency	96	%	
	Rectifier efficiency	94	%	
	Lifetime	15	Years	
	COST	Capital cost	400	\$/Kw
		Replacement cost	350	\$/kW
Operation and maintenance cost		15	\$/year	

### 3.7.4 SIZING OF DIESEL GENERATOR

The diesel generator is used during period of peak demand or periods of low availability of renewable energy generation. The diesel generator is also used in period where the renewable energy sources of generation and the battery system are under either routine or corrective maintenance.

Ikot Inyang community has a peak load of 58.62kW. Applying the error margin of 5% and the capacity factor of 0.9, we have:

$$P_d = \frac{58.62 \times 1.05}{0.9} = 68.39 \approx 68.4\text{kW} \quad (3.18)$$

Where  $P_d$  is the power generated from the diesel generator (in this case diesel) generator. A 75kW and 50kW diesel generator will be used for the initial design simulation, HOMER optimizer will choose the optimal solution considering other related factors. Hence the cost of the generator will depend on the size eventually chosen after simulation.

Table 3.8: Diesel generator design variables (inputs) consideration

INPUT TYPE	VARIABLES	VALUE	UNIT
TECHNICAL	Generator model	Generic Generator	Nil
	Fuel type	Diesel	Nil
	Operational lifetime	15,000	Hours
	Minimum efficiency	85	%
	Fuel curve gradient	0.33	1/h/kW rated
	Fuel curve intercept	0.05	1/h/kW rated
	Minimum load ratio	30	%
	COST	Capital cost	300
Replacement cost		300	\$/kW
Operation and maintenance cost		0.3	\$/hour
Fuel cost		0.65	\$

#### 3.7.4.1 METHOD FOR DISPATCHING THE DIESEL GENERATOR

The determining factors for the diesel generator dispatch plan (strategy) includes the following:

- i. Amount of renewable energy resources available
- ii. Size/capacity of the renewable energy generators available

- iii. Size/capacity of energy storage (battery) system
- iv. Price of diesel (fuel)
- v. Size of the diesel generator
- vi. Cost of maintenance and operation of the diesel generator

### 3.7.5 SIZING OF WIND TURBINE

To accurately determine the size of wind turbine, it necessary to take into consideration several factors that are different for every site such as minimum and maximum wind speed and also know the range in which different wind turbine operates accordingly.

To adequately size the wind turbine, the HOMER simulation optimizer is used. The wind turbine is the Bergey Excel 10 with the generation capacity of 10kW. The capital and replacement cost of Bergey Excel 10 is \$25,000 while it's operational and maintenance cost is set at \$50.00/year.

## 4.0 RESULTS AND ANALYSIS OF RESULTS

The result is also summarized based on the design plan we have in table 3.3, is clearly given in table 4.1. This design plan result does not follow the alphabetical order but it is arranged the order of the most optimal system based on the least Net Present Cost.

Table 4.1: Showing the NPC, COE and RF of design plan A – H in USD

PLANS	Dis patch	COE (\$)	NPC (\$)	Ren Frac (%)	Combinations
H	LF	0.228	1.07M	84.8	D+W+S+B
E	LF	0.234	1.09M	80.6	D+S+B
F	CC	0.285	1.33M	28.5	D+W+B
C	CC	0.305	1.42M	16.6	S+W+D
B	CC	0.308	1.43M	0	D+B
G	CC	0.342	1.60M	100	S+W+B
A	CC	0.376	1.75M	0	D

Table 3.9: Wind turbine design variable (input) consideration

INPUT TYPE	VARIABLES	VALUE	UNIT
TECHNICAL	Turbine model	Bergey Excel 10	Nil
	Starting wind speed	3	m/s
	Operational lifetime	25	Years
	Cut-off wind speed	25	m/s
	Hub height	80	Metres
	Rating	10	kW
	COST	Capital cost	25,000
Replacement cost		25,000	\$/10kW
Operation and maintenance cost		50	\$/year/turbine

					W+B
D	CC	0.821	3.83M	100	

From the table 4.1 it shows clearly that the most optimal system design is the H design plan which comprises of a diesel generator, wind turbines, solar PV and the battery storage system which in our initial system design was in design plan H.

### 4.2 ANALYSIS OF THE MOST OPTIMUM SYSTEM FOR IKOT INYANG RURAL COMMUNITY

The most optimum system is a hybrid energy system comprising of a diesel generator, wind turbine, solar PV system, converter and an energy storage system.

Table: 4.2: System architecture for the most optimal system for Ikot Inyang rural community

Component	Type	Rating	Quantity in Use
Diesel Generator	Generic Diesel Generator	50kW	1
Wind Turbine	Bergey Excel 10	10kW	5
Solar PV	Generic flat plate PV	134kW	Nil
Converter	Leonics MTP-413F 25kW	25kW	2

Battery	Hoppecke 12 OPzS 1500	3.59kW	204 strings
Dispatch Method	Homer Load following	N/A	N/A

Table 4.2. shows the system architecture of the most optimal system, the system comprises of 1 diesel generator of any choice, 5 Bergey Excel 10 wind turbine which is a 10kW wind turbine, 134 kW solar models of any type, 2 Leonics

From Fig. 4.1 and table 4.2 respectively, it is seen that the component with the highest capital cost is the Solar PV model which is \$334,792, followed by the wind turbine with the capital cost of \$125,000 and then the converter model with capital cost of \$81,600 in this category, the diesel generator has the lowest capital cost of \$15,000, but when it comes to replacement cost, the converter leads in this category with a total lifetime replacement cost of \$103,555 and it also has the highest salvage value of -\$20,690 nevertheless, the renewable energy equipment has no fuel requirement, hence under the cost of resources the renewable energy sources incur no cost at all but the cost of resource for the diesel generator although the operating lifetime is as much as \$164,349, all this cost accumulates and takes to total Net Present Cost of the system to \$1.07M. Table 4.3 also concludes the same which gives the annualized cost of the system for the total of 25years lifetime.

#### 4.3 COST SUMMARY FOR SYSTEM H

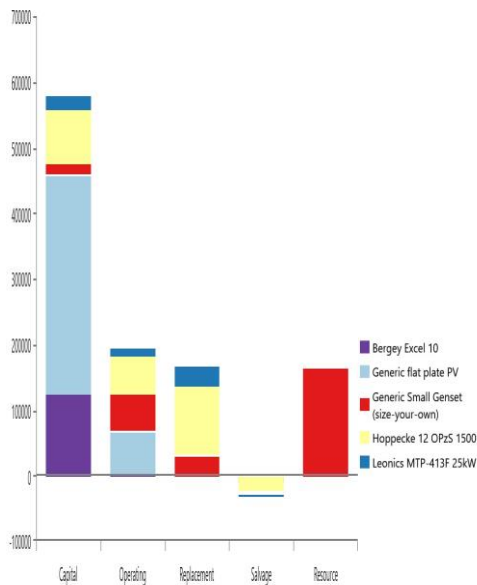


Figure 4.1: A chart of total cost summary for system H

#### 4.4 ELECTRICAL ENERGY RESULTS

Table 4.3: Excess electricity production and Unmet load

Quantity	Value	Units
Excess Electricity	36,766	kWh/yr

MTP-413F 25kW converter and 204 strings of Hoppecke 12 OPzS 1500 battery system. The dispatch method of the most optimal system is the Load Following dispatch strategy, where the generator only supplies the load but the excess renewable energy available charges the battery respectively. This configuration and design make up the most optimal system, meet the required energy demand at the lowest Net Present Cost (NPC), with the highest renewable fraction thereby reducing fuel consumption and hence reduction in greenhouse gas emissions.

Unmet Load	Electric	Value	Units
		0	kWh/yr
Capacity Shortage		4.83	kWh/yr

Table 4.4: Production Summary of individual energy sources

Component	Production (kWh/yr)	Percent
Generic flat plate PV	220,000	72.7
Generic Small Genset (Diesel)	37,291	12.3
Bergey Excel 10 Wind turbine	45,457	15.0
<b>Total</b>	<b>302,748</b>	<b>100</b>

From table 4.3 and table 4.4, it shows that all the system load were total met during the 25 years period proposed for the project, it shows that out of the 302,748kWh of energy generated by year by all the sources in the system, 36,766kWh of energy was excess energy generated per year. It also shows that 72.2% (220MWh) of all electrical energy generated per year was generated by the Solar PV this is because of the solar energy resource in the area, the wind turbine generated as much as 15% (45.5MWh) per year but the least energy generated per year came from the diesel generator which contributed only 12.3% (7.3MWh) which gave a total of 303MWh of electrical energy per year. It can also be seen that the renewable energy sources produced a total of 87.2% of all electrical energy produced per year compared to 12.3% of electrical energy produced per year, this made the Load Following dispatch strategy the best method of utilizing the diesel generator.

#### 4.5 SYSTEM EMISSIONS RESULTS

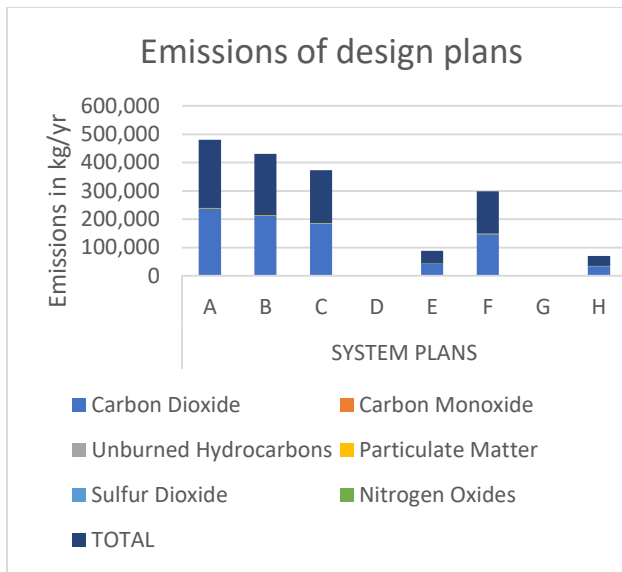


Fig. 4.2: A chart showing the net emission of each system plan per year

From figure 4.2, it is accurately shown that system Plan D (wind turbine + Battery) and G (Solar PV + wind turbine + battery) has no emissions because the sources of energy are total renewable, hence no emission, however these systems are not optimal because:

- i. High Net Present Cost
- ii. Unmet Electrical load

The unmet electrical load for system Plan D (wind turbine + Battery) and G (Solar PV + wind turbine + battery) are 109 kWh/yr and 85.5kWh/yr respective. The optimal system H is the system with a considerably low emissions, the lowest Net Present Cost and the Lowest LCOE. The systems with the most undesired A (Diesel only) and B (Diesel + Battery) which has the highest emissions.

#### 4.6 RENEWABLE FRACTIONS

From Fig. 4.3, it seen that system Plan D (wind turbine + Battery) and G (Solar PV + wind turbine + battery) have the highest renewable fractions of 100% this is very favourable but it's high Net Present Cost and Unmet electrical load per years makes it economically and technically infeasible. Systems plan A (Diesel only) and B (Diesel + Battery) are not even considered has they have the lowest renewable fraction owing to the fact that they do not possess any renewable energy source. But the most optimal system is seen to be system plan H (Diesel + Wind turbine + Solar PV + Battery) which has one of the highest Renewable Fraction, one of the least emissions, the lowest Net present cost and the least Levelized cost of energy. Hence the most optimal system for Ikot Inyang rural community is the H system plan.

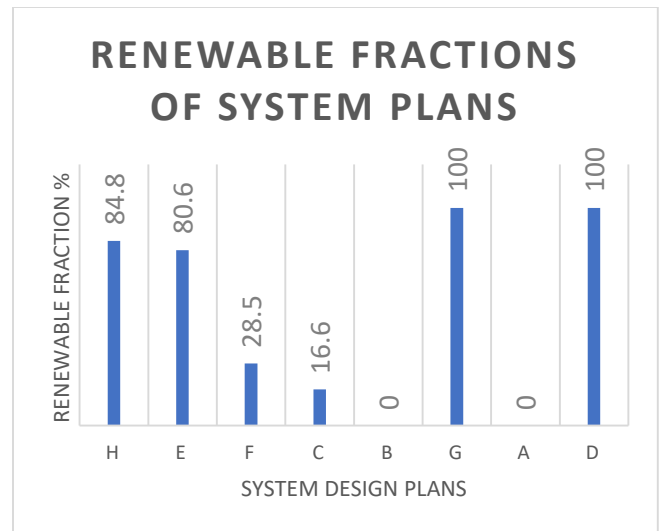


Fig 4.3: Renewable Fractions of different system design plans

#### 5.0 SUMMARY AND CONCLUSION

Optimal hybrid energy systems are very crucial in modern life as the population growth is geometrical rates, dependence on bulk energy generation and grid supply cannot be sustained, hence the use of hybrid energy systems as a form of distributed generation must be encouraged and implemented. Many developed nations have employed this method in order to ensure that energy supply reaches every citizen including the local population in order to discourage rural-urban migration with lack of adequate supply of energy as an excuse. Hybrid renewable energy systems is meant to supply energy that is reliable, efficient, dependable and affordable for the consumption of the local population and also preserve the environment by reducing the greenhouse gases emission per kilowatt-hour of electrical energy generated. A hybrid renewable energy system was designed for Ikot Inyang rural community in Nigeria, was consisted of 50 houses, 8 shops, a school and a primary health care facility. The system designed was aimed at supply 24 hours constant power supply to the area for a 25 years period. The electrical energy supplies were to be cheap, reliable and green as possible. This project when implemented would improve and promote business growth in the area, increase the farming population, hence greater family yield, promote other socio-economic activity as well as improve the living conditions of the residence of Ikot Inyang. After system design, calculations and simulations, the most optimal system in terms of technical and economic considerations included a 50kW diesel generator, 5 Bergey Excel 10 wind turbine, 134kW solar model, 204 strings of Hoppecke 12 OPzS 1500 battery and 2 Leonics MTP-413F 25kW converter. The dispatch method used for this system was the Load Following dispatch method. This method produced at least Net Present Cost of \$1.7M (₦349.36M), Levelized Cost of Energy of \$0.228 (₦74.74), considerably high

Renewable Fraction of 84.7% and above all met all its proposed loads for the period of 25 years.

## 6.0 REFERENCES

- [1] Rehman, S., Badeer, M.A. & Al-Moallem, S.A., 2007. Cost of solar energy generated using pv panels. *Renewable and Sustainable Energy Reviews* 11 (8): 1843-857.
  - [2] Elusakin J. E., Ajide O.O. & Diji J. C., 2014; Challenges of sustaining off-grid power generation in Nigeria rural communities.
  - [3] Ajayi O O, Fagbenle R O, Katende J. Assessment of wind power potential and wind electricity generation using WECS of two sites in South West, Nigeria. *International Journal of Energy Science*, 2011, 1(2): 78-92
  - [4] Rohit S, 2013; Off grid Electricity Generation with Renewable Energy Technologies in India; an application of HOMER. Retrieved on the 3rd of May 2019.
  - [5] Dekker, J., Chowdhuryand, S. & Chowdhury, S.P., 2010. Economic viability of pv/diesel hybrid power systems in different climatic zones in south africa IEEE Power and Energy Society General Meeting, Minneapolis, MN.
  - [6] Al-Badi, A.H. & Bourdoucen, H., 2011. Study and design of hybrid diesel-wind standalone system for remote area in oman. *International journal of Sustainable Energy* 31 (2): 85-94.
  - [7] Jose´, L., Bernal-Agustin, R. & Dufo-Lo´, P., 2009. Simulation and optimization of stand-alone hybrid renewable energy systems *Renewable and Sustainable Energy Reviews* 13: 2111-2118.
  - [8] Ohunakin OS. Energy utilization and renewable energy sources in Nigeria. *J Eng Appl Sci* 2010;5(2):171e7.
  - [9] García-Valverde, R., Miguel, C., Martínez-Béjar, R. & Urbina, A., 2009. Life cycle assessment study of a 4.2 kw stand-alone photovoltaic. *Solar Energy* 83 (9): 1434-1445.
  - [10] Kumar US, Manoharan P. Economic analysis of hybrid power systems (PV/ diesel) in different climatic zones of Tamil Nadu. *Energy Convers Manag* 2014;80:469e76.
  - [11] Perez R, 2006. USA Today, Home Power Magazine. Retrieved: April 15, 2013.
  - [12] Erdinc O, Uzunoglu M. Optimum design of hybrid renewable energy systems: overview of different approaches. *Renew Sustain Energy Rev* 2012;16:1412-25.
  - [13] Bhattacharyya SC. Review of alternative methodologies for analysing off-grid electricity supply. *Renew Sustain Energy Rev* 2012;16:677-94.
  - [14] Kaundinya DP, Balachandra P, Ravindranath NH. Grid-connected versus stand-alone energy systems for decentralized power—a review of literature. *Renew Sustain Energy Rev* 2009;13:2041-50.
  - [15] Bajpai P, Dash V. Hybrid renewable energy systems for power generation in stand-alone applications: A review. *Renew Sustain Energy Rev* 2012;16:2926-39.
  - [16] Bernal-Agustín JL, Dufo-López R. Simulation and optimization of stand-alone hybrid renewable energy systems. *Renew Sustain Energy Rev* 2009;13:2111-8.
  - [17] Fathima AH, Palanisamy K. Optimization in microgrids with hybrid energy systems—a review. *Renew Sustain Energy Rev* 2015;45:431-46.
  - [18] Mahesh A, Sandhu KS. Hybrid wind/photovoltaic energy system developments: critical review and findings. *Renew Sustain Energy Rev* 2015;52:1135-47.
  - [19] Upadhyay S, Sharma MP. A review on configurations, control and sizing methodologies of hybrid energy systems. *Renew Sustain Energy Rev* 2014;38:47-63.
  - [20] Shivarama Krishna K, Sathish Kumar K. A review on hybrid renewable energy systems. *Renew Sustain Energy Rev* 2015;52:907-16.
  - [21] Dusabe, D., Munda, J.L. & Jimoh, A.A., 2009. Rural village electrification in south africa: Role of energy efficient in off-grid pv/dg system. [active.cput.ac.za/energy/past\\_paper](http://active.cput.ac.za/energy/past_paper).
  - [22] Anwari, M., Rashid, M.I.M., Muhyiddin, H.T.M. & Ali, A.R.M., 2012. An evaluation of hybrid wind/diesel energy potential in pemanggil island malaysia IEEE Conference on Power Engineering and Renewable Energy, Bali, Indonesia 17-21.
  - [23] Seyed, J. & Mohammad, F., 2011. Analysis of hybrid wind/fuel cell /battery/ diesel energy system under alaska condition. The 8th Electrical Engineering and Electronics, Computer, Telecommunications and University, Thailand, 917-920.
  - [24] Nfaha, E.M., Ngundamb, J.M. & Tchindaa, R., 2007. Modelling of solar/diesel/battery hybrid power systems for far-north cameroon. *Renewable Energy* 32: 832-844.
  - [25] Mekhilef, S. & Chandrasegaran, D., Year. Assessment of off-shore wind farms in malaysia IEEE Region 10 conference (TENCON 2011), Bali, Indonesia, 13511355.
  - [26] Barsoum, N.N. & Vacent, P., 2007. Balancing cost, operation and performance in integrated hydrogen hybrid energy system First Asia International Conference on Modelling & Simulation.
  - [27] Ashok, S. & Balamurugan, P., 2007. Biomass gasifier-based hybrid energy system for rural areas IEEE Canada Electrical Power Conference, Canada.
  - [28] Rashayi, E. & Chikuni, E., 2012. The potential of grid connected photovoltaic array in zimbabwe. IEEE Mediterranean Electrotechnical Conference. Yasmine, Hammamet.
  - [29] Sekgoele, K., Chowdhury, S.P. & Chowdhury, S., 2011. Technical and economic assessment of power generation from landfill gas in south Africa. IEEE Power and Energy Society General Meeting. San Diego, CA, 1-8.
- Environmental effects of energy policy in sicily: The role of renewable energy. *Renewable and Sustainable Energy Reviews* 11: 282-298.
- [30] Nahari, A. & Dashti, R., 2011. Technical and economic analysis of different micropowers in providing network load and optimal selection with real load analysis of a 20kv/400v station in bushehr province of iran. The

International Conference on Advanced Power System Automation and Protection. Beijing, China.

- [31] Castañeda, M., Fernández, L.M., Sánchez, H., Cano, A. & Jurado, F., 2012. Sizing methods for stand-alone hybrid systems based on renewable energies and hydrogen. IEEE Mediterranean Electrotechnical Conference (MELECON). Yasmine, Hammamet, Tunisia.
- [32] Akella, A.K., Sharma, M.P. & Saini, R.P., 2007. Optimum utilization of renewable energy sources in a remote area. Renewable and Sustainable Energy Reviews 11: 894-908.
- [34] Adekoya L O, Adewale A A. Wind energy potential of Nigeria. Renewable Energy, 1992, 2(1): 35–39
- [35] Fagbenle R O, Karayiannis T G. On the wind energy resources of Nigeria. International Journal of Energy Research, 1994, 18(5): 493–508
- [36] Ngala G M, Alkali B, Aji M A. Viability of wind energy as a power generation source in Maiduguri, Borno state, Nigeria. Renewable Energy, 2007, 32(13): 2242–2246
- [37] Ajayi O O. The potential for wind energy in Nigeria. Wind Engineering, 2008, 34(3): 303–311
- [38] Chiemeka I. U and Chineke T. C (2009). Evaluating the global solar energy potential at Uturu, Nigeria, *International Journal of Physical Sciences* Vol. 4 (3), pp. 115-119

# Effect of Maghemite ( $\gamma$ -Fe<sub>2</sub>O<sub>3</sub>) Nano-Powder Mixed Dielectric Medium on Material Removal Rate (MRR) During Micro-EDM of AL6061

Nagwa Mejid Ibrahim  
Benghazi University, Industrial and  
Manufacturing System Engineering Benghazi,  
Libya

Zienab B. Mohamed  
Benghazi University, Industrial and Manufacturing  
System Engineering Benghazi  
Libya

**Abstract:** AL6061 alloys are high-potential materials for many manufacturing sectors including automobiles, aerospace, electrical, military, sports and engineering components, owing to their better technological properties. Through the thermal erosion process of Electrical Discharge Machining (EDM), an electrically-produced spark vaporizes materials that are electrically conductive. This study examines the viability of improvement of material removal rate in the micro-electric discharge machining of AL6061 alloy using Fe<sub>2</sub>O<sub>3</sub> nano-powder-mixed dielectric fluid. For the purpose of this research, a copper electrode with 500 $\mu$ m diameter and positive polarity was used. The performance measures of the machining process were investigated regarding the material removal rate (MRR). one concentration of nano-powder were added to dielectric (4g/l). Results showed that if Iron oxide nano-powders (Fe<sub>2</sub>O<sub>3</sub>) exists in the dielectric, MRR can be significantly improved.

**Keywords:** Powder-mixed Micro -EDM, Fe<sub>2</sub>O<sub>3</sub> nano-powder, Material removal rate (MRR).

## 1. INTRODUCTION

process currently applied to the production of various tools and molding industries is electrical discharge machining (EDM) that can be properly used for machining of electrically-conductive parts and also this method is capable of generating complex shapes with no limitation in the material hardness [1]. One of the most proficient modern machining processes regarding the size and the precision of products is Micro-EDM, which outperforms other fabrication processes like a laser, LIGA, ultrasonic ion beam, and so on. [2]. Micro-EDM ( $\mu$ EDM) is broadly applied to the field of micro-mould making and the generation of dies, cavities, and complex 3D structures [3]. In the technologies of EDM/ $\mu$ EDM, one of the latest advancements is powder-mixed electric discharge machining (PMEDM) that works with the addition of powder particles to dielectric for improving machining rate. Suspended particles cause a reduction in the dielectric overall electrical resistivity, and they allow sparking to occur from a larger distance. Flushing conditions and the improved spark frequency together with multiple sparks lead to the simultaneous improvement of material removal rate [4]. AL6061 alloy is widely used in dies and moulds industry. The 6000 series aluminum have many alloys with different names and properties. Al 6061 alloy is one of the most extensively used of these series [5].

Various researchers have added different powders to dielectric fluids for improving the material removal rate. The investigation of (Jahan, M P et., al 2010) employed nano-powders of graphite, Al, and Al<sub>2</sub>O<sub>3</sub> for PM $\mu$ EDM of WC10%Co alloy [6]. The authors reported no significant effect was found with Al<sub>2</sub>O<sub>3</sub> while Al and graphite powders significantly improved MRR and surface quality. The study by (Assarzadeh and Ghoreishi, 2012) investigated the effect of electrical and non-electrical process parameters on MRR and SR during PMEDM of CK45 alloy. The selected dielectric additives used were Al<sub>2</sub>O<sub>3</sub>, Cu, and SiC. The experiments were conducted using RSM design whereas

optimization was determined using the desirability approach [7]. (Kansal *et al.*, 2007) found that The suspension of silicon powder into the dielectric fluid of EDM appreciably enhances material removal rate [8]. In a separate study (Jahan *et al.*, 2011) investigated the feasibility of improving the surface characteristics of cemented tungsten carbide (WC-Co)- die and mould material during micro-EDM. Comparative performance analysis of powder-mixed sinking and milling micro-EDM has been examined. It was observed that semi-conductive nano-size graphite powder in the dielectric significantly improved surface finish, MRR and reduced EWR [9]. In addition, according to (NM elsit *et al.*, 2017) MRR can be significantly improved when Fe<sub>2</sub>O<sub>3</sub> nano powder was added to dielectric fluid during micro-EDM of Co-Cr- Mo [10].

## 2. EXPERIMENTAL DETAILS

The experiments in the present research were conducted on an AG40L Sodick electrical discharge machine (see Fig.2). Copper electrodes with a diameter of 500 $\mu$ m were selected and utilized as tool material. This is due to its low cost, good machinability, and fine surface finish potentials. The commercially available "EDM 23" oil was selected as the dielectric fluid in this study. The weights of the electrodes and workpiece(s) were measured using the Precision Balance (Model: Pioneer™) before and after each micro-EDM process. This is a digital weighing scale capable of obtaining 0.0001-g precision and maximum weights of 200 g. The results of the Micro-EDM of AL6061 was planned and analyzed using Design of Experiments (DoE) software, Design-Expert *version 7*. The maghemite nano-particles ( $\gamma$ -Fe<sub>2</sub>O<sub>3</sub>) with size <10 nm, were added to the dielectric fluid in concentration (4g/l). The powder mixed EDM experiments were conducted in an in-house designed machining tank with dimensions; 46 cm  $\times$  35 cm  $\times$  24 cm. The tank was fabricated with 1.5 mm thick stainless steel sheets as shown in Figure 3.22. The selected process parameters were; peak current (A), voltage (B), and pulse-on time (C). The measured response

was MRR. Table 3.9 illustrates the experimental plan and design.

**Table 1. Experimental plan and design**

Exp no	A (Current) (Ip)	B (Voltage) (V)	C (Pulse on) (µs)
1	1.5	60	10
2	3	60	10
3	1.5	120	10
4	3	120	10
5	1.5	60	200
6	3	60	200
7	1.5	120	200
8	3	120	200
9	2.25	90	105
10	2.25	90	105
11	2.25	90	105

The MMR is calculated from the mathematical expression in Eq 1:

$$MRR = [(W1 - W2) / (t \times \rho)] \times 1000 \text{ (mm}^3/\text{min)} \quad (1)$$

The terms  $W1$  and  $W2$  represent the initial and final weights of the workpiece, respectively. The terms  $\rho$  denote the density ( $\text{g}/\text{mm}^3$ ) of the workpiece whereas  $t$  denotes the machining time (min).



Figure 1. Working Tank



Figure 2. AG40L Sinker EDM

### 3. RESULTS AND DISCUSSION

As observed from the table 3, the factors A and C significantly influence the Material Removal Rate (MRR1). The results indicate that the interaction between the process parameters peak current and pulse on time is significant for MRR1. The effect plot of the process parameters on MRR 1 are shown in Figures 3. The material removal rate (MMR) during EDM is a function of the electrical discharge energy. In principle, an increase of peak current generates high energy intensity resulting in increased melting of the workpiece material. According to Figure 4, the MRR2 increases with a corresponding increase in gap voltage and current. This is because higher voltage increases the spark gap, thereby

improving flushing conditions during the machining process. It is evident from same figure that there is a strong interaction between current and voltage. Pulse on time also had significant effect on MRR2. As observed, the lack of fit had an insignificant effect as expected for the MRR1 and MRR2 responses. As a result, all of the insignificant factors were removed to improve the models. The results for MRR1,2 demonstrated that R-squared value (0.8139,8563), which are ~ 1, is desirable. Hence, there was only a marginal difference (< 0.2) between the Adj.  $R^2$  and Pred.  $R^2$ . This indicates a suitable correlation exists between the input and output parameters of the model. Accordingly, the final regression models based on actual prediction factors for MRR1,2 are presented in Eq. 2,3.

$$MRR1 = 0.053 + 0.028 * A - 0.042 * C - 0.025 * AC \quad (2)$$

$$MRR2 = 0.12 + 0.095 * A + 0.02 * B - 0.041C + 0.033 * AB \quad (3)$$

In addition, findings in figure 7 showed that the addition of 4 g/l of  $\text{Fe}_2\text{O}_3$  nano-powder to the dielectric fluid increased the MRR. Likewise, the increase in powder concentration from 0 to 4 g/l enhanced the MRR.

**Table 2. Experimental plan and results**

Exp no	Ip	V	ton	MRR1 Without nanopowder ( $\text{mm}^3/\text{min}$ )	MRR2 4g/l-nanopowder ( $\text{mm}^3/\text{min}$ )
1	1.5	60	10	0.0743027	0.09816
2	3	60	10	0.173766	0.235063
3	1.5	120	10	0.0214707	0.0476361
4	3	120	10	0.132275	0.345598
5	1.5	60	200	0.00643004	0.0186865
6	3	60	200	0.0182997	0.129199
7	1.5	120	200	0.0182516	0.019114
8	3	120	200	0.0203687	0.230719
9	2.25	90	105	0.026936	0.0305747
10	2.25	90	105	0.0124634	0.0733407
11	2.25	90	105	0.0838939	0.0979274

**Table 3: Analysis of variance (ANOVA) test for MRR1**

Source	Sum of squares	DF	Mean Square	F Value	Prob>F
A-Current	6.28E-	1	6.286E	7.57	0.0285
C-Pulse on	0.014	1	0.014	17.24	0.0043
AC	4.816E	1	4.816E	5.8	0.0469
Residual	5.814E	7	8.306E		
Lack of fit	2.962E	5	5.925E	0.42	0.8147
Core total	0.031	10			
$R^2$	0.8139	Adj- $R^2$	0.7341	Pred $R^2$	0.5909

**Table 4: Analysis of variance (ANOVA) test for MRR2**

Source	Sum of squares	DF	Mean Square	F Value	Prob>F
A- Current	0.072	1	0.072	78.17	0.0003
B- Voltage	3.279E-	1	3.279E-	3.58	0.1171
C-Pulse on	0.014	1	0.014	14.74	0.0121
AB	8.590E-	1	8.590E-	9.37	0.028
Residual	4.582E-	5	9.163E-		
Lack of fit	2.258E-	3	7.528E-	0.65	0.6539
Core total	0.11	10			
R <sup>2</sup> -	0.8563	Adj-R <sup>2</sup>	0.7604	Pred R <sup>2</sup>	0.5968

#### 4. CONCLUSION

The current study was aimed to examine the possibility of the improvement of material removal rate of AL6061 in Micro-EDM using Fe<sub>2</sub>O<sub>3</sub> nano-powder-mixed dielectric. The conclusions of this experimental study are as follow:

- The ANOVA analysis for MRR1 and MRR2 responses summarized that current, voltage, and two-level interaction between voltage and current were significant factors. Findings showed that with the increase of current, MRR increased, too. This was due to the rising amount of heat and energy transmitted to the workpiece for melting and vaporization.
- During the fine-finish powder-mixed Micro-EDM of AL6061, if 4g/l Fe<sub>2</sub>O<sub>3</sub> nano-powder is added to dielectric liquid, MRR can be improved.

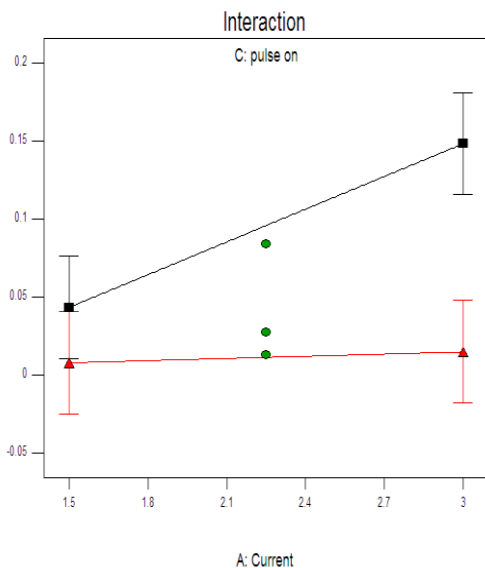


**Fig 3.** Effect plot showing variation of MRR1 with process parameters

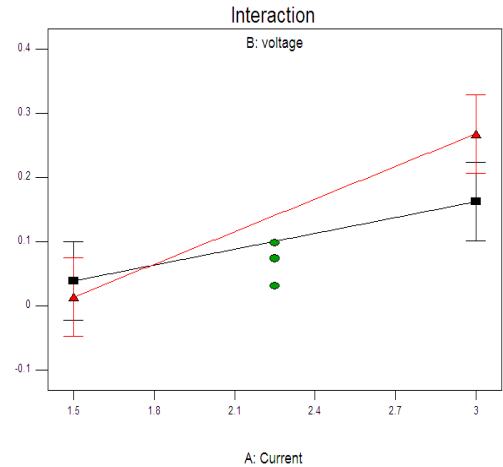


**Fig 4.** Effect plot showing variation of MRR2 with process parameters

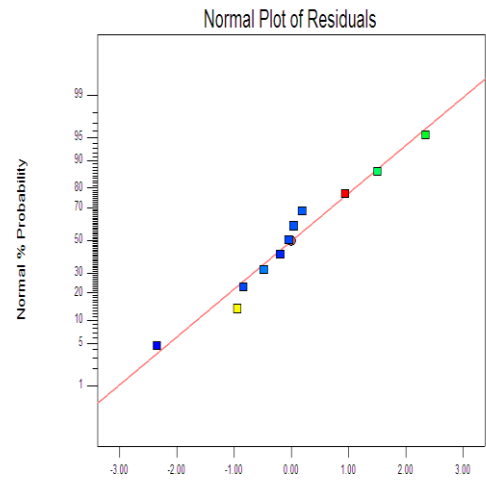


**Fig 5.** Show normal plot of residuals for MRR1

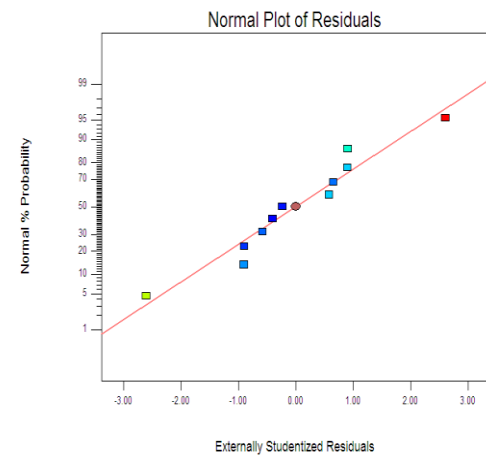


**Fig 6.** Show normal plot of residuals for MRR2

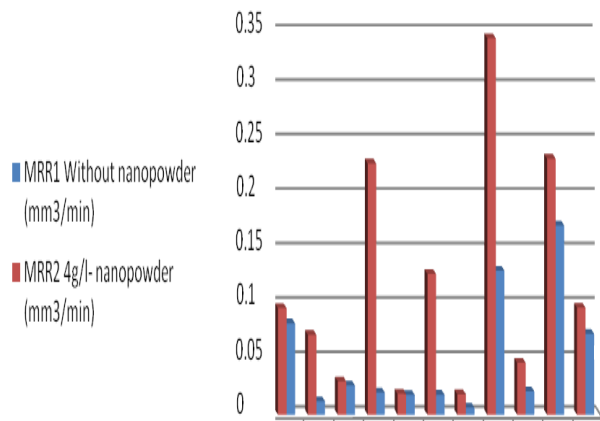


Fig 7. Material removal values

## 5. REFERENCES

1. Singh, S., S. Maheshwari, and P.C. Pandey, *Some investigations into the electric discharge machining of hardened tool steel using different electrode materials*. Journal of Materials Processing Technology, 2004. **149**: p. 272-277.
2. Bilal, A., et al., *Electro-Discharge Machining of Ceramics: A Review*. Micromachines, 2019. **10**(1): p. 10.
3. Maity, K.P. and M. Choubey, *A review on vibration-assisted EDM, micro-EDM and WEDM*. Surface Review and Letters, 2018. **26**.
4. Joshi, A.Y. and A.Y. Joshi, *A systematic review on powder mixed electrical discharge machining*. Heliyon, 2019. **5**(12): p. e02963-e02963.
5. Sankaran, K.K. and R.S. Mishra, *Chapter 4 - Aluminum Alloys*, in *Metallurgy and Design of Alloys with Hierarchical Microstructures*, K.K. Sankaran and R.S. Mishra, Editors. 2017, Elsevier. p. 57-176.
6. Jahan, M.P., M. Rahman, and Y.S. Wong, *Modelling and experimental investigation on the effect of nanopowder-mixed dielectric in micro-electrodischarge machining of tungsten carbide*. Proceedings of the Institution of Mechanical Engineers, Part B: Journal of Engineering Manufacture, 2010. **224**(11): p. 1725-1739.
7. Assarzadeh, S. and M. Ghoreishi, *A dual response surface-desirability approach to process modeling and optimization of Al<sub>2</sub>O<sub>3</sub> powder-mixed electrical discharge machining (PMEDM) parameters*. The International Journal of Advanced Manufacturing Technology, 2012. **64**.
8. Kansal, H.K., S. Sehijpal, and P. Kumar, *Effect of silicon powder mixed EDM on machining rate of AISI D2 die steel*. Journal of Manufacturing Processes, 2007. **9**: p. 13-22.
9. Jahan, M.P., M. Rahman, and Y.S. Wong, *Study on the nano-powder-mixed sinking and milling micro-EDM of WC-Co*. The International Journal of Advanced Manufacturing Technology, 2011. **53**(1): p. 167-180.
10. Elsitei, N.M. and M.Y. Noordin, *Experimental Investigations into the Effect of Process Parameters and Nano-Powder (Fe<sub>2</sub>O<sub>3</sub>) on Material Removal Rate during Micro-EDM of Co-Cr-Mo*. Key Engineering Materials, 2017. **740**: p. 125-132.

# The Optical Properties of Indocyanine Green suspended in Solution as Observed under Near Infrared LED and LASER Light Conditions

Angharad Curtis  
Wireless &  
Optoelectronics  
Research and  
Innovation Centre,  
University of South  
Wales  
Pontypridd, Wales,  
UK

Kang Li  
Wireless &  
Optoelectronics  
Research and  
Innovation Centre,  
University of South  
Wales  
Pontypridd, Wales,  
UK

Mohammed Ali  
Roula  
School of  
Engineering,  
University of South  
Wales  
Pontypridd, Wales,  
UK

Nigel Copner  
Wireless &  
Optoelectronics  
Research and  
Innovation Centre,  
University of South  
Wales  
Pontypridd, Wales,  
UK

**Abstract:** The use of Indocyanine Green (ICG) as a fluorescent marker at Near Infrared (NIR) excitation wavelengths is well established in clinical imaging. Typical systems comprise multiple LED sources for optimal imaging which can result in unnecessary energy transfer to patients and contribute to tissue damage. An experimental setup comprising a 780 nm excitation channel generating up to 10 mW of optical power is used in order to determine if there is potential to exploit the optical properties of ICG, in order to reduce the total excitation power through pulsing. We demonstrate in this work that a single 1.6 Megapixel CMOS camera with quantum efficiency of less than 30% is appropriate to capture both fluorescent and non-fluorescent landmarks at NIR wavelengths. Experimental results verify that all ICG solutions tested yielded detectable fluorescence and that degradation of fluorescence intensity over time is multifaceted.

**Keywords:** Fluorescence Imaging, Indocyanine Green (ICG), Fluorescence Endoscopy, In-Vitro Testing, Fluorescence Spectrometry

## 1. INTRODUCTION

There are a number of detailed reviews in the literature related to the fluorescent chemical marker Indocyanine Green (ICG) and its importance in clinical imaging [1, 2]. ICG is excited with either LED, Xenon or LASER light at NIR wavelengths causing fluorescence. This essentially illuminates cells which have absorbed and retained the fluorescent marker during minimally invasive surgery, allowing for a more efficient and complete resection of diseased tissue. ICG is currently one of two FDA approved dyes at this wavelength range [3] and has been approved for medical use since the 50's [1].

The fluorescence decay rate and photobleaching properties of ICG for fluorescence endoscopy are not well documented but are crucial to understand. The literature related to the photobleaching effect of ICG appears conflicting [4-6] and there is currently no standardization regarding test procedures and no consistency in findings. If the optical properties are identified, there could be opportunity to exploit them so that ICG usage in general can be optimized resulting in enhanced patient safety.

Typically, when using ICG as an identifying marker for diseased tissue, a white light channel is required in order to view non-fluorescent/unmarked landmarks within the frame such as blood vessels. The NIR and white light channels individually, do not allow for a complete resection of diseased tissue with minimal removal of healthy tissue as the imaging conditions are not optimal and this can prove dangerous [7]. The most successful protocol is to combine data from both channels which involves possible risks and complications. The main risk being excessive excitation used thus exposing the patient to a higher risk of thermal damage during minimally invasive surgical conditions

An experimental four channel LED multiplexer [8], awaiting clinical trials, designed to replace the 'light box' component

in fluorescence endoscopy focuses red, green blue and near infrared LED light to a liquid light guide. The small aperture of the liquid light guide sets the etendue limit. Heat is produced as a by-product from the illumination source and can become intense causing permanent damage to tissue [9, 10]. Optical power of the NIR source needs to reach the desired penetration depth without adding to the unwanted thermal output [11]. Optical power used in this research is between 5 mW and 10 mW in agreement with relevant work in the literature [12-14]. The literature also suggests that excitation could be pulsed to reduce the thermal effects [15].

In this work we demonstrate the viability of a system comprising a pulsed excitation channel and a single CMOS detector with the aim to image ICG-stained samples using an inexpensive camera in order to capture residual fluorescence and determine the relationship between thermal decay and photobleaching. While this work relates to an endoscopy application for the detection of cancerous tissue in the breast using ICG as a chemical marker, the experimental work is conducted in a laboratory environment using a wide-field approach for various reasons.

## 2. MATERIAL AND METHODS

Samples of various concentrations of ICG solution were prepared for this experimental research. The ICG (Tokyo Chemical Industry UK Ltd) is mixed with Human Serum Albumin (HSA) in order to enhance stability and fluorescence [12-13, 16]. The samples are illuminated with either LED or LASER excitation at 780 nm (Thorlabs L780P010 and Thorlabs LED780E respectively) in order to excite the chemical marker causing it to fluoresce. This fluorescence is detected using a spectrometer (Ocean Optics USB4000) and captured via a CMOS camera with signal to noise ratio of 40.48 dB. Data collected is processed to determine if it is possible to detect any residual fluorescence at the instant

excitation is removed as well as confirming the decay rate of fluorescence and the parameters contributing to this.

## 2.1 ICG Sample Preparation

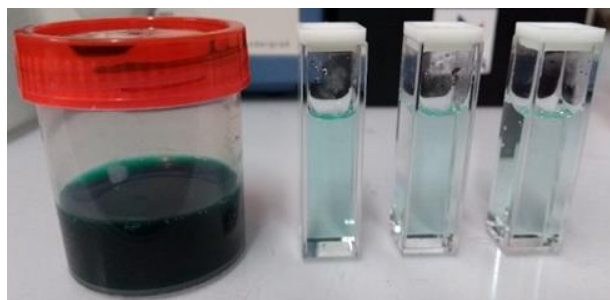


Figure 1: An image showing the ICG stock solution and diluted samples in cuvettes

ICG and HSA (PAN Biotech UK Ltd) are mixed in a 1:1 molar ratio consistent with relevant literature [12, 15-16]. A 1000  $\mu\text{Mol}$  solution was prepared allowing for a sufficient dilution level for the desired range of concentrations analyzed. In order to prepare 30ml of stock solution at a concentration of  $1 \times 10^{-4}$  Mol, 111.7 mg of HSA and 23.2 mg ICG are dissolved in 30 ml deionized water. This solution is diluted down to 1000  $\mu\text{Mol}$  or  $1 \times 10^{-6}$  Mol by pipetting 0.10 ml of stock solution into 9.90 ml of deionized water. A solution is prepared daily and kept under dark conditions. The temperature of the ambient environment is monitored throughout using a thermometer fitted with an external probe and recorded frequently. There was no significant change in ambient temperature to note. Figure 1 shows the stock solution stored in a plastic container alongside three cuvettes filled with diluted samples of varying concentration. The stock solution does not fluoresce and is the lowest concentration of ICG:HSA achievable with the available apparatus. It is essential to use a transparent mixing vessel to prepare the sample to ensure that the dry constituents are dissolved however, this is kept covered to protect the sample from ultraviolet (UV) degradation.

## 2.2 Experimental Setup

Two similarly arranged systems are assembled for this experiment. One comprises a LA-SER (insert A) light source while the other utilizes a single LED (insert B) as shown in Figure 2. Both the LASER and LED emit light at a central wavelength of 780 nm. The output power of the LASER is manually set to either 5 mW or 10 mW by adjusting the current in mA. A calibration curve is plotted to convert the corresponding current to output power by reading the results from a power meter (Thorlabs PM100A fitted with a S302C Head) while adjusting the current in small increments. Once the power threshold has been met, the relationship between current and optical power is linear. A simple circuit is setup to control the LED providing 1.75 V and comprising an LED controller unit (Gardasoft CC320) for computer controlled on/off and pulsing. Forward optical power for the LED is documented as 7.2 mW within the technical specifications which corresponds with the power meter readings taken from the perspective and positioning of the cuvette. Table 1 shows the subsequent power at the surface of the sample.

Table 1: Power conversion for each illumination condition

Illumination Source	Power (mW)	Power at the sample surface (mW/cm <sup>2</sup> )
LED	7.2	36.67
LASER	5.0	70.74
LASER	10.0	141.47

For continuity, key apparatus such as the spectrometer, power meter, thermometer and CMOS camera are disconnected and swapped out as and when needed so that the optical stages and mounts can remain fixed. The camera used is a BlackFly 16S2M CMOS which is powered and controlled via a USB 3 port, the quantum efficiency of the incorporated sensor (SONY IMX273) at 800 nm is around 26 %. The camera resolution is 1440×1080 and the pixel size is 3.45  $\mu\text{m}$ . The power meter detector and the fiber end of the spectrometer can interfere with imaging due to reflection, so these are arranged in a flexible mode whereby they are simply set out of the frame when unused. Two thermometers with external probes are also used during data collection. One is used to monitor the temperature of the ambient environment while the other can be placed inside the cuvette and sub-merged in its liquid contents. All experiments are completed under dark conditions with the analysis post data acquisition. The insert C in Figure 2 shows a schematic of the sample as seen from the perspective of the CMOS camera which is arranged perpendicular to the excitation source. (1) contains the liquid sample only, (2) contains the liquid sample with the probe end of the thermometer in position and (3) shows the fiber end of the spectrometer visible through the liquid contents. Images are not collected under condition (2) or (3) from the figure due to the unwanted reflection caused from the surface of the temperature probe and the spectrometer fiber respectively.

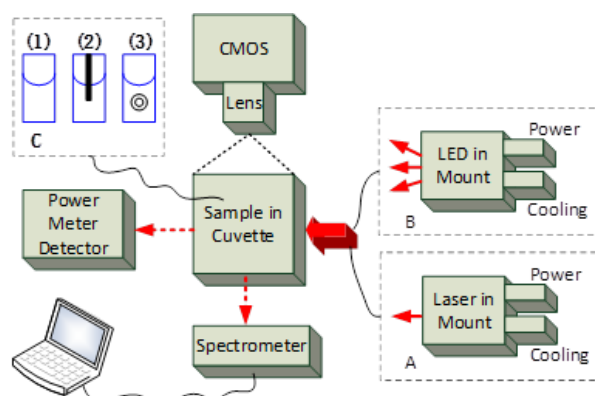


Figure 2: A schematic showing the arrangement of apparatus used during testing (not drawn to scale). Part A features a LASER diode as the excitation source while part B uses a single LED. All other equipment is swapped between the two arrangements.

Although 780 nm is visible to the naked eye, a beam viewer card was used during the LASER setup to ensure that the beam is striking the cuvette at the center of the first surface and exiting the final cuvette surface without distortion. The beam is not collimated but an aspheric lens is used to minimize optical aberration. The spot size, 3 mm was reflected only with inaccurate placement, no reflection is detected within the cuvette following correct positioning in parallel to the source. As the cuvette is positioned manually, inaccurate positioning can result in reflection and scatter which are visible at the furthest corners of the cuvette with respect to the source. This is evident from the images collected such as that seen in Figure 3 and can be rectified with very gentle twisting of the vessel. The housing of the LED allows for a much simpler aligning to the central face of the cuvette which is achieved with the LED off.

### 2.3 Data Collection

Data collected from the CMOS camera is analyzed in a custom LabVIEW programme utilizing the vision and motion palette. The programme displays an intensity analysis of pixels within a user-controlled Region of Interest (ROI). This ROI is saved to memory to keep the position and size consistent between images and can also be re-sized and re-positioned when needed. Data from the images is available in real-time and with units according to the parameter under investigation. These numerical values are entered into a spreadsheet ready for plotting using software visualization and analysis tools. The Lab-VIEW programme allows extraction of various features such as the mean intensity of the region given in grayscale values and the minimum and maximum intensity which provides the contrast available for example, at the border of fluorescence. This can also be useful when looking at the intensity of the fluorescence across the pathlength of the cuvette to understand the effect of absorption of the fluorescent material.

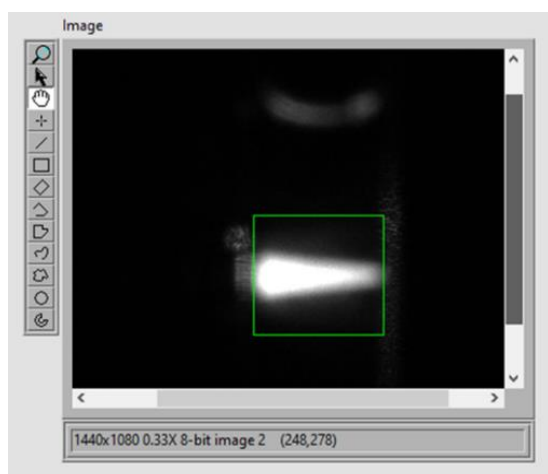


Figure 3: Front end view of the ROI selection of an image showing a 1000  $\mu\text{Mol}$  ICG:HSA solution fluorescing within a cuvette. The excitation source is a 10 mW LASER at 780 nm and exposure time is 249998  $\mu\text{s}$ . The cuvette walls and meniscus are useful landmarks for analysis and are visible due to scattering.

Spectrometer data is exported from the OceanView software in csv format which is then analyzed. Data collection was repeated six times to enable computation of the mean and standard error. Unfortunately, the spectrometer traces collected show noise across the wavelength range for all repetitions and so a Savitzky-Golay smoothing function was applied to filter out the noise while preserving the shape of the peak. The smoothed spectrometer data is plotted to show the relative intensity of fluorescence for each excitation source and concentration on test. The power meter and temperature data are recorded manually from their respective display interfaces and processed before plotting, processing again involves calculation of the mean and the corresponding standard error.

The camera frame rate and LED pulses are software controlled. SpinView is used to set the camera frame rate through adjusting the exposure time in microseconds to a minimum of 4855  $\mu\text{s}$  resulting in a maximum of 199.98 frames per second  $\sim 200$  Hz. Gardasoft Maintenance software connects the LED controller to the laptop via Ethernet connection. The values are entered manually with a minimum available pulse rate of 0.1 ms. The LED can also be set high (on) or low (off) and the time on phase and time off phase set independently. Timings and pulse rates are recorded in a spreadsheet before each repetition and assigned an alphanumeric code with images saved under a file name with a corresponding code. The SpinView software allows for consecutive images to be collected as either a specified number of frames whereby the frame rate is known or, as a specified number of seconds worth of data capture, again assuming that the frame rate is known and does not exceed the maximum limit of the hardware resulting in dropped frames. Consecutive images can then be analyzed in LabVIEW by simply running through them frame by frame in a similar fashion to if each data set were a video clip. Figure 3 shows the image loaded into LabVIEW with the ROI appearing as the Green boundary. The sides of the cuvette and meniscus of the solution are visible due to scattering which are useful landmarks for analysis.

### 3. RESULTS

Fluorescence data is collected under each excitation condition and the results are presented in Figure 4. Here we can see that the fluorescence wavelength is centered around 815 nm, 35 nm longer than the excitation. Each figure shows the wavelength range of the spectrometer along the x-axis with the y-axis representing the relative intensity of fluorescence in spectrometer units. There are three spectra per figure to correspond with the three excitation conditions. Figure 4 displays the fluorescence spectra detected at each concentration of ICG in solution and illumination condition on test. Fluorescence intensity is highest under 10 mW LASER excitation with the LED producing a more intense fluorescence than the 5 mW LASER condition. Consistent with literature [13, 18-19], the lowest concentration on test provided the highest fluorescence intensity under each excitation condition, this is due to secondary mechanisms

related to formation of molecule aggregation. The data presented in Figure 4 represent repeat testing as to avoid errors due to rogue mixing or dilution calculations. The spectrometer collects fluorescence data at intervals of 0.2 nm, an error analysis is displayed in Table 2 representing the peak wave-length value ~818 nm for simplicity. The power values at 818nm are displayed in Figure 4(f).

The reference cuvette containing deionized water shows no fluorescence in Figure 4(e) as expected when excited with the 5 mW and 10 mW LASER source. Figure 4(e) shows the LED spectra with a central peak at 780 nm. The reason for this is due to the di-vergence of the LED beam, the light that travels through the cuvette containing water at the excitation wavelength is detected by the spectrometer head. No fluorescence is detected due to the lack of ICG in the sample. As the results presented in Figure 4(e) represent the excitation wavelength of the LED only, we have a better understanding of the “intensity” which accounts for the y-axis of the spectra in Figure 4. The spectrometer and accompanying software define fluorescence as a measurement of the relative irradiance which is not a quantified numerical value. The LED provides just over 7 mW of forward optical power and so the peak represented by the cuvette containing water only represents a fraction of the source which has travelled through two cuvette walls (optical glass) and a volume of water to reach the detector positioned perpendicular to the source. For reference, the cuvettes have a pathlength of 10 mm and the glass thickness is 1.25 mm.

which would saturate the image, consideration of exposure time, excitation power and ICG concentration will yield the most useful images whereby all fluorescent regions are clearly visible without any areas of saturation.

No filtering was applied to the camera setup as confirmed by the spectrometer results. With the exception of water under LED excitation, there is no source wavelength within the results. The camera is in an equivalent position to the spectrometer, in parallel to the source so that the cuvette and its contents are imaged. Images are collected every 60 seconds for 10 minutes at an exposure time of 124998  $\mu$ s, a power meter reading is recorded manually at 5 seconds intervals to confirm the camera data and assess the presence of photobleaching or decay in fluorescence over time.

The power meter readings are presented in Figure 6(a), (b) and (c) and the camera data for the 10 mW excitation with the corresponding camera data are shown in Figure 6(d), (e) and (f). For clarity, no filter has been applied.

**Table 2: Error analysis at the fluorescence wavelength peak of 818 nm**

<b>Solution</b>	<b>5mW LASER Excitation</b>	<b>10mW LASER Excitation</b>	<b>LED Excitation</b>
400 $\mu$ Mol	$\pm 5.02$ nm	$\pm 5.39$ nm	$\pm 4.1$ nm
600 $\mu$ Mol	$\pm 3.91$ nm	$\pm 3.91$ nm	$\pm 2.43$ nm
800 $\mu$ Mol	$\pm 3.91$ nm	$\pm 3.54$ nm	$\pm 0.96$ nm
1000 $\mu$ Mol	$\pm 2.07$ nm	$\pm 2.07$ nm	$\pm 0.22$ nm

To quantify the intensity of the fluorescence, the spectrometer data is used in support of an analysis using images captured with a single CMOS camera. Figure 5(a), (b) and (c) show the maximum, mean and total intensity of the ROI respectively for each concentration and excitation source on test. Images collected are opened in LabVIEW and a region of interest is drawn manually encompassing the contents of the cuvette and excluding the light source. An analysis was conducted in order to obtain the intensity values for pixels within the selected region. These values are plotted and presented to complement the data collected via spectrometry. The CMOS camera images are unfiltered hence the reason for a higher intensity under LED excitation, not observed in the spectrometer results. Figure 5(a) displays the maximum intensity of pixels within the region and Figure 5(b) the mean in-tensity. The upper intensity limit is 256 grayscale units

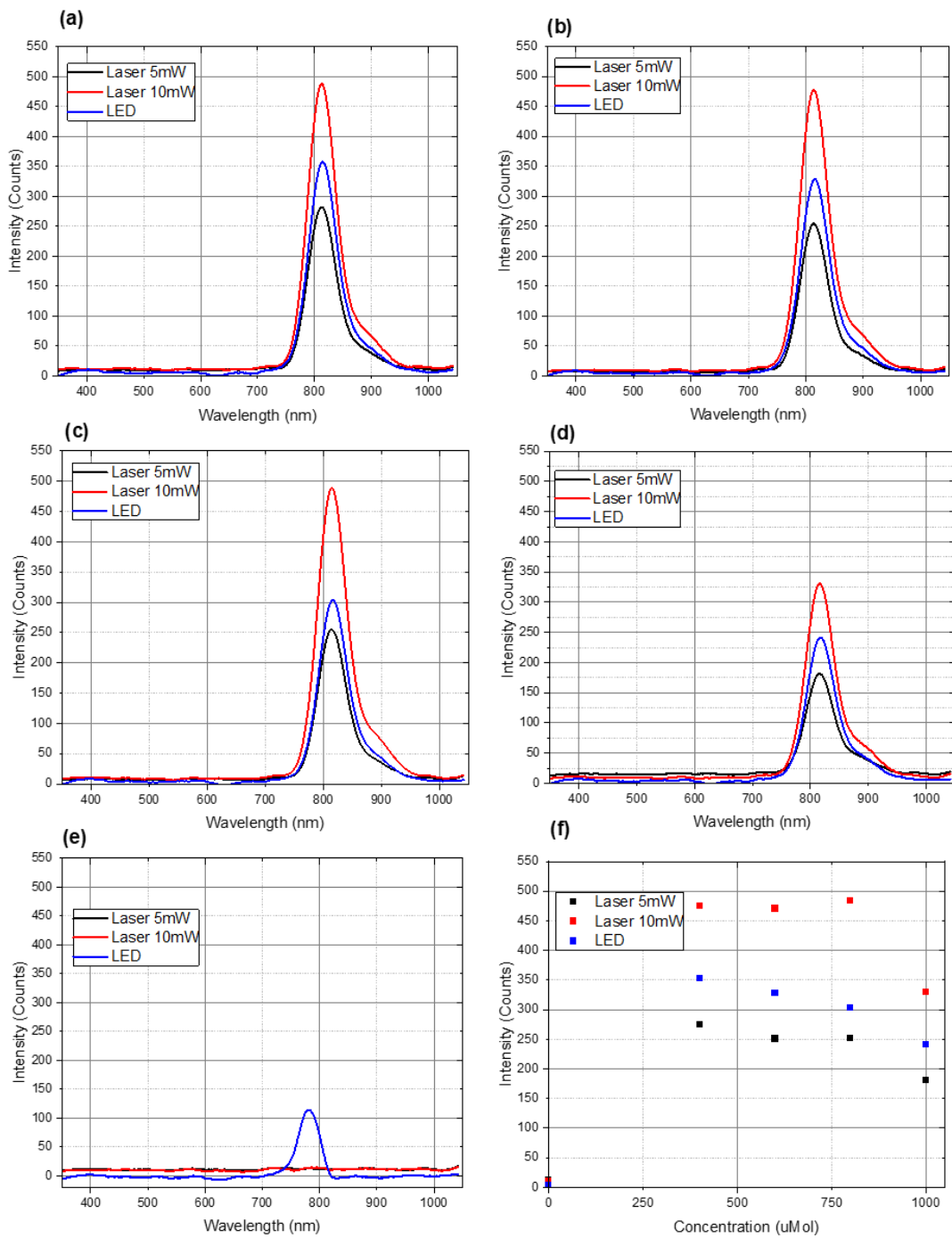


Figure. 4. Averaged and smoothed emission spectrometer data for a 400 μMol (a), 600 μMol (b), 800 μMol (c), 1000 μMol (d) solution of ICG:HSA, Water (e) as a reference and the peak power of fluorescence at 818nm (f), n=6

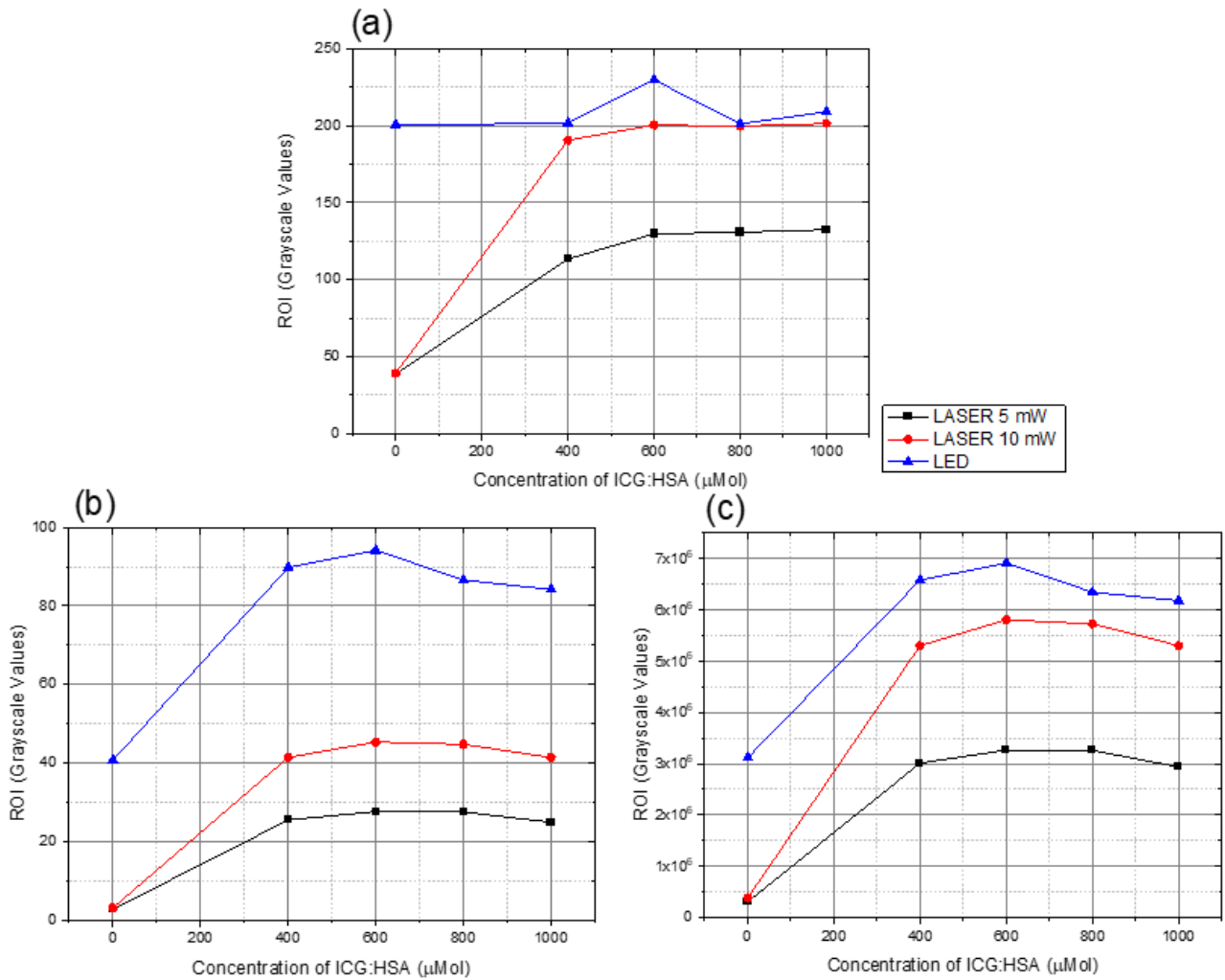


Figure 5. The maximum (a), mean (b), and total (c) intensity of pixels within the selected region for each concentration of ICG:HSA under each excitation condition,  $n=1$ . Image captured at an exposure of  $78124 \mu\text{s}$  and the ROI represents an average area of 107618 pixels

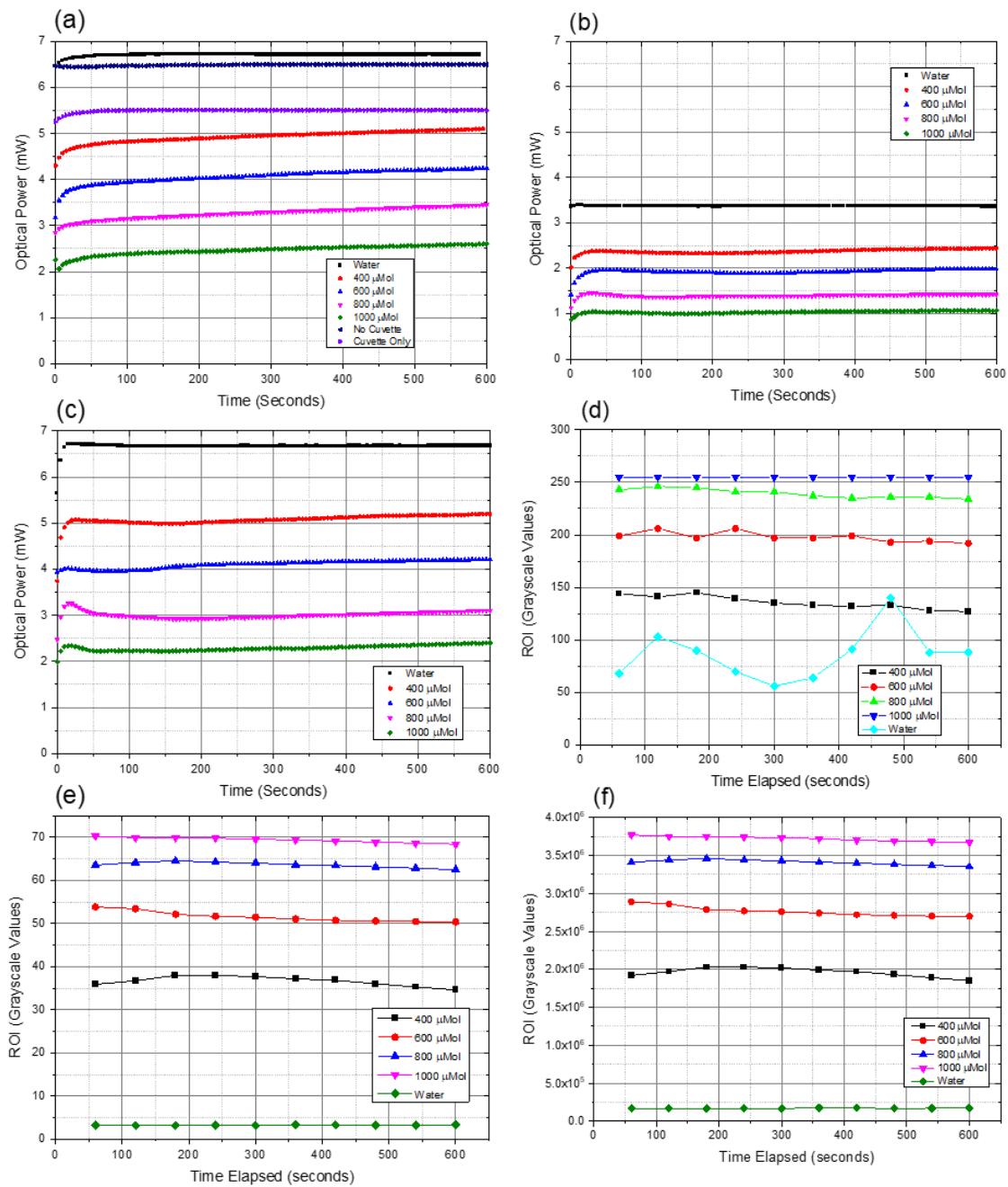


Figure 6: A plot showing the change in optical power with time using a power meter linear to the LED (a), 5mW LASER (b), and 10mW LASER (c), n=3; and maximum (d), mean (e), and total (f) intensity of pixels within the selected region for each concentration of ICG:HSA under 10 mW LASER excitation over a time period of 10 minutes, n=1. The image was captured at an exposure of 124998 μs and the ROI represents an area of 53578 pixels

Figure 6(a), (b) and (c) show how the optical power changes with time for each excitation condition with a range of samples on test. The power meter detector is arranged in parallel with the excitation source so that excitation light passes through the sample before detection. Optical power values were recorded every 5 seconds and plotted to determine the relationship between the cuvette contents, the optical power, the excitation source and time.

Figure 6(d), (e) and (f) present the maximum, mean and total pixel intensities respectively calculated in LabVIEW. Images are analyzed with a region of interest protocol as per the previous figure, Figure 5(a), (b) and (c) however, a string of images are analyzed in sequence in order to understand the relationship between the pixel intensity and time under excitation. With this data we can determine if there is any photobleaching present and which excitation condition and sample is most affected.

**Table 3: Degradation of the fluorescence (T=0 minutes – T=10 minutes)**

Solution	10mW LASER Excitation with Camera Perpendicular to Source (Grayscale values per minute)	10mW LASER Excitation with Power Meter Opposite the Source (mW per minute)
400 $\mu\text{Mol}$	0.13	-0.14
600 $\mu\text{Mol}$	3.47	-0.03
800 $\mu\text{Mol}$	1.08	-0.06
1000 $\mu\text{Mol}$	1.84	-0.04
Water	-0.10	-0.10

The results indicate degradation of the fluorescence at a varying rate as displayed in Table 3, the mean pixel intensity values are used in column 2 taken from Figure 6(e) and optical power for column 3 taken from Figure 6(c). It is important to note the apparatus orientation as this can provide explanation as to why the power meter values are negative. The power meter is arranged opposite the source as seen in Figure 2 which would not necessarily indicate the rate of fluorescence decay. The optical power detected at the beginning of the experiment is less than that after an observation period of 10 minutes hence the negative values. It is reasonable to assume that over time the fluorescent material within the cuvette absorbs energy and will begin to photobleach once the threshold has been reached. More source energy is detected as absorption reduces following a reduction in available fluorophores, which also reduces the overall intensity of fluorescence. Source energy passing through the cuvette without absorption will be detected as the power meter cannot distinguish spectra. The power detected with the power meter is composed of fluorescence and source spectra. Without using a filter this cannot be verified but is an observation from experimental work as we have confirmed that fluorescence has also de-decreased over time. No filter was used so as to simplify the system and to verify that a filter is not essential when using a single camera detection technique.

Temperature within the cuvette is recorded and the average temperature increase over a period of 11 minutes is presented in Table 4. The LASER is connected to a thermoelectric cooler in order to maintain the operating temperature for output stability, the LED is not connected to an active thermal management system during experiment as it is mounted in a custom aluminium holder. The differences in thermal management is likely to have a significant effect on temperature within the cuvette as shown in the following Table 4.

**Table 4: Temperature within the cuvette**

Illumination	Temperature Change
5 mW LASER	+0.13 $^{\circ}\text{C}$
10 mW LASER	+0.30 $^{\circ}\text{C}$
LED	+0.60 $^{\circ}\text{C}$

A GPIO trigger was connected between the LED controller and the camera in order to synchronize data collection. The lowest framerate possible at 4855  $\mu\text{s}$  was selected so that once the LED channel is set low, the camera channel is set high and an image is captured. The following figure (Figure 7) shows a schematic representation of the protocol followed whereby  $\Delta K$  is the time the LED is on,  $\Delta T$  is the time between the LED channel off and camera channel on and  $\Delta S$  is the exposure time, all are changeable parameters. No combination of testing conditions has resulted in any detectable fluorescence in the frame captured as soon as the excitation is switched off. This confirms that the ICG:HSA solutions on test do not have a lasting fluorescence decay that is detectable at frame rates of 199.98 Hz or lower. There is no present residual “glow effect” following excitation and therefore the fluorescent marker cannot be exploited by imaging it using a pulsed source and a corresponding negatively pulsed detector at a rate of 200 Hz or lower. This could have had a significant impact on patient safety during endoscopic diagnostics and therapy if viable. Literature indicates that femtosecond [20] and picosecond [21] pulse rates are appropriate for capturing ICG decay however, this system is limited by the human eye in regards to visible residual fluorescence. The cost of a high-speed camera system for fluorescence endoscopy would be exponentially higher than the proposed design and would not hold any value in real-world applications. If the fluorescence decay could have been detected via a camera capturing at millisecond speeds, then this would allow surgeons to visualize fluorescent material (diseased tissue) during endoscopic procedures in real-time.

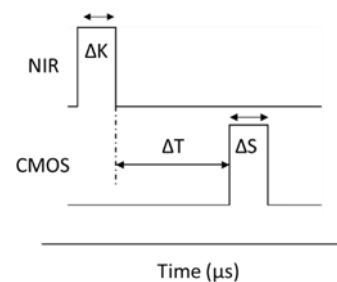


Figure 7: A schematic of the triggered pulses controlled via the Gardasoft LED controller with the NIR LED channel and the CMOS camera channel

#### 4. DISCUSSION

This research confirms that at an exposure time equivalent to 200 Hz, there is no detectable residual fluorescence when a sample containing ICG in solution is excited at 780 nm. If any residual fluorescence existed, then this could have a significant impact on medical imaging techniques such as minimally invasive fluorescence endoscopy as it would allow for a pulsed excitation. Pulsing the excitation would reduce the total time whereby the source is emitting, thus reducing the energy that the patient is exposed to during the procedure. Currently at least one NIR channel is mixed with a white light channel with both remaining on throughout the surgery. The risk of damage through excess heat is significantly higher when the channels remain on. Should there be any residual fluorescence in the moments following the excitation off,  $\Delta K=0$  then a faster exposure time should be used to detect its presence,  $\Delta T=0$  and  $\Delta S < 4855 \mu s$ .

The experiments verify that fluorescence, generated from excitation of ICG in a solution, degrades with time during exposure to light at the excitation wavelength. The changes in fluorescence intensity observed during this study do not indicate a proportional relationship between concentration of ICG in solution and degradation of fluorescence. Data collected indicates that there are most likely secondary mechanisms occurring at a molecular level within the solution that have an effect on absorption and consequently on fluorescence.

The results show that there is a relationship between the rate of degradation of fluorescence and the optical power of the excitation source but again, this is not proportional. In general, as expected, the higher the optical power of the excitation, the quicker the rate of degradation of fluorescence. Temperature inside the cuvette was recorded for each excitation source. The LED recorded a temperature increase 50 % higher than the 10 mW LASER and 80 % higher than the 5 mW LASER however, this data does not suggest any proportional relationship with fluorescence decay. The thermal differences observed are likely to impact on changes in the solution at a molecular level which contributes to the overall effect of photodegradation. According to the experimental findings, after a period of 10 minutes there will be a detectable difference in fluorescence intensity however, this difference is not significant and may not even be detectable to the naked eye.

Results from this experimental work verify that exposing a solution containing ICG to a 780 nm excitation source generates detectable fluorescence that cannot be seen by the naked eye. Over time, a reduction in fluorescence intensity is observed and this can be detected using either a power meter or an off-the-shelf CMOS camera. The camera used recorded a quantum efficiency of less than 30 % at NIR wavelengths however, both fluorescent and non-fluorescent regions could be detected with good contrast. This refers to the ICG sample within the cuvette and the non-fluorescing background within the frame respectively. For liquid samples, the experimental setup is able to confirm the presence of ICG without the need for filters.

#### 5. CONCLUSIONS

From this experimental work, the optical properties of ICG in solution are investigated using an excitation wavelength of 780 nm. Apparatus including a single monochrome camera and LED controller are assembled for synchronized data collection, whereby aqueous solutions of ICG are exposed to controlled pulses of excitation wavelength. The main

objective is to understand more about the optical properties of ICG in solution in order to exploit its properties and enhance its usage.

With the safety surrounding fluorescence endoscopy as the motivation for this work, significantly reducing energy exposure through pulsing of the NIR channel would result in an improvement in patient wellbeing. This experiment has confirmed that there is no detectable fluorescence post-excitation-pulse at frame rates of 200 Hz and lower with a slight delay in signal generation (0.1 ms). This indicates that in order to detect fluorescence at a frame rate of 200 Hz, the source must always be present and subsequently filtered out of the frame. This research shows that at 780 nm, both fluorescent and non-fluorescent regions of the frame can be detected using a single CMOS camera. This may be of benefit in future work as the excitation wavelength is visible to the naked eye but the fluorescence is not and this has been the most significant finding. If an accurate and effective method for detecting the presence of ICG in a sample is required, this can be accomplished using a cheap monochrome camera and an illumination source at 780nm. If fluorescence is pre-sent through the camera but not by eye then ICG is present.

With regards to photobleaching and photostability of ICG in solution, a variety of parameters and conditions have been investigated to demonstrate that there is no one parameter that proportionally affects the decrease in fluorescence intensity observed. Instead, it is likely that a combination of parameters influence the rate of fluorescence decay and some of which, should be considered at a molecular level.

#### 6. FUNDING

Knowledge Economy Skills Scholarships (KESS) is a pan-Wales higher level skills initiative led by Bangor University on behalf of the HE sector in Wales. It is part funded by the Welsh Government's European Social Fund (ESF) convergence programme for West Wales and the Valleys



#### 7. ACKNOWLEDGEMENTS

A special thank you to KESS and to the Faculty of Computing, Engineering and Science at the University of South Wales.

#### 8. CONFLICTS OF INTEREST

The authors declare no conflict of interest. The funders had no role in the design of the study; in the collection, analyses, or interpretation of data; in the writing of the manuscript, or in the decision to publish the results.

## 9. REFERENCES

- [1] Alander, J.T.; Kaartinen, I.; Laakso, A.; Pätilä, T.; Spillmann, T.; Tuchin, V.V.; Venermo, M. and Välsuö, P. A Review of Indocyanine Green Fluorescent Imaging in Surgery. *International Journal of Biomedical Imaging* Volume 2012; 2012:940585.
- [2] Lade, U.; Bhojar, P. and Hingankar, M. Newly Developed Application of NIR Dyes in Cancer Targeting and Imaging: A Review. *World Journal of Pharmacy and Pharmaceutical Sciences*. 2014 Volume 3, Issue 2, 2193-2201
- [3] Gibbs, S.L. Near infrared fluorescence for image-guided surgery. *Quantitative Imaging in Medical Surgery* 2012 Sep; 2(3): 177-187
- [4] Jonak, C.; Skvara, H.; Kunstfeld, R.; Trautinger, F. and Schmid, J.A. Intradermal Indocyanine Green for In Vivo Fluorescence Laser Scanning Microscopy of Human Skin: A Pilot Study. *PLoS ONE*. 2011; 6(8):e23972
- [5] Yaqoob, Z.; McDowell, E.; Wu, J.; Heng, X.; Fingler, J. and Yang, C. Molecular contrast optical coherence tomography: A pump-probe scheme using indocyanine green as a contrast agent. *Journal of Biomedical Optics* 2006, Sept-Oct; 11(5):054017
- [6] Haj-Hosseini, N.; Behm, P.; Shabo, I. and Wårdell, K. Fluorescence spectroscopy using indocyanine green for lymph node mapping. *Proceedings of SPIE, the international Society for Optical Engineering* 2014, (8935), 893504, 1-6
- [7] Frangioni, J. New Technologies for Human Cancer Imaging. *American Society of Clinical Oncology*. August 2008 Volume 26 Number 24
- [8] Qi, J.; Nabavi, E.; Hu, Y.; Rees-Whippey, D.; Curtis, A.; Price, C.; Copner, N.; Sanassy, C.; Leiloglou, M.; Leff, D.; Hanna, G. and Elson, D. A light-weight near infrared fluorescence endoscope based on a single color camera: a proof-of-concept study. *Conference on Lasers and Electro-Optics Pacific Rim (CLEO-PR)* 31 July-4 Aug. 2017
- [9] Kozin, E.D.; Lehmann, A.; Carter, M.; Hight, E.; Cohen, M.; Nakajima, H.H. and Lee, D.J. Thermal effects of endoscopy in human temporal bone model: implications for endoscopic ear surgery. *Laryngoscope* 2014 Aug; 124(8): E332-E339
- [10] Modlin, I.M.; Begos, D.G. and Ballantyne, G.H. *Laparoscopic Gastrointestinal Surgery: Current State of the Art*. Edr. Spiro HM. *Clinical Gastroenterology* 2010
- [11] Envemeka, C.S. Attenuation and penetration of visible 632.8 nm and invisible infra-red 904nm light in soft tissues. *LASER Therapy* Volume 13, 2001 95-101
- [12] Ohnishi, S.; Lomnes, S.; Laurence, R.; Gogbashian, A.; Mariani, G. and Frangioni, J. Organic Alternatives to Quantum Dots for Intraoperative Near-Infrared Fluorescent Sentinel Lymph Node Mapping. *Molecular Imaging* Vo 4. No. 3 July 2005 pp 172-181
- [13] Hutteman, M.; Mieog, J.; van der Voost, J.; Liefers, G.; Putter, H.; Löwik, C.; Frangioni, J.; van de Velde, C. and Vahrmeijer, A. Randomized, double-blind comparison of indocyanine green with or without albumin premixing for near-infrared fluorescence imaging of sentinel lymph nodes in breast cancer patients. *Breast Cancer Research and Treatment*. 2011 May; 127(1): 163-170
- [14] Gioux, S.; Choi, H. and Frangioni, J. Image-Guided Surgery using Invisible Near-Infrared Light: Fundamentals of Clinical Translation. *Molecular Imaging* 2010 October; 9(5): 237-255
- [15] Bozkurt, A. and Onaral, B. Safety assessment of near infrared light emitting diodes for diffuse optical measurements. *Bio-medical Engineering OnLine* 2004, 3:9
- [16] Hachey, K.; Gilmore, D.; Armstrong, K.; Harris, S.; Hornick, J.; Colson, Y. and Wee, J. Safety and Feasibility of Near Infrared Image-Guided Lymphatic Mapping of Regional Lymph Nodes in Esophageal Cancer. *Journal of Thoracic Cardiovascular Surgery*. 2016 August; 152(2): 546-554
- [17] Nairat, M.; Konar, A.; Kaniecki, M.; Lozovoy, V. and Dantus, M. Investigating the role of human serum albumin protein pocket on the excited state dynamics of indocyanine green using shaped femtosecond laser pulses. *Royal Society of Chemistry PCCP* 2015, 17, 5872
- [18] Crull, J.W. and Schafer, S.A. Indocyanine Green Degradation During High-Intensity Laser Irradiation. *SPIE 2671, Lasers in surgery: Advanced Characterization, Therapeutics, and Systems VI*, (17 May 1996)
- [19] Yuan, B.; Chen, N. and Zhu, Q. Emission and absorption properties of indocyanine green in Intralipid solution. *Journal of Biomedical Optics* 2004; 9(3): 497-503
- [20] Gerega, A.; Zolek, N.; Soltysinski, T.; Milej, D.; Sawosz, P.; Toczyłowska, B. and Liebert, A. Wavelength-resolved measurements of fluorescence lifetime of indocyanine green," *J. Biomed. Opt.* 16(6), 067,010. 2011
- [21] Homulle, H.A.R.; Powolny, F.; Stegehuis, P. L.; Dijkstra, J.; Li, D.U.; Homicsko, K.; Rimoldi, D.; Muehlethaler, K.; Prior, J.O.; Sinisi, R.; Dubikovskaya, E.; Charbon, E. and Bruschini, C. Compact solid-state CMOS single-photon detector array for in vivo NIR fluorescence lifetime oncology measurements. *Biomedical Optics Express*, 7(5), 1797-1814, 2016

# Why Should we Use Inclined Tables in Engineering Drawing Works?

Abdelaty E. Abdelgawad  
Industrial Engineering  
Department, Faculty of  
Engineering, King Saud  
University, Saudi Arabia, P.O.  
Box 800, Riyadh, 11421, Saudi  
Arabia

Ahmed T. Soliman  
Industrial Engineering  
Department, Faculty of  
Engineering, King Saud  
University, Saudi Arabia, P.O.  
Box 800, Riyadh, 11421, Saudi  
Arabia

Mohamed Z. Ramadan  
Industrial Engineering  
Department, Faculty of  
Engineering, King Saud  
University, Saudi Arabia, P.O.  
Box 800, Riyadh, 11421, Saudi  
Arabia

---

**Abstract:** One of the primary purposes of studying human Factors is to relieve work stresses imposed on the workers during their jobs. The current study consisted of two stages. The first phase aimed to develop a microcomputer biomechanically based to analyze clerk body postures. The second phase was to test that developed model on studying table tapes (i.g., adjustable inclined versus table vs. fixed horizontal table) during drawing engineering designs. The results showed the capability of the proposed model for analyzing the clerks' jobs. In addition, the inclined furniture was superior in reducing the stresses associated with doing jobs using furniture compared with fixed horizontal tables. Finally, it would be better to use a simple tool such as the developed one to analyze complicated tasks that force workers to take awkward postures and sustained that posture for an extended period.

**Keywords:** Biomechanics, Furniture, Human Factors, Engineering.

---

## 1. INTRODUCTION

The majority of engineering drawing jobs require a man to remain at his posture for the workday duration, and many employees spend their entire careers in one occupation. The cumulative effects of several years of work at insufficiently designed workplaces in terms of capacities and measurements can be highly detrimental to the musculoskeletal systems.

Musculoskeletal injuries were the top priority in daily medical practice in most cases [1,2]. Recent research in the revelation claims that over one million people with MSD were unable to function last year, with an annual economic loss exceeding \$50 billion [3]. Approximately 6.4% of Australia's entire workforce (who have worked at least one year after a work-related injury) has reported at least one injury or illness in the past year [4]. A large number of injuries and diseases are connected to jobs in the U.S. That equates to roughly 15-20% of all Americans [5].

Oakman et al. [6] identified an association between MSP and adverse physical and psychosocial job characteristics in their study of the relationship between pain site and workplace characteristics for use by individual participants. Organizations must conduct a thorough assessment of their work environments to ensure that all potential workplace risks, both physical and psychosocial, are recognized and then mitigated for all age groups. According to Jay et al. [7], increased stress and musculoskeletal discomfort are associated with decreased work capacity in female laboratory technicians. Floyd and Ward [8] demonstrated how two operators' bent upper spines resulted in them operating at a too low pace for their heights. One of the numerous studies has addressed the importance of correcting work postures to improve work efficiency and productivity. Brideger [9] showed that sloping furniture significantly decreased trunk flexion. The knee, hip joints, and pelvis adapted to the forward-sloping chair, while the neck and trunk inclination adapted to the eloping table floor. Additionally, sloping furniture was viewed as providing a more relaxing feeling than standard furniture. Even with humans come in different sizes where there are differences between different national, ethnic groups, there are gender differences.

With the rapid computing capabilities of modern microcomputers, it becomes both scientifically beneficial and economically feasible to conduct comprehensive mechanical analyses of people's interactions with their tasks and work environment. A generalized model capable of predicting and quantifying work-related stresses may be helpful. This article describes a microcomputer-based model for calculating the compression load on body joints in the upper limbs. This interactive model will assist job designers in evaluating secure compression loads for workplace design, optimize material handling, optimize physical (seat, worktop, etc.), and visual (display and tool placement) posture. In addition, the program will test its capability to identify which furniture is appropriate to be used for engineering drawing task supporting with applying Electromyography (EMGs) signals and subjective measures.

## 2. METHODS

This article is divided into two phases. The first phase was developing the micro-computer biomechanical model. Then, the second phase was testing and applying this model to differentiate between furniture designs.

### 2.1 Phase I. Developing the Microcomputer Model

The proposed model is similar to that one developed by Khalid and Ramadan [10], except that the proposed model allowed the person to support his/her hands or arms on an object. The proportions of the individual body's components are just as significant as the total size and weight. A popular approach is to view the human body as a series of pieces, as illustrated in Figure 1. The components are linked through articulation points.

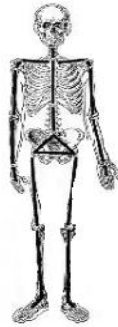


Figure. 1 Body Link System.

The biomechanical model aimed to determine the stresses placed on the musculoskeletal system's critical points. The model uses currently available data on body segment parameters, assuming that the body is composed of rigid links connected at predetermined articulations. The reactive forces and torques equations at the various articulations of the body in various configurations could be constructed using these segment parameters and Newtonian mechanics. The human body is modeled in Figure 2 as a two-dimensional, eight-link structure representing movement across seven joints. The foot, knee, back, L5/S1, shoulder, elbow, and wrist are all included. Since most back injuries occur in the lower back at the level of the fifth lumbar and first sacral vertebrae (L5/S1) and their adjacent disc, cumulative loads impose stresses on that area. The trunk was divided into two parts to allow for the measurement of spinal compressive forces and moments at the L5/S1 disk: (1) Hip joint to L5/S1 disc center; (2) L5/S1 disc center to shoulder joint. The ankle joint is believed to be fixed in place, serving as a reference point for the model.

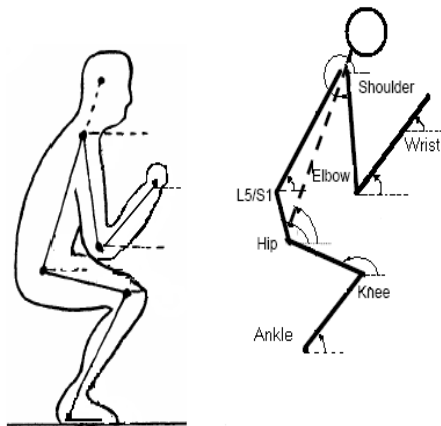


Fig. 2. Linkage system used in body model.

Angles between body links and the horizontal, measured in an anticlockwise direction, describe posture. Angles  $\theta_3$  and  $\theta_4$  are calculated in the model using the inclination of the trunk and knee relative to the horizontal  $\theta_8$  and  $\theta_2$  [11]. The model will be implemented using an advanced Visual Basic program. The software will make use of both stored and user-supplied data. The data that is stored includes the following:

- 1) The weight of the body segment links which is based on the ratios of segment weight to body weight based on data provided by Miller and Morrison [12] as shown in Table 1.
- 2) Location of the center of gravity for each link based on data provided by Garg and Chaffin [13] as shown in Table 2.

- 3) Radius of rotation for each link as given by Chaffin and Anderson [14].

To ensure that the L5/S1 disc does not experience excessive stress during static and dynamic analysis, the model assumes that safe stress exists when the maximum compression force measured on the spine is less than the compressive force limits specified by Chaffin and Anderson [14]. Males have a mass of 5670 N (578 kg), and females have a mass of 3394 N (346 kg). The maximum weight lifted in a given configuration is determined by assuming that the same permissible weight limit on the L5/S1 is not exceeded. Biomechanical analysis may be conducted in either a dynamic or static mode using the model.

**Table 1. Body segment weight as a presented regression equation  $SW = a + b * TW$  based on Miller and Morrison [12].**

Body segment	a	b
Hand	+0.7	+0.01
Forearms	-0.5	+0.04
Upper arms	-2.9	+0.8
Head, neck and trunk	+12.0	+0.47
Upper legs	+3.2	+0.18
Lower legs	-1.9	+0.11
Feet	+1.5	+0.02

TW= total body weight in lbs. SW= segment weight in lbs.

**Table 2. Link centers of mass as a percentage of segment length based on Garg and Chaffine [13].**

Segment	from proximal end	from distal end
Hand	50.6%	49.4%
Forearms	43.0	57.0
Upper arms	43.6	56.4
Head, neck and trunk above L5/S1	43.21	56.79
Trunk below L5/S1 disk	50.0	50.0
Upper legs	56.7	43.3
Lower legs	56.	43.3
Feet	57.1	42.9

### 2.1.1 Static mode analysis

The static analysis mode uses the same body segment data as the dynamic analysis mode, except all accelerations are set to zero, and  $\sum F_x$  and  $\sum F_y$  are equal to zero. By defining the body posture, the static model is initiated. Six articulation angles can be used to describe a person's stance. These are the angles at the ankle, knee, trunk, shoulder, elbow, and wrist. These could be determined using photographic techniques based on a lateral photograph of a worker in the role understudy and similar to that used in Chaffin and Anderson [14]. All angles are determined in the opposite direction of the horizontal plane, counter-clockwise. After defining a body position, the model measures the inclination angles of both the hip-L5/S1 and L5/S1 shoulder links using the trunk and knee angles with the horizontal plane. The masses of the body segments produce the joint forces and torques.

A function of the model is intended to identify essential postures associated with a given task at a given height. This is the case of the position in which the L5/S1 stresses exceed the compressive force maximum. Within the range of motion, the body articulation angles are incremented using maximum,

minimum, and increment values stored in the software memory. Each articulation angle is then decreased or increased incrementally to create a logically balanced posture. This process is repeated for each articulation angle until all possible positions have been considered.

### 2.1.2 Dynamic mode analysis

For dynamic analysis, the body's inertia generates forces that are a component of the overall kinematics mechanism. This model is based on a relationship established many years ago by Slot and Stone [15] to explain the displacement—time relationship for arm movement. By examining segment displacements concerning time, the angular velocity and acceleration are calculated using the displacement equation's first and second derivatives. Beginning with the ankle joint, the tangential and regular accelerations, as well as their horizontal and vertical components, will be calculated at each segment's center of gravity using the following equations:

$$\text{Tangential acceleration} = \omega_i * r_i$$

$$\text{Normal acceleration} = \alpha_i * r_i$$

Where:

$r_i$  = the distance of the center of gravity of segment  $i$  to the articulation;

$\omega_i$  = angular velocity of segment  $i$ ;

$\alpha_i$  = angular acceleration of segment  $i$ .

At the center of mass of each segment, the inertial force components in the X and Y directions are determined by multiplying the link mass by the corresponding linear acceleration components. Forces and torques are measured at each joint using the equilibrium equations, taking into account the mass of the body segments, the mass of the handled weight, and the additive effects of acceleration on both the weight handled and the body segments. This study requires a detailed explanation of the motion of each connection during work activities. This can be accomplished using photographic data captured with either a goniometric or video spot locator device [14]. The entire movement should be photographed from start to finish. The data are entered into the computer program either by specifying postures at constant time intervals or by specifying the posture that corresponds to the actual elapsed time.

### 2.1.3 Model input/output

The required input data include the subject's weight, gender, and connection lengths (i.e., the straight-line distances between the articulation points). The latter is calculated either from actual body dimensions or from a displaced table of percentile values. At this point in the program's implementation, two choices would be available for calculating the mechanical stresses in the body. The user can choose any choice from the menu. If the static choice is chosen, the user must enter body posture parameters that correspond to the links' angle relative to the horizontal. If the dynamic choice is chosen, the consumer must supply body posture angles at various time intervals along the motion trajectory.

The seven postural angles are defined as follows:

- 1) Trunk Flexion Angle (TF): The angle between the upper trunk line and the upward extension of the pelvic line. The angle TF increases with increased bending of the trunk.
- 2) Hip Flexion Angle (HF): The angle between the thigh and the downward extension of the pelvic line. The angle HF increases as the hip joints are flexed.

- 3) Pelvic Inclination Angle (PI): The inclination of the pelvic line with respect to the horizon. PI decreases as the pelvis tilts backward.
- 4) Trunk Inclination Angle (TI): The inclination of the trunk with respect to the horizontal. Large values of TI represent an upright posture, whereas small values are observed when the trunk is inclined over the work surface.
- 5) Thigh Angle (TH): The inclination of the thigh with respect to the horizontal. TH increases as the thighs are pointed downward. TH was given a negative sign if the thighs pointed above the horizontal.
- 6) Neck Flexion Angle (NF): The angle between the upward extension of the trunk line and the line from the seventh cervical marker through the subject's eye. NF increases as the head is bent forward with respect to the trunk.
- 7) Knee Flexion Angle (KF): The angle between the lower leg line and the extension of the thigh line. KF increases as the knee is flexed.

Those angles are inputted in the model microcomputer with other measures (weight, anthropometric measurements) to get results.

The following output data will be printed by the microcomputer model:

- 1) A complete configuration for a given motion or for a defined posture.
- 2) Position of each joint in the space (Cartesian Coordinates) considering the ankle joint as a reference.
- 3) Angular velocity and acceleration for each link.
- 4) Forces in the X and Y directions at each joint.
- 5) Torque at each joint.
- 6) Compression force at L5/S1 joint.

In addition to the above information, special messages may appear depending on the option selected.

## 2.2 Phase II. Model Testing

In the second phase, an experimental method was employed to test the developed biomechanical model and the significance of using inclined adjustable furniture. Again, biomechanical body stresses, muscular activities, and subjective measures were the dependable factors; while table types (e.g., adjustable inclined versus fixed horizontal table) were independent factors.

### 2.2.1 Participants

The participants were eight unpaid male engineering students. The mean age of the participants was 23 years, their average height was 167.7 cm, and their average weight was 75.2 kg. The experiment excluded all participants who were obese or had a history of musculoskeletal disorders. The experiment requires participants to draw on two different kinds of tables: a horizontal surface and an adjustable inclined table, as shown in Figure 4, over a forty-five-minute period for each run.

### 2.2.2 Dependent variables

#### 2.2.2.1 Biomechanical model

It is described in detail in phase I.

#### 2.2.2.2 Electromyography (EMG)

Electromyography is a medical procedure used to determine the response of muscles to nerve stimulation. Electromyography measures the electrical potential produced by contracting muscle cells. When a muscle fiber twitches, a small electrical potential is produced that can be measured by inserting an electrode into the muscle or above the muscle on the skin's surface. (Surface electrodes are usually less invasive and are used in laboratory and workplace experiments.) Since the relationship between muscle force and electrical output is

monotonic, calibration procedures are used to translate EMG signals to estimates of muscle force output.

During execution sessions, EMG values such as root mean square (RMS) and rectified absolute mean (RAM) will be computed as dependent variables. The dorsal neck muscle on the left side of the body was analyzed to determine the difference in sitting criteria between the two set styles. The two electrodes were connected to the body on the opposite side of the face to eliminate the signal interference caused by hand-arm device motions. The experimental conditions were presented so that the participants were randomized to minimize the possibility of order effects due to the repeated-measures nature of the experimental design.

### 2.2.2.3 Subjective assessments

After each photography day, participants completed a survey that included questions about body part discomfort, headaches, visual discomfort, rest breaks frequency, and workstation preferences. Participants will use the Borg CR scale [16] to characterize body parts and headache pain at the end of the workday, as shown in Figure 3. In addition, each of the seven signs will signify the presence or absence of visual discomfort (burning, itching, aching, watering, blurring, tired, or dry).

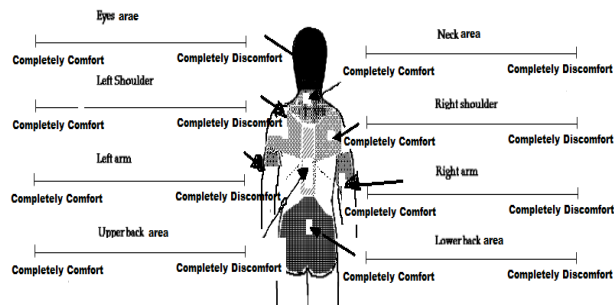


Fig.3 Visual analogue discomfort scale rated from `no pain to `extreme pain in 8 body areas

### 2.2.3 Independent Variables

A horizontal surface table and an adjustable inclined surface table were employed. Both tables are commercial well-known in the local market, as shown in Figure 4.



Fig 4. Some frames are used in different surface table types.

## 2.3 Apparatus

The equipment that was used to perform this experiment were:

- 1) A horizontal surface table and an adjustable inclined surface table.

- 2) Digital camera (Canon EOS 4000D DSLR, Germany).
- 3) Digital timer (Marathon TI080006-BK Digital Big Digits).
- 4) Electromyography (EMG) system (CASSY Lab., Leybold Didactic GmbH, Germany).

## 2.4 Experimental Design and Procedures

Five adhesive markers were mounted on the skin of the right ankle, knee, shoulder, elbow, and wrist joints, as well as one marker at the hip joint to determine posture. The positions of joints in different anatomical regions were estimated using these markers. Articulation is determined by the angles of the lines that connect them. For example, the angle between the hip/trunk line and a line drawn from the trunk through the subject's eyes is used to approximate neck flexion. Additionally, surface electrodes were mounted on the subject's lower back and neck, just above the muscle. The EMG technique will be used to determine the relationship between the forces exerted by a muscle and its electrical activity. The participants' postures were captured using a digital camera.

The chair height must be adjusted so that the desk and sitting elbow lengths are approximately the same. At the end of the experiment, participants rated each workspace on a seven-point discomfort scale in which a score of 1, 3, 5, and 7 associated with completely comfortable, quite comfortable, just noticeable discomfort, and entirely discomfort, respectively. It is felt that the modifying body part discomfort would provide more acceptable discrimination than that obtaining by having subjects choose a number between one and seven and placing that number on the picture body part in discomfort. The reading of EMG was recorded and analyzed.

## 3. Results

### 3.1 Biomechanical Analysis

#### 3.1.1 Estimated Erector-Spinae Muscle Force

The erector-spinae muscle forces were computed based on the average values of each forty-five working minutes. In addition, the average back muscle forces for a complete duration were employed for the statistical analysis. There was a significant difference between the horizontal and inclined table,  $F(1,7)=81.793, p<0.000$ . As shown in Figure 5, there was more significantly biomechanical stress when participants worked on the horizontal table (840N) than on the inclined table (705N).

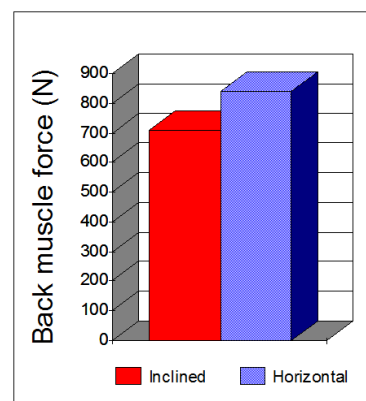


Fig.5. Effect of the table types on estimated erector-spinae muscle force.

#### 3.1.2 Estimated Compression Force acting at L5/S1

The estimated compression forces acting at L5/S1 were computed based on the average values of each forty-five working minutes, and it was employed for the statistical analysis. There was significant differences between the

horizontal and inclined table,  $F(1,7) = 19.495$ ,  $p < 0.003$ . As shown in Figure 6 there was more significantly biomechanical stress at working on the horizontal table (1250N) compared to working on the inclined table (1080N).

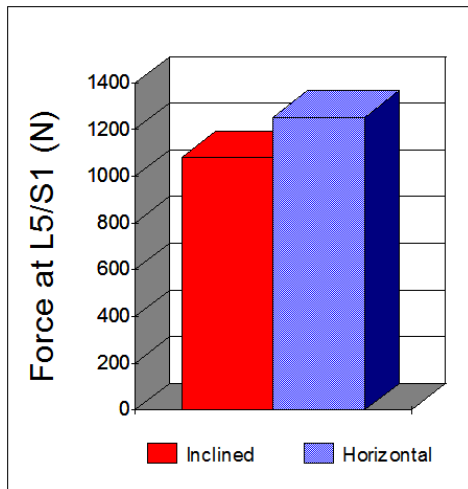


Fig.6. Effect of the table types on compression force acting at L5/S1

### 3.2 Results of EMG

There are two types of data (e.g., the mean and root-mean-square values). The average of neck muscle showed that there were significant differences between the horizontal and inclined table, for the mean values  $F(1,7) = 29.726$ ,  $p < 0.001$ , as well as for root-mean-square value  $F(1,7) = 18.099$ ,  $p < 0.004$ . As shown in Figure 7 there were more significantly muscular stresses at working on a horizontal table compared to working on the inclined table.

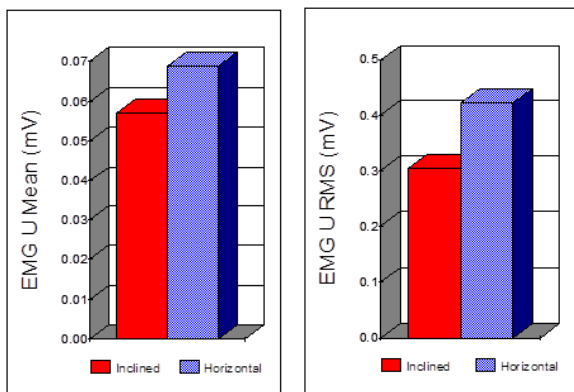


Fig.7. Effect of table types on neck muscular activities using EMG values.

### 3.3 Subjective Assessments

Each discomfort measure of the neck, right shoulder, left shoulder, right arm, left arm, upper back, and lower back for each subjective was computed based on the average values for a complete forty-five minutes period. Those values were employed for the statistical analysis. There were significant differences between the horizontal and inclined table as shown in Figure 8:

The neck muscle:  $F(1,7) = 1519.298$ ,  $p < 0.000$   
 The right shoulder muscle:  $F(1,7) = 31.047$ ,  $p < 0.001$   
 The left shoulder muscle:  $F(1,7) = 6.250E-04$ ,  $p < 0.001$

The right arm muscle:  $F(1,7) = 5.760$ ,  $p < 0.000$   
 The lower back muscle:  $F(1,7) = 5.130$ ,  $p < 0.000$

As shown in Figure 8, there were more significant stresses at working on a horizontal table compared to working on an inclined table in terms of discomfort measures. Also, there were no significant differences between horizontal and inclined tables on the discomfort scale at the lift arm muscle and the upper back muscle.

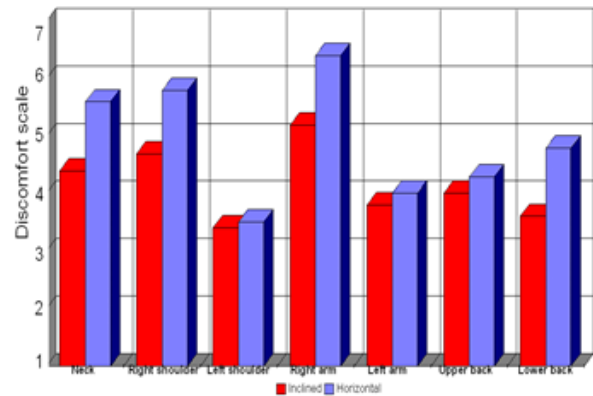


Fig.8. Effect of table types on neck, right shoulder, left shoulder, right arm, left arm, upper back and lower back discomfort scales.

## 4. Discussions and Conclusions

Using biomechanical models to predict musculoskeletal stresses is one of the best and most practical methods used by task designers and medical professionals. A biomechanical model's efficacy is contingent upon its ability to capture the human body's complex features accurately. The proposed model showed its capability for evaluating stresses imposed on the participants' backs in the furniture application. This evaluation was similar to the model used in Khalil and Ramadan [10] for assessing manual lifting tasks. The majority of these models examine the stresses imposed on the human body when it is in a static position. Just a few employ dynamic analysis of the body's motion trajectory. Dynamic analysis is far more complex and time-consuming than static analysis and as the number of links in the model rises, the computational complexity increases exponentially. It should be noted that using biomechanical models to assess musculoskeletal system stresses has both advantages and disadvantages.

Among the benefits is collecting objective data on the forces and torques applied to different joints, bones, and muscles without resorting to often dangerous and psychologically inappropriate invasive techniques. Consequently, when interpreting the findings, one should be thoroughly familiar with the model's assumptions and limitations. Another common occurrence is the absence of reliable in vivo data on the stress limits of soft and hard human tissues. Again, considerable judgment should be exercised in interpreting model output data. However, the model outputs can also provide a handy approximation of otherwise unavailable stress values. These principles can be used in combination with work analysis and design guidelines.

Microcomputers' widespread usage in recent years enables analysts to more openly using complex biomechanical models to investigate the relationship between posture, task type, and stresses placed on different joints and muscles of the human body. The model established in this article views the human

body as an eight-link structure. It differs from more simplistic biomechanical models in that it considers the hip stress as distinct from the L5/S1 stress by separating the two articulation points.

The findings of this study showed that students who used an adjustable inclined surface table experienced less biomechanical tension and a more relaxed posture than students who used a horizontal surface table. The adjustable inclined surface table did also maintain a stress-free position for the muscle system. The study was conducted using a biomechanical model to manage both static and dynamic modes to predict musculoskeletal stresses. Additionally, the study was accompanied by the use of EMG to assess neck muscle tension and by the psychophysical measure of comfort. As a result, the drafting table must be revamped to accommodate versatility. Mobility here refers to adjusting the table height and angle of the surface to stand or sit more upright and with less neck flexion.

Additionally, the study established that the current horizontal table compelled students to lean forward and that prolonged trunk effort resulted in complete muscle fatigue. This result is consistent with the findings of other researchers who assessed the use of furniture using various posture assessment techniques [17, 18]. Additional research on sloping furniture may benefit from factoring out visual and anatomical determinants of posture and attempting to define and evaluate complex changes in posture.

The evidence from the agreement of biomechanical stress measures, EMG values, and psychophysical comfort scales proved the capability of the new available approaches. As a result, the findings in this study demonstrate the efficacy of a methodology that utilizes a body posture recording and analysis technique while the subject is working. The versatility of this methodology enables the designer to use the model in both field and laboratory studies. Additionally, the model overcomes the limitations of previous methodologies by incorporating the postures' time histories and the dynamic model of the entire movement.

## 5. REFERENCES

- [1] Reiso, H., Nygard, J.F., Brage, S., et al., 2000. Work ability assessed by patients and their GPs in new episodes of sickness certification. *Family Practice* 17, 139–144.
- [2] Weevers, H.-Ja, Van Der Beek, A.J., Anema Jr., et al., 2005. Work-related disease in general practice: a systematic review. *Family Practice* 22, 197–204.
- [3] National Academy of Sciences, 1999. Work related musculoskeletal disorders: report, workshop summary, and workshop papers. National Academy of Sciences, National Research Council, Institute of Medicine, Washington, D.C., 1–240.
- [4] Australian Bureau of Statistics, 2007. Work related injury. *Australian Social Trends*.
- [5] Melhorn, J.M., 1996. A prospective study for upper-extremity cumulative trauma disorders of workers in aircraft manufacturing. *Journal of Occupational and Environmental Medicine* 38 (12), 1264–1271.
- [6] Oakman J., Wind A., Heuvel S.G., Beek J.A. 2017. Work characteristics predict the development of multi-site musculoskeletal pain. *Int Arch Occup Environ Health*, 90:653–661. DOI 10.1007/s00420-017-1228-9
- [7] Jay K, Friborg M.K., Sjøgaard G., Jakobsen M.D., Sundstrup E., Brandt M., and Andersen L.L. 2015. The Consequence of Combined Pain and Stress on Work Ability in Female Laboratory Technicians: A Cross-Sectional Study. *Int. J. Environ. Res. Public Health* 2015, 12, 15834–15842; doi:10.3390/ijerph121215024
- [8] Floyd, W.F. and Ward, J.S', "Posture in industry...", *Int. of Prod. Re.*, 5, 213-224 (1966).
- [9] Bridger, R.S., "Postural adaptations to a sloping chair and work surface, *Human Factors* 30, 237-247 (1988).
- [10] Khalil, T.M. and Ramadan, M.Z., " Biomechanical evaluation of lifting tasks: a microcomputer-based model," *An international Journal of Computers & Industrial Engineering*, 14 (2), 1988, pp. 153-160.
- [11] Freivalds, D. B. Chaffin. A. Garg and K. S. Lee A dynamic biomechanical evaluation of lifting maximum acceptable loads. *7. Biomechanics* 17(4), 251-262 (1984).
- [12] Miller and Morrison. Prediction of segmental parameter. *Medicine Sci. Sports*, 207-212 (1975).
- [13] Garg, A., Chaffin, D.B. (1975). A biomechanical computerized simulation of human strength. *AIIE Transactions*, 7(1):1-15. EX.26-122
- [14] Chaffin, D.B., Andersson, G.B. (1991). *Occupational Biomechanics*. Second edition. New York: John Wiley and Sons. EX.26-420.
- [15] L. Slote and G. Stone. Biomechanical power generated by forearm flexion. *Human Factors* 5, 5 443452 (1963).
- [16] Borg, G.A.V. (1998). *Borg's Perceived Exertion and Pain Scales*. Champaign, IL: Human Kinetics. EX.26-721.
- [17] Tunay M. and Melemez K. An analysis of biomechanical and anthropometric parameters on classroom furniture design. *African Journal of Biotechnology* Vol. 7 (8), pp. 1081-1086, 2008.
- [18] Carcone S.M., Keirb P.J. Effects of backrest design on biomechanics and comfort during seated work. *Applied Ergonomics* 38 (2007) 755–764.